

**Modelling Impacts of Climate Change on Snow Drought, Groundwater
Drought, and their Feedback Mechanism in a Snow Dominated Watershed in
Western Canada**

By

Yinlong Huang

A thesis submitted in partial fulfillment of the requirements of the degree of

Master of Science

Department of Earth and Atmospheric Sciences

University of Alberta

© Yinlong Huang, 2023

Abstract

In snow-dominated regions, snow storage is a primary water resource contributing to surface water (SW) and groundwater (GW) supplies. Snow drought is defined as either lack of snow storage or high-temperature-induced early snowmelt, leading to a loss of snow water resources. GW drought refers to a period of decreased GW levels that results in insufficient water supply in GW-dependent regions. Due to snowmelt infiltration to the soil, an interaction mechanism between snow drought and GW drought is possible, requiring attention. Most of the recent studies focused on assessing the hydrological, meteorological, and agricultural droughts, and in some cases, the relationship between some of them was studied.

Since snow is a primary driver of hydrologic processes in most cold watersheds of the mid-to-high latitude regions, the overarching goal of this study was to assess the relationship between snow drought and GW drought, which can inform water management and environmental protection in these regions. Two physical process-based SW and GW models were calibrated and coupled to simulate the interactions and feedback mechanism between snow and GW droughts for a historical period (i.e., 1980-2013) under different eco-hydro(geo)logical (EHG) settings, including Mountains, Foothills, and Plains. Using a set of downscaled climate data, projected from an ensemble of five Global Climate Models of the Coupled Model Intercomparison Project 6, the coupled SW-GW model was forced to simulate physical processes associated with snow and groundwater droughts for the 2040-2073 period under two Shared Socioeconomic Pathways (SSP126, and SSP585). With a drainage area of about 59,000 km², comprising heterogeneous EHG conditions, the North Saskatchewan River Basin, Alberta, Canada was selected as the study area. The study results indicated that characteristics of snow and GW droughts were reversed across different EHG regions under future SSP scenarios compared to the historical period. Mountains

experienced the worst historical snow drought compared to Foothills and Plains. The multi-model ensemble mean projections indicated more intensified and prolonged snow droughts with higher frequency in Mountains, leading to lower snow accumulation in Mountains. Among all regions, Plains experienced worst historical GW drought, and it was projected to experience lower intensity GW droughts in the future. On the other hand, mountains were projected to experience relatively less frequent and low intensity GW droughts compared to other regions. This implies a potential shift of snow drought events to GW droughts in Plains and the opposite processes in the Mountains in the future.

The statistical analysis of the simulated snow water equivalent and GW heads for historical period indicated that the propagation time from snow to GW drought varies across regions, with 4 months in Mountains, 5 months in Foothills, and 6 months in Plains. Both future scenarios projected decreased propagation time for all regions, suggesting accelerated water cycle. The Least Absolute Shrinkage and Selection Operator analysis of the simulated results indicated that dominant physical process that control GW head and its connection to snow processes varies across EHG regions. All regions showed sensitive response to soil water content and percolation. Mountains and Foothills were more sensitive to curve number than Plains, whereas Foothills and Plains were more sensitive to total water yield, with Plains alone being extremely sensitive to evapotranspiration.

This study provides a basis for further studies concerning the GW management strategies due to changes in snow processes that results from global warming effects in cold watersheds of the mid-to-high latitude regions. It also provides a unified approach for analyzing snow drought and GW drought relationship.

PREFACE

This master's research thesis is an original work by Yinlong Huang. It is a paper-based thesis that is organized into three chapters. Chapter 2 is in the final stage of preparation to be submitted to a peer-reviewed journal to be announced with further edits to the current manuscript prior to submission to the journal. Chapters 1 and 3 represent the general introduction, summary, and conclusions of the research, respectively.

I (Yinlong Huang) designed the framework of the thesis, wrote most of the text contained in it and created all figures. For the manuscript (Chapter 2), the co-authors are Dr. Monireh Faramarzi, an Associate Professor in the Department of Earth and Atmospheric Sciences who supervised this research and provided constructive feedback and edits throughout the formulation of this thesis. Other co-authors are Yangdi Jiang, a Ph.D student from the faculty of Mathematical and Statistical Science department, University of Alberta; and Dr. Bei Jiang, an Assistant Professor from the faculty of Mathematical and Statistical Science department, University of Alberta, who collaboratively provided feedback on the statistical analysis used for post-processing of the model outputs. Dr. Ryan T Bailey, an Associate Professor from Civil and Environmental Engineering Department, Colorado State University provided feedback on the groundwater model development; and Dr. Badrul Masud, a former post-doctoral researcher at University of Alberta, who supervised early steps of the post-processing of the model outputs related to calculation of drought indices.

DEDICATION

I hold my utmost gratitude to my supervisor, Dr. Monrieh Faramarzi. She provided me the chance to pursue my research interest, and she trusted and encouraged me throughout my entire research period. She taught me the necessary knowledge and extended my vision, sharpened my skills, and enhanced my confidence in my research, and she showed me how to be a good scientist, and I will always remember, and hold my appreciation.

Many thanks to my fellow lab members and many other experts from different fields, who have shown me their warmest welcome and provided me the most help since I started my master's program. You have shared your expertise and your knowledge generously with me and helped me on countless occasions. Due to the interdisciplinary nature of this project, experts from different fields provided their most helpful knowledge and skills. Yangdi Jiang and Dr. Bei Jiang have been more than helpful in this research, with their exceptional and abundant statistical knowledge and skill, willingness to share and teach me with concise and clear scientific methods. Dr. Ryan T Bailey provided the most help in assisting me in providing feedback and debugging errors related to the groundwater model. Dr. Badrul Masud supervised me in early stage of my research in development of drought indices. I also would like to acknowledge Dr. Daniel Alessi for agreeing to serve as a supervisory committee member who also led the larger project, where this research contributed to, and his broader viewpoints helped me learn the bigger picture of the research. I am also grateful to Dr. Brian Smerdon who agreed to serve as an examiner and Dr. Long Lee who served as a chair to facilitate my master's thesis defense.

I also would like to acknowledge Alberta Innovates and EPCOR for providing the funding needed to complete this thesis. Without their generous support, this project would not have been possible.

Finally, I would like to thank my parents and my partner, without whom I would not have been able to persist and continue to pursue my scientific career. This work is dedicated to them. More thanks to my friends and all the people who supported me along the way both physically and mentally.

TABLE OF CONTENTS

Abstract	ii
PREFACE	iv
DEDICATION	v
TABLE OF CONTENTS	vii
LIST OF FIGURES	ix
CHAPTER I – Introduction	1
1.1 Overview	1
1.2. Research Objectives	5
1.3. Thesis structure	6
1.4. References	7
CHAPTER II – MANUSCRIPT 1	13
1. Introduction	14
2. Material and methods	18
2.1 Study area	18
2.2 Data.....	21
2.2.1 Input data for hydrology and snow simulator (SWAT)	21
2.2.2 Input data for MODFLOW GW simulator	23
2.3 Surface water and GW modeling.....	24
2.3.1 SWAT model and calibration – validation procedure	24
2.3.2 MODFLOW model and calibration – validation procedure	27
2.4 Snow drought and GW drought calculation	29
2.5 Assessment of propagation and response time	31
2.6 Assessment of driving physical processes.....	32
3. Results and discussion.....	34
3.1 Model calibration, validation, and verification	35
3.1.1 SWAT model calibration and validation results.....	35
3.1.2 MODFLOW model calibration and validation results.....	36
3.2 Drought characteristics (frequency, duration and intensity)	37
3.2.1 Snow drought	37
3.2.2 GW drought	43
3.3 Propagation time for GW response to SWE.....	46

3.4 Dominant driving physical processes	51
4. Implication of the study results	54
5. Study caveats and future directions.....	57
6. Summary and conclusion	58
Acknowledgment	61
Declaration of Competing Interest	61
Credit authorship contribution statement	61
References	62
CHAPTER III – CONCLUSION	77
Research Summary.....	77
Study Conclusions and Implications.....	79
Study Limitations and Future Directions	83
BIBLIOGRAPHY	86
APPENDICES.....	104

LIST OF FIGURES

Figure 1. (a) Geographic extent of study area illustrating topographic information, hydrometric stations used for calibration of streamflow, climate stations used for model input, and the three Eco-hydro(geo)logical (EHG) regions. (b) North Saskatchewan River Basin Land Cover-Land Use Information.

Figure 2. Model calibration performance for selected hydrometric stations across different EHG regions (left column). The shaded range indicates the 95PPU based on calibrated parameter range. Comparison of model simulated snow depth (red) with the observed (blue) used for model verification (right column).

Figure 3. Historical and future snow drought characteristics: cumulative snow drought intensity (upper row), snow drought duration for each class of drought (middle row), and snow drought frequency (bottom row). Upper row: illustrates the cumulative probability of snow drought intensity for historical and future periods. The x-axis illustrates the snow drought intensity (SWEI), whereas y-axis indicate the cumulative probability for a particular snow drought intensity. The black curve in the center shows the historical snow drought intensity and shaded area around elaborates possible future intensity.

Figure 4. Historical and future standardized GW index (SGWI) characteristics for (a) cumulative GW drought intensity. The black line shows the historical GW drought intensity and shaded area around elaborates possible future intensity. (b) GW drought duration for each class of drought, and (c) GW drought frequency for each EHG region.

Figure 5. Cross-correlation analysis result for (a) Mountains, (b) Foothills and (c) Plains. The x-axis indicates lag time between SWE and GW levels. The negative lag months indicates that in SWE and GW time series, the variation of SWE occur before GW variations (i.e., GW responds to changes in SWE), whereas right-hand-side means GW time series leads SWE time series (not realistic and usually below the horizontal threshold, suggesting meaningless correlation, or negative CCF values, suggesting inverse correlation).

Figure 6. Heat plot indicating dominant physical processes for each EHG region. More cells with red-like color indicate that the particular parameter is more influential on GW head variation.

CHAPTER I – INTRODUCTION

1.1 Overview

Drought is a complicated, recurring natural disaster that can cause severe environmental, ecological or social-economic challenges (Lee et al., 2018; Pathak & Dodamani, 2021). Drought is often a slow-onset disaster that can occur worldwide and sometimes lasts for months and years (Beran & Rodier, 1985; Sheffield & Wood, 2011). Climate anomalies are the root cause of most droughts, nevertheless depending on the other natural processes involved in developing droughts and based on their potential impacts, the droughts are categorized into different types. The most commonly studied drought types are meteorological, hydrological, and agricultural droughts (He et al., 2018; Liu et al., 2016; M. B. Masud et al., 2015; Pathak & Dodamani, 2021). Snow and groundwater droughts are relatively new concepts which require extensive research, especially in the context of cold regions (Fendeková & Fendek, 2012; Hatchett & McEvoy, 2018; Huang et al., 2021; Huning & AghaKouchak, 2020; Lee et al., 2018; Staudinger et al., 2014).

Snow drought is explained as a deficit in snow accumulation due to variations in temperature or precipitation or both (NOAA, 2018). Groundwater (referred as GW) drought refers to a period of decreased GW levels that results in insufficient water supply in GW-dependent regions (USGS, 2016; Van Lanen & Peters, 2000; Huang et.al, 2021). It is projected that global warming and the resulting anomalies in climate in the future will impact the frequency, intensity, and duration of extreme events, such as droughts (IPCC, 2022b, 2022a; Stocker et al., 2013). In snow-dominated and groundwater abundant regions, such as mid-to-high latitude areas, the projected changes in climate and hydrological cycle, can impact snow accumulation, snow coverage, and snowmelt, which can then affect groundwater recharge. A prolonged deficit in precipitation or accelerated

snowmelt due to warming can initiate, develop, and intensify snow drought (Pendergrass et al., 2020), which can be propagated to the development and intensification of GW drought.

Snow and GW (particularly, unconfined aquifer) are connected through various physical processes through soil media. During the warm season when the frozen soil starts thawing and retains adequate permeability, snow can slowly melt and partially infiltrate into the soil, which can then travel to feed the underlying aquifer. Compared to rainfall precipitation, snowmelt can infiltrate more effectively below the root zone (Earman et al., 2006; W. Y. Wu et al., 2020), and some studies have shown that a large portion of GW recharge originates from snowmelt (Ajami et al., 2012; Earman et al., 2006). In mid-to-high latitude regions, where snow is a primary controlling factor of the hydrologic cycle, it is important to study snow drought, its potential impact on GW drought, and the physical processes that regulate their propagation and feedback mechanism. Essentially, the regions where snowmelt has a large contribution to GW, the occurrence of snow drought can affect snowmelt and infiltration feeding the aquifer, leading to potential GW drought. However, this propagation mechanism and the response of GW to changes in snow variation are not linear, and they depend on numerous eco-hydro (geo)logical (EHG) processes. Therefore, a key question that motivates the objectives of this study is “how under different ecological, geological, and hydrological settings, the time for snow drought to propagate to GW differs?”. The following question is, “what features can take major control of such propagation time?”. Hence, the main goal of this study is not only the assessment of characteristics of snow drought and GW drought, but also the mechanism of snow drought propagation to GW drought and the dominant physical processes driving such mechanism.

The existing drought assessment studies in cold regions, focused either on snow drought (Dierauer et al., 2019; Hatchett et al., 2021; Hatchett & McEvoy, 2018; Huning & AghaKouchak,

2020; Shrestha et al., 2021; Staudinger et al., 2014) or GW drought (Bloomfield et al., 2015; Bloomfield & Marchant, 2013; Fendeková & Fendek, 2012; B. Li & Rodell, 2015; Villholth et al., 2013), lacking a comprehensive assessment of the physical processes driving snow drought and GW drought connection and their feedback mechanism. Moreover, the current studies are mainly conducted at a local scale (Dierauer et al., 2021; Staudinger et al., 2014; Yeh, 2021), and regional-scale snow drought and GW drought assessments are limited. As a result, conclusions from small-scale studies are limited to the EHG settings of their local environments, and often they cannot be up-scaled to the large regional watersheds with varying geospatial, eco-hydrological, and climate conditions.

In order to study snow drought and GW drought characteristics and their connection and propagation mechanism at a regional scale, a coupled surface water (SW)-GW hydrological modelling framework is inevitable. A physical and process-based SW-GW model can facilitate the simulation of snow accumulation, snowmelt, evapotranspiration, and soil water content (Neitsch et al., 2011), as well as GW recharge and GW flow. The Soil and Water Assessment Tool (SWAT) hydrologic model (Arnold, J., Kiniry, R., Williams, E., Haney, S., Neitsch, 2012; Neitsch et al., 2011) and the MODFLOW model (Harbaugh, 2005) are widely-used process-based tools to simulate surface and groundwater processes at various geographical scales (Abbaspour et al., 2015; Bailey et al., 2016; Faramarzi et al., 2015; Schuol et al., 2008; Tanachaichoksirikun et al., 2020; Wu et al., 2013; Baily et al., 2016). The SWAT and MODFLOW models were recently coupled through a user-friendly interface that facilitates SW-GW modelling for eco-hydro(geo)logical studies at a regional scale (Baily et al., 2016). While effectiveness of these models have been reported in numerous studies, similar to many regional-scale studies, these models are subject to several sources of uncertainties. The major drawback of process-based SW-GW modelling at a

regional scale is the insufficient input data availability which can result in simulation uncertainty (Bailey et al., 2016; Barthel & Banzhaf, 2016; Candela et al., 2014; Faramarzi et al., 2015a; Refsgaard et al., 2010). For example, Faramarzi et al (2015) developed a regional hydrologic model including all of the main watersheds of the province of Alberta, Canada, which required climate data including precipitation, temperature, relative humidity, wind speed and solar radiation; and topographic and geospatial data including DEM (digital elevation model), land cover and soil type, as well as management data including reservoir operation. The study addressed the inevitable model uncertainty related to model input data, especially at large regional studies, and concluded that a careful data discrimination process prior to model development is required. Also, Bailey et al (2016) assessed SW-GW interaction using a coupled SWAT-MODFLOW model at a regional scale, and investigated model inputs, such as soil hydraulic conductivity, specific yield, specific storage, geologic formation, and GW observation well data, and argued that insufficient data can cause model uncertainty. Although the process-based models are capable of simulating various physical processes involved in snow and GW hydrology, the extensive requirement of input data is not often available for large study areas, especially in the mountainous region where access of climate data is difficult. Subsequently, an uncertainty assessment in model calibration is often suggested (K. C. Abbaspour et al., 2015; K. C. Abbaspour et al., 2017; Faramarzi et al., 2015).

In this research, the North Saskatchewan River Basin (NSRB) with a drainage area of around 59000 km² in central Alberta, Canada, was selected as a study area. The SWAT hydrologic model was coupled with MODFLOW groundwater model, through the most recently developed interface (Bailey & Park, 2019). The SWAT and MODFLOW models of NSRB were calibrated and validated based on monthly streamflow data available from 13 hydrometric stations and monthly GW head data available from 20 observational wells for the 1983-2007 period, and uncertainty

analysis was performed. The model outputs were then used for assessment of snow and GW drought characteristics and their propagation mechanism in three different EHG regions of the NSRB including Mountains, Foothills, and Plains. Mountains contains the headwater of the entire NSRB, with multiple mountain glaciers and covers a portion of Rocky Mountain area. Foothills exhibits alpine environment, with large area of boreal forests and parkland ecosystems. Plains mainly consists of agricultural land, pasture and urban regions among other land cover types.

Overall, the results of this research provide insights for water management and planning in snow-dominated regions such as Canadian watersheds. This is partly because, snowmelt during the warming season can contribute a significant portion of the annual water cycle to river networks and open water bodies, supplying water for industrial, agricultural or municipal sectors (T. P. Barnett et al., 2008; Corriveau et al., 2011; Gray & Landine, 1988; Qin et al., 2020; Wang et al., 2022). Studies have reported that snowmelt supplies freshwater to more than one-sixth of the global population (T. P. Barnett et al., 2005; Huning & AghaKouchak, 2020). On the other hand, GW, as one of the prominent entities of the hydrosphere, provides resilience to several water use sectors as well as the environment and ecosystem during drought events (Hughes et al., 2012; Mussá et al., 2015). Given the connectivity of surface and groundwater hydrologic processes (Han et al., 2019; Pathak & Dodamani, 2021; Yeh, 2021), and the predicted drought impacts (Beran & Rodier, 2020; Castle et al., 2014; Dierauer et al., 2021; Svoboda et al., 2002), assessment of snow and GW droughts, and their relationships can inform management and planning of water resources. The results and conclusions from this study can also help with informed decisions for developing adaption strategies to projected global warming effects in the future.

1.2. Research Objectives

The overarching goal of this Master of Science thesis is to understand the snow drought and GW drought characteristics, their changes under global warming scenarios, and their interconnection and propagation mechanism, including propagation time and dominant physical processes at a regional scale. This is achieved by implementing a process-based SW-GW modelling framework and statistical analysis of the model outputs. To achieve the main goal, the below specific objectives were designed and tested in different EHG regions of the NSRB, including Mountains, Foothills, and Plains:

1. Develop, calibrate, and validate SWAT surface water model and MODFLOW groundwater model, and couple these models into SWAT-MODFLOW modelling framework, to simulate historical (1980-2013) and future (2040-2073) snow water equivalent (SWE) and groundwater level time series, as well as the time series of key physical processes, such as evapotranspiration, snowmelt, soil water content, or percolation, that drives snow and GW changes in Mountains, Foothills, and Plains.
2. Determine snow drought and GW drought characteristics, including their intensity, duration, and frequency for both study periods, and assess the spatiotemporal variation of each type of droughts under different EHG settings.
3. Assess response time of GW to changes in SWE and determine the physical processes driving their feedback mechanism in different EHG regions and under historical and future scenarios.

1.3. Thesis structure

Chapter 2 is the main body of this research prepared in a paper format to be submitted for publication in a peer-reviewed journal. This chapter provides description of the study area, various

input data used for model development and simulations under historical and future scenarios. It introduces the detailed development, calibration-validation and verification analysis of SWAT and MODFLOW models, and their coupling process. It provides a description of the state-of-the-art approaches used for snow and GW drought assessment, and their intensity, duration, and frequency assessments. Details of the statistical techniques for assessment of drought propagation mechanism and response time are explained. Finally, the study implications, its assumption, and caveats are discussed, followed by providing future directions.

Chapter 3 is the general summary of previous chapter and then the drawing of general conclusion for future snow drought and GW drought assessments and their relationships, which is followed by discussion of the implication for future water resource adaptation and mitigation measures.

1.4. References

- Abbaspour, K. C., Rouholahnejad, E., Vaghefi, S., Srinivasan, R., Yang, H., & Kløve, B. (2015). A continental-scale hydrology and water quality model for Europe: Calibration and uncertainty of a high-resolution large-scale SWAT model. *Journal of Hydrology*, 524, 733–752. <https://doi.org/10.1016/j.jhydrol.2015.03.027>
- Abbaspour, K. C., Vaghefi, S. A., & Srinivasan, R. (2017). A guideline for successful calibration and uncertainty analysis for soil and water assessment: A review of papers from the 2016 international SWAT conference. *Water (Switzerland)*, 10(1). <https://doi.org/10.3390/w10010006>
- Ajami, H., Meixner, T., Dominguez, F., Hogan, J., & Maddock, T. (2012). Seasonalizing Mountain System Recharge in Semi-Arid Basins-Climate Change Impacts. *Ground Water*, 50(4), 585–597. <https://doi.org/10.1111/j.1745-6584.2011.00881.x>
- Arnold, J., Kiniry, R., Williams, E., Haney, S., Neitsch, S. (2012). *Soil & Water Assessment Tool, Texas Water Resources Institute-TR-439*.
- Bailey, R. T., & Park, S. (2019). *SWAT-MODFLOW Tutorial—Documentation for Preparing and Running SWAT-MODFLOW Simulations*.

- Bailey, R. T., Wible, T. C., Arabi, M., Records, R. M., & Ditty, J. (2016). Assessing regional-scale spatio-temporal patterns of groundwater–surface water interactions using a coupled SWAT-MODFLOW model. *Hydrological Processes*, 30(23), 4420–4433. <https://doi.org/10.1002/hyp.10933>
- Barnett, T. P., Adam, J. C., & Lettenmaier, D. P. (2005). Potential impacts of a warming climate on water availability in snow-dominated regions. *Nature*, 438(7066), 303–309. <https://doi.org/10.1038/nature04141>
- Barnett, T. P., Pierce, D. W., Hidalgo, H. G., Bonfils, C., Santer, B. D., Das, T., Bala, G., Wood, A. W., Nozawa, T., Mirin, A. a, Cayan, D. R., & Dettinger, M. D. (2008). Human-Induced Changes United States. *Science*, 319(February), 1080–1083.
- Barthel, R., & Banzhaf, S. (2016). Groundwater and Surface Water Interaction at the Regional-scale – A Review with Focus on Regional Integrated Models. *Water Resources Management*, 30(1), 1–32. <https://doi.org/10.1007/s11269-015-1163-z>
- Beran, M. ., & Rodier, J. . (1985). Hydrological aspects of drought: a contribution to the International Hydrological Programme. In *Studies and Reports in Hydrology* (Vol. 39, p. 149). UNESCO-WMO.
- Bloomfield, J. P., & Marchant, B. P. (2013). Analysis of groundwater drought building on the standardised precipitation index approach. *Hydrology and Earth System Sciences*, 17(12), 4769–4787. <https://doi.org/10.5194/hess-17-4769-2013>
- Bloomfield, J. P., Marchant, B. P., Bricker, S. H., & Morgan, R. B. (2015). Regional analysis of groundwater droughts using hydrograph classification. *Hydrology and Earth System Sciences*, 19(10), 4327–4344. <https://doi.org/10.5194/hess-19-4327-2015>
- Castle, S. L., Thomas, B. F., John T. Reager, M. R., & Sean C. Swenson, J. S. F. (2014). future water security of the Colorado River Basin. *Geophysical Research Letters*, 41, 5904–5911. <https://doi.org/10.1002/2014GL061055>.Received
- Candela, L., Elorza, F. J., Tamoh, K., Jiménez-Martínez, J., & Aureli, A. (2014). Groundwater modelling with limited data sets: The Chari-Logone area (Lake Chad Basin, Chad). *Hydrological Processes*, 28(11), 3714–3727. <https://doi.org/10.1002/hyp.9901>
- Corriveau, J., Chambers, P. A., Yates, A. G., & Culp, J. M. (2011). Snowmelt and its role in the hydrologic and nutrient budgets of prairie streams. *Water Science and Technology*, 64(8), 1590–1596. <https://doi.org/10.2166/wst.2011.676>
- Dierauer, J. R., Allen, D. M., & Whitfield, P. H. (2019). Snow Drought Risk and Susceptibility in the Western United States and Southwestern Canada. *Water Resources Research*, 55(4), 3076–3091. <https://doi.org/10.1029/2018WR023229>

- Dierauer, J. R., Allen, D. M., & Whitfield, P. H. (2021). Climate change impacts on snow and streamflow drought regimes in four ecoregions of British Columbia. *Canadian Water Resources Journal*, 46(4), 168–193. <https://doi.org/10.1080/07011784.2021.1960894>
- Earman, S., Campbell, A. R., Phillips, F. M., & Newman, B. D. (2006). Isotopic exchange between snow and atmospheric water vapor: Estimation of the snowmelt component of groundwater recharge in the southwestern United States. *Journal of Geophysical Research Atmospheres*, 111(9), 1–18. <https://doi.org/10.1029/2005JD006470>
- Faramarzi, M., Srinivasan, R., Iravani, M., Bladon, K. D., Abbaspour, K. C., Zehnder, A. J. B., & Goss, G. G. (2015). Setting up a hydrological model of Alberta: Data discrimination analyses prior to calibration. *Environmental Modelling and Software*, 74, 48–65. <https://doi.org/10.1016/j.envsoft.2015.09.006>
- Fendeková, M., & Fendek, M. (2012). Groundwater drought in the nitra river basin - Identification and classification. *Journal of Hydrology and Hydromechanics*, 60(3), 185–193. <https://doi.org/10.2478/v10098-012-0016-1>
- Han, Z., Huang, S., Huang, Q., Leng, G., Wang, H., Bai, Q., Zhao, J., Ma, L., Wang, L., & Du, M. (2019). Propagation dynamics from meteorological to groundwater drought and their possible influence factors. *Journal of Hydrology*, 578(September). <https://doi.org/10.1016/j.jhydrol.2019.124102>
- Harbaugh, A. W. (2005). *MODFLOW-2005: the U.S. Geological Survey modular groundwater model - the groundwater flow process*. <https://doi.org/10.3133/tm6A16>
- Harpold, A. A., & Kohler, M. (2017). Potential for Changing Extreme Snowmelt and Rainfall Events in the Mountains of the Western United States. *Journal of Geophysical Research: Atmospheres*, 122(24), 13,219–13,228. <https://doi.org/10.1002/2017JD027704>
- Hatchett, B. J., & McEvoy, D. J. (2018). Exploring the origins of snow drought in the northern sierra nevada, california. *Earth Interactions*, 22(2), 1–13. <https://doi.org/10.1175/EI-D-17-0027.1>
- Hatchett, B. J., Rhoades, A. M., & Mcevoy, D. J. (2021). *Monitoring the Daily Evolution and Extent of Snow Drought*. July, 1–29.
- He, Z., Liang, H., Yang, C., Huang, F., & Zeng, X. (2018). Temporal–spatial evolution of the hydrologic drought characteristics of the karst drainage basins in South China. *International Journal of Applied Earth Observation and Geoinformation*, 64(August 2017), 22–30. <https://doi.org/10.1016/j.jag.2017.08.010>
- Huang, J., Cao, L., Yu, F., Liu, X., & Wang, L. (2021). Groundwater Drought and Cycles in Xuchang City, China. *Frontiers in Earth Science*, 9(September), 1–13. <https://doi.org/10.3389/feart.2021.736305>

- Hughes, J. D., Petrone, K. C., & Silberstein, R. P. (2012). Drought, GW storage and stream flow decline in southwestern Australia. *Geophysical Research Letters*, 39(3), 1–6. <https://doi.org/10.1029/2011GL050797>
- Huning, L. S., & AghaKouchak, A. (2020). Global snow drought hot spots and characteristics. *Proceedings of the National Academy of Sciences of the United States of America*, 117(33), 19753–19759. <https://doi.org/10.1073/PNAS.1915921117>
- IPCC. (2022). Climate Change 2022 - Mitigation of Climate Change - Working Group III. Cambridge University Press, 1454. <https://www.ipcc.ch/site/assets/uploads/2018/05/uncertainty-guidance-note.pdf>.%0Awww.cambridge.org
- IPCC. (2022). Summary for Policymakers: Climate Change 2022_ Impacts, Adaptation and Vulnerability_Working Group II contribution to the Sixth Assessment Report of the Intergovernmental Panel on Climate Change. In *Working Group II contribution to the Sixth Assessment Report of the Intergovernmental Panel on Climate Change*. <https://doi.org/10.1017/9781009325844>.Front
- Lee, J. M., Park, J. H., Chung, E., & Woo, N. C. (2018). Assessment of groundwater drought in the Mangyeong River Basin, Korea. *Sustainability (Switzerland)*, 10(3). <https://doi.org/10.3390/su10030831>
- Li, B., & Rodell, M. (2015). Evaluation of a model-based groundwater drought indicator in the conterminous U.S. *Journal of Hydrology*, 526, 78–88. <https://doi.org/10.1016/j.jhydrol.2014.09.027>
- Liu, X., Zhu, X., Pan, Y., Li, S., Liu, Y., & Ma, Y. (2016). Agricultural drought monitoring: Progress, challenges, and prospects. *Journal of Geographical Sciences*, 26(6), 750–767. <https://doi.org/10.1007/s11442-016-1297-9>
- Masud, M. B., Khaliq, M. N., & Wheeler, H. S. (2015). Analysis of meteorological droughts for the Saskatchewan River Basin using univariate and bivariate approaches. *Journal of Hydrology*, 522, 452–466. <https://doi.org/10.1016/j.jhydrol.2014.12.058>
- Mussá, F. E. F., Zhou, Y., Maskey, S., Masih, I., & Uhlenbrook, S. (2015). GW as an emergency source for drought mitigation in the Crocodile River catchment, South Africa. *Hydrology and Earth System Sciences*, 19(2), 1093–1106. <https://doi.org/10.5194/hess-19-1093-2015>
- National Oceanic and Atmospheric Administration. (2018). Snow drought. Drought.gov. <https://www.drought.gov/what-is-drought/snow-drought>. (accessed 3.12.20).
- Neitsch, S. ., Arnold, J. ., Kiniry, J. ., & Williams, J. . (2011). Soil & Water Assessment Tool Theoretical Documentation Version 2009. *Texas Water Resources Institute*, 1–647. <https://doi.org/10.1016/j.scitotenv.2015.11.063>

- Pathak, A. A., & Dodamani, B. M. (2021). Connection between Meteorological and Groundwater Drought with Copula-Based Bivariate Frequency Analysis. *Journal of Hydrologic Engineering*, 26(7), 05021015. [https://doi.org/10.1061/\(asce\)he.1943-5584.0002089](https://doi.org/10.1061/(asce)he.1943-5584.0002089)
- Pendergrass, A. G., Meehl, G. A., Pulwarty, R., Hobbins, M., Hoell, A., AghaKouchak, A., Bonfils, C. J. W., Gallant, A. J. E., Hoerling, M., Hoffmann, D., Kaatz, L., Lehner, F., Llewellyn, D., Mote, P., Neale, R. B., Overpeck, J. T., Sheffield, A., Stahl, K., Svoboda, M., ... Woodhouse, C. A. (2020). Flash droughts present a new challenge for subseasonal-to-seasonal prediction. *Nature Climate Change*, 10(3), 191–199. <https://doi.org/10.1038/s41558-020-0709-0>
- Qin, Y., Abatzoglou, J. T., Siebert, S., Huning, L. S., AghaKouchak, A., Mankin, J. S., Hong, C., Tong, D., Davis, S. J., & Mueller, N. D. (2020). Agricultural risks from changing snowmelt. *Nature Climate Change*, 10(5), 459–465. <https://doi.org/10.1038/s41558-020-0746-8>
- Refsgaard, J. C., Højberg, A. L., Møller, I., Hansen, M., & Søndergaard, V. (2010). Groundwater modeling in integrated water resources management - visions for 2020. *Ground Water*, 48(5), 633–648. <https://doi.org/10.1111/j.1745-6584.2009.00634.x>
- Sheffield, J., & Wood, E. . (2011). Drought: Past Problems and Future Scenarios, Earthscan, London, UK, Washington DC, USA
- Shrestha, R. R., Bonsal, B. R., Bonnyman, J. M., Cannon, A. J., & Najafi, M. R. (2021). Heterogeneous snowpack response and snow drought occurrence across river basins of northwestern North America under 1.0°C to 4.0°C global warming. *Climatic Change*, 164(3–4), 1–21. <https://doi.org/10.1007/s10584-021-02968-7>
- Staudinger, M., Stahl, K., & Seibert, J. (2014). *A drought index accounting for snow*. 5375–5377. <https://doi.org/10.1002/2013WR014979.Reply>
- Stocker, T. ., Qin, D., Plattner, G.-K., Tignor, M., Allen, S. ., Boschung, J., Nauels, A., Xia, Y., Bex, V., & Midgley, P. . (2013). Climate Change 2013: The Physical Science Basis. Contribution of Working Group I to the Fifth Assessment Report of the Intergovernmental Panel on Climate Change. In *Cambridge University Press*.
- Svoboda, M. D., LeComte, D., Hayes, M., Heim, R., & Gleason, K. (2002). The Drought Monitor. In *Bull. Amer. Meteorol. Soc* (pp. 1181–1190).
- Tanachaichoksirikun, P., Seeboonruang, U., Fogg, G.E., 2020. Improving Groundwater Model in Regional Sedimentary Basin Using Hydraulic Gradients. *KSCE Journal of Civil Engineering* 24, 1655–1669. <https://doi.org/10.1007/s12205-020-1781-8>
- United States Geological Survey. (2016). USGS: Groundwater and Drought. <https://water.usgs.gov/ogw/drought/#:%7E:text=A%20groundwater%20drought%20typically%20refers,for%20humans%20and%20the%20environment>. (accessed 3.12.20).

- Van Lanen, H. A. J., & Peters, E. (2000). *Definition, Effects and Assessment of Groundwater Droughts*. 49–61. https://doi.org/10.1007/978-94-015-9472-1_4
- Van Loon, A. F. (2015). Hydrological drought explained. *Wiley Interdisciplinary Reviews: Water*, 2(4), 359–392. <https://doi.org/10.1002/WAT2.1085>
- Van Loon, A. F., & Van Lanen, H. A. J. (2012). A process-based typology of hydrological drought. *Hydrology and Earth System Sciences*, 16(7), 1915–1946. <https://doi.org/10.5194/hess-16-1915-2012>
- Villholth, K. G., Tøttrup, C., Stendel, M., & Maherry, A. (2013). Integrated Mapping of Groundwater Drought Risk in the Southern African Development Community (SADC) region. *Hydrogeology Journal*, 21(4), 863–885. <https://doi.org/10.1007/s10040-013-0968-1>
- Wang, B., Guo, S., Feng, J., Huang, J., & Gong, X. (2022). Simulation on Effect of Snowmelt on Cropland Soil Moisture within Basin in High Latitude Cold Region Using SWAT. *Nongye Jixie Xuebao/Transactions of the Chinese Society for Agricultural Machinery*, 53(1), 271–278. <https://doi.org/10.6041/j.issn.1000-1298.2022.01.030>
- Wu, H., Chen, B., & Li, P. (2013). Comparison of sequential uncertainty fitting algorithm (SUFI-2) and parameter solution (ParaSol) method for analyzing uncertainties in distributed hydrological modeling - A case study. *Proceedings, Annual Conference - Canadian Society for Civil Engineering*, 4(January), 3453–3456.
- Wu, W. Y., Lo, M. H., Wada, Y., Famiglietti, J. S., Reager, J. T., Yeh, P. J. F., Ducharne, A., & Yang, Z. L. (2020). Divergent effects of climate change on future groundwater availability in key mid-latitude aquifers. *Nature Communications*, 11(1), 1–9. <https://doi.org/10.1038/s41467-020-17581-y>
- Yeh, H.-F. (2021). Spatiotemporal Variation of the Meteorological and Groundwater Droughts in Central Taiwan. *Frontiers in Water*, 3(February), 1–12. <https://doi.org/10.3389/frwa.2021.636792>

CHAPTER II – MANUSCRIPT 1

Modelling Impacts of Climate Change on Snow Drought, Groundwater Drought, and their Feedback Mechanism in a Snow Dominated Watershed in Western Canada

1. Introduction

Traditional drought categorization is approached from various meteorological, hydrological, agricultural, and socio-economical perspectives. Over the past few decades, however, novel types of drought categorization, including snow and groundwater droughts, have emerged. Groundwater (GW) drought can be defined based on changes in GW recharge, GW levels, and GW discharge over various timescales (Han et al., 2019). Snow drought is explained as a deficit in snow accumulation due to variation in temperature or precipitation or both (NOAA, 2018). Snow accumulation and GW resources are connected through soil-plant-water systems and within the hydrologic cycle (T. P. Barnett et al., 2005; Earman et al., 2006; Jódar et al., 2017; Lundberg et al., 2016; Meng et al., 2015). Various processes such as precipitation types (snow or rain), temperature, vegetation growth, evapotranspiration rates, runoff, and infiltration can define the extent of GW recharge and discharge, their rates, and their spatiotemporal dynamics (Hayashi & Rosenberry, 2002; Hayashi, 2020; Jódar et al., 2017; Paznekas & Hayashi, 2016). For mid-to-high latitude countries, snow accumulation usually contributes a large portion to surface water resources during melt seasons (USGS, 2019; Hayashi, 2020; DeBeer, 2012) and to GW resources through infiltration (Flerchinger et al., 1993). Snow accumulation in a region can be affected by changes in meteorological factors. It can fall below the long-term average, causing snow accumulation deficiencies and snow droughts (NOAA, 2018). Recent studies have reported that the frequency, duration, and intensity of droughts have increased due to global warming (Huning & AghaKouchak, 2020). Studies have also shown that the increasing trend in the impacts of climate change will likely amplify hydrologic processes such as changes in snow, rain, melt and runoff, infiltration, and GW recharge (Kriauciuniene et al., 2008), and as a result the feedback mechanisms between GW and surface water across time and space. Such changes can lead to consequent

changes in how droughts propagate from snow to GW. Therefore, assessing spatiotemporal variation in drought propagation patterns from snow to GW and their changes under historical and future scenarios of climate change becomes increasingly crucial, especially in mid-to-high latitude regions.

Snow drought, also defined as snow deficit, can be described as warm snow drought (WSD) or dry snow drought (DSD). WSD is a deficit of snow accumulation despite near-normal precipitation, caused by warm temperatures and precipitation falling as rain rather than snow or unusually early snowmelt. DSD is defined as a shortage of overall precipitation (NOAA, 2018). WSD can be affected by hydrologic and climatic factors, whereas DSD can be affected by climatic factors (Dierauer et al., 2019). Different processes related to hydrological cycle (e.g., evapotranspiration, soil moisture, snowmelt, and runoff), climate variation (e.g., wind speed, relative humidity, solar radiation, temperature, and precipitation type), and geospatial characteristics (e.g., landuse/landcover, surficial soil type in plant root zone, topography) determine the extent of SD across regions. These processes are referred to here as eco-hydro(geo)logical (EHG) processes. The EHG processes of watersheds determine how water moves, and they lead to spatial variations in hydrologic behavior, and therefore, snow accumulation or ablation and consequently GW and surface water interactions. Several studies have focused on revealing snow drought hotspots at different scales, such as the global-scale (Huning and Aghakouchak, 2020), regional scale (Dierauer et al., 2019), or local-scale watersheds (Van Loon et al., 2010; Kapnick et al., 2012; Dierauer et al., 2019). Many of these studies have emphasized the spatiotemporal variation of snow droughts. However, they do not identify the driving forces behind the formation of snow drought and how snow drought develops or evolves

under different EHG settings. Therefore, conclusions from these studies cannot be up-scaled or applied to other regions that have differing EHG conditions.

GW drought is a relatively new concept that typically refers to a period of decreased GW levels that results in insufficient water supply in GW-dependent regions, low water well yields, low spring flows, low based flows in the streams, and even a total dry-up of wells or rivers (USGS, 2016; Van Lanen & Peters, 2000; Huang et.al, 2021). Similar to snow drought variation, GW drought formation can also vary across spatiotemporal scales (Yeh, 2021). To date, multiple studies have focused on GW drought formation, providing various insights. Bloomfield et al. (2013) conducted a study across the entire UK. They depicted a wide range of unconfined consolidated aquifers, including a fractured limestone aquifer and chalk aquifer, described as dual porosity, dual permeability carbonate aquifers comprised of local karstic Permo-Triassic sandstone. They argued that in different sites in the UK, the GW drought trend shows similar broad scale structures across all sites. In contrast, Pathak & Dodamani (2019), researching western India, argued that GW drought is strongly affected by seasonal variations in precipitation patterns. For example, they found that nearly half of the study sites were experiencing GW level increases for a single pre-monsoon season, and the other half was going through GW level decreases at the same time due to diminishing rainfall or severe GW exploitation (Pathak & Dodamani, 2019). Comparison of the results of these studies (i.e., Bloomfield & Marchant, 2013; Pathak & Dodamani, 2019) indicate that geographic location, management factors, and the related EHG settings are crucial in determining the extent and scale of the GW drought variations.

Many studies have revealed a relationship between surface water and GW. Some studies pointed out that GW drought formation is mainly due to rainfall deficit (e.g., Pathak & Dodamani, 2019), which indicates communication between surface water and GW systems. The influence and

relationships between multiple variables, including short-term climate variation, glacial deposit types, surficial geology, and topography on the GW table and GW flow have been a topic of fewer studies (Hokanson et al., 2019; Bloomfield et.al, 2015). Topography was found to be a primary control of water table position and the scale of GW flow in some studies (Hokanson et al., 2019), whereas the main control for hydrologic connectivity between GW and surface water was reported to be precipitation and evapotranspiration in other studies (Han et al., 2019; Wu et.al, 2016). All these evidence explain why groundwater-surface water (GW-SW) interaction mechanisms can be spatially and temporally variable and they are driven by numerous factors affecting the hydrologic cycle in the region. However, the response time of GW levels to changes in surface water cycle (e.g., snowmelt and infiltration) can vary across spatial scales. A wide range of response times are reported, from 6 to 12 months accumulation time steps, meaning that for certain regions, it takes 6, 7, 8... 12 months for the GW table to change in response to surface water changes, including snow accumulation or rainfall precipitation quantity on the surface. The GW response to changes in surface water is as a result of changes in climate across different regions (Castle et al., 2014; Bloomfield et al., 2015; Pathak et.al, 2019), or hydrologic factors (Li & Rodell et.al, 2015). The differences in the reported response times is partially related to the scale of the study region (e.g., small plains catchments versus large watersheds originating from a mountain and ending in a river delta), and the EHG conditions of the study sites (e.g., coastal regions experiencing temperate oceanic climate versus sub-tropical regions experiencing monsoon climate). Therefore, it is imperative to consider that not only the surface processes (e.g., snow accumulation, snowmelt) and GW processes (e.g., GW recharge, GW discharge) themselves, but also the feedback mechanisms between them, are impacted by variations in the EHG settings. Noteworthy is that there is little information (e.g., how quick can GW variation response to SWE change) about the

factors (e.g., air temperature, soil temperature, water permeability of HRU) or physical drivers (e.g., soil moisture content, infiltration, evapotranspiration, etc.) that control these response mechanisms. Moreover, there is limited information how such response time will change under future global warming scenarios.

The overarching goal of this study is to fill this gap by assessing historical and future drought characteristics and propagation mechanisms from snow to GW in different EHG settings, taking the North Saskatchewan River Basin, a relatively large watershed in western Canada, as a study region. To achieve the main goal of this research, a coupled physical and process-based hydrological and hydrogeological model was used to simulate the most important physical drivers controlling GW and surface water interactions (GW-SW) under historical (1980-2013) and future (2040-2073) global warming scenarios. The simulated processes facilitated examination of the specific objectives of this research which are assessment of: (1) characteristics of historical and future snow drought under different EHG settings including Mountains, Foothills, and Plains; (2) characteristics of historical and future GW drought in various EHG settings; (3) propagation and response time of GW to changes in snow drought under historical and future scenarios; and (4) dominant physical processes controlling propagation of snow to GW droughts across different EHG regions.

2. Material and methods

2.1 Study area

The North Saskatchewan River Basin (NSRB) is located in central Alberta, Canada, and the head water tributaries are originated from several glaciers of Rocky Mountains in the west and

they collectively flow east to the Alberta-Saskatchewan border and ultimately draining into Hudson Bay after passing through Saskatchewan and Manitoba (Figure 1a). The NSRB is relatively a large watershed with a drainage area of about 59,000 km², comprising a heterogeneous geospatial and topographic conditions (North Saskatchewan Watershed Alliance, 2005). The entire watershed is climatically, hydrologically, and ecologically diverse, moving from mountain glaciers and rocky areas in the upstream (called mountains, hereafter); to alpine, boreal forests, and parkland ecosystems in the foothill regions (called foothills, hereafter); and ending with agricultural, pasture, and urban regions among other land cover types in the majority of downstream plain region of the watershed (called plains, hereafter) (North Saskatchewan River Alliance, 2005). Several glaciers of different sizes exist upstream in the Rocky Mountains, feeding tributaries to the North Saskatchewan River (NSR) such as Clearwater River, Ram River and North Ram River. These tributaries join the NSR in the foothills region, which cover evergreen needle leaf forests and other minor forests.

The NSRB elevation ranges from a maximum of 3478 m above mean sea level to a minimum of 480 m (Figure 1a). The watershed encompasses diverse land cover-land use types (Figure 1b). The major land cover in NSRB is agricultural land-row crops and pastures, followed by evergreen needle leaf forests and other minor forests. The total amount of grassland and shrub lands is greater than other land cover types, such as urban areas and wetlands. There are also two dams located on the upstream part of the watershed that regulate seasonal flow in the NSR (Figure 1 a,b). The Brazeau dam is located on the northern tributary in the mountains and the Bighorn dam sits on the southern tributary in the foothills. According to Government of Alberta River Basins database, the Bighorn dam releases larger volumes of water than the Brazeau dam (Government of Alberta, 2021). The flow from these reservoirs is essential in maintaining consistent flow in the downstream

river, especially during the cold season, to protect the mainstream from very low flow that might cause ecological issues, such as impacts to aquatic life or insufficient water supply for downstream water users.

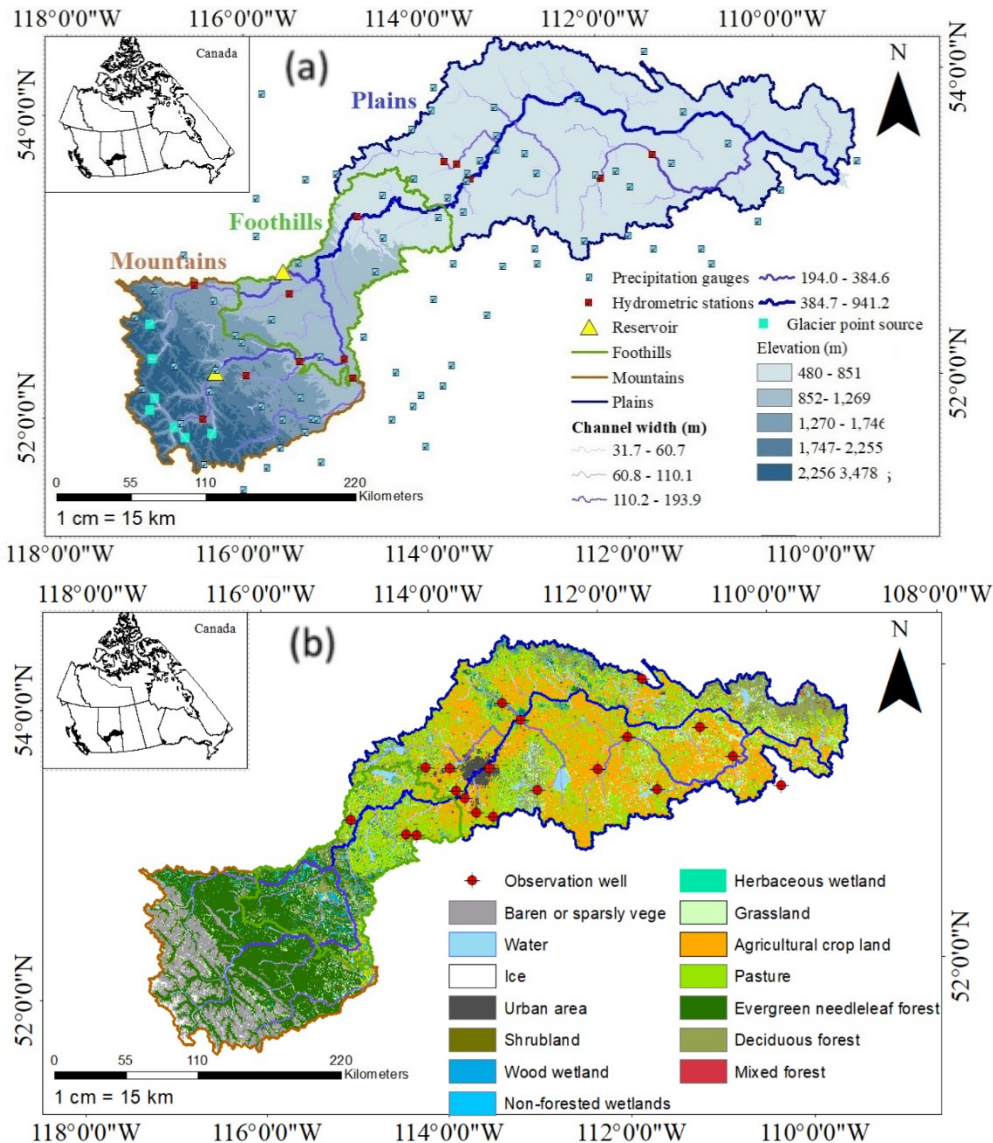


Figure 1. (a) Geographic extent of study area illustrating topographic information, hydrometric stations used for calibration of streamflow, climate stations used for model input, and the three Eco-hydro(geo)logical (EHG) regions. (b) North Saskatchewan River Basin Land Cover-Land Use Information and location of GW observation wells.

There is no dominant soil type in the North Saskatchewan River Basin, but several major soil types were discovered in the Agriculture Agri-Food Canada, Soil Landscapes of Canada

database (AAFC, 2011). According to the soil database, loam and clay loam near downstream areas and silty loam on the upstream area are common types of soil texture. Historical climate data for the NSRB suggests that during 1980-2010, the historical high and low temperature can range from -30°C in the winter to +30 °C in the summer (Government of Canada, 2020), with annual total precipitation ranging from 800 mm at upstream mountainous regions to almost 500 mm in downstream plains regions (Government of Alberta, 2012). MacDonald et.al (2012) argued that even though little change in annual maximum snow water equivalent accumulation is observed in the NSRB, early snowmelt in spring would occur under the existing climate change pattern, and the rainfall proportion of precipitation will prevail as compared to the snow proportion (MacDonald et al., 2012). Sauchyn et al. (2020) noted that GW in NSRB is prone to changes in precipitation and mean temperature, and is controlled by inter-decadal climate oscillations, with unconfined aquifers and confined aquifers exhibiting different behaviors. In unconfined aquifers, the groundwater level is positively related to mean air temperature, whereas in confined aquifers, the groundwater level is inversely related to mean air temperature (Sauchyn et al., 2020).

2.2 Data

2.2.1 Input data for hydrology and snow simulator (SWAT)

Soil and Water Assessment Tool (SWAT) is a semi-distributed, process-based hydrologic model that has been widely applied to simulate water quantity and water quality at various scales from small catchment to large continents (Faramarzi et al., 2017; Abbaspour et al., 2015; Staudinger et al., 2014; Teshager et al., 2016). To develop a SWAT model of the NSRB, various input data were obtained, processed, and reformatted (see Table S1), including climate data that involves precipitation, maximum and minimum temperature, solar radiation, relative humidity and wind speed. Historical precipitation, temperature, solar radiation, wind speed and relative humidity

data quality have been retrieved and validated by Faramarzi et al. (2015, 2017), which are in various formats including gauged data from weather stations and gridded data for the production of historical streamflow throughout the province of Alberta. Hydrologic response units (HRUs) are small units of larger sub basins that are delineated using topographic maps and characterized based on land use-land cover and soil properties, and slope classes in the study watershed (Arnold et al., 2012). Using a DEM data of 10m×10m the stream network were carefully delineated in an earlier work (Faramarzi et al., 2015, 2017). This pre-delineated stream network and a DEM of 90m×90m were used as an input to the SWAT model to delineate a total of 174 sub basins for the NSRB. In order to characterize soil properties for water balance simulation, the SWAT model uses a total of 24 physical parameters including the number of soil layers, including dominant hydrologic groups, soil depths, soil bulk density, soil saturated hydraulic conductivity and others which are assigned to each specified soil layer. These physical properties used by SWAT, govern the movement of water and air through soil profiles, and impact water cycling within each soil layer and in spatial units (Arnold et al., 2012). All data involved in SWAT model of NSRB is displayed in Table S1.

For future projections of the hydrological cycle, GW levels, and snow processes, the climate data were incorporated from an ensemble of five Global Climate Models (GCMs) of the Coupled Model Inter-comparison Project Phase 6 (CMIP6) including BCC-CSM2-MR, CNRM-CM6-1, EC-Earth3, EC-Earth3-veg and MRI-ESM2.0 (Table S2) (Eyring et al., 2016). Based on an earlier study by Masud et al. (2021), the future climate data were statistically downscaled based on historical daily gridded climate data from WFDEI [GPCC] (Weedon et al., 2014) at roughly 0.5° grid resolution for all of Alberta watersheds. We used the GCMs' simulated data based on two contrasting Shared Socio-economic Pathways, SSP126 and SSP585. The major difference between

these two scenarios is the minimum and maximum radiative forcing levels projected for the year 2100 based on IPCC Assessment Report 6 scenarios (O'Neill et al., 2016). Nevertheless, for hydrologic model simulation two levels of atmospheric carbon dioxide, i.e., 400 ppmv CO₂ for SSP126 and 700 ppmv CO₂ SSP585 scenarios, were set based on available data from IPCC (2022). The timespan for future climate data is consistent with that of historical, which ranges from 2040 to 2073.

2.2.2 Input data for MODFLOW GW simulator

To setup the MODFLOW model of the NSRB, five vertical layers were used, each corresponding to a specific geologic formation in the study region. Information about geologic units and their physical properties, including hydraulic conductivity and storability, are required to setup MODFLOW model. Corresponding elevation data, as well as hydraulic properties for each layer were obtained from the Alberta Geologic Survey (Alberta Geological Survey, 2019). For horizontal hydraulic conductivity, the maximum and minimum values for each formation were obtained from a previous study conducted using borehole tests in west-central Alberta (Smerdon et al., 2017). Table S3 displays the bedrock geologic formation name and properties acquired from Zaremehrijardy et al (2022). Due to the limitations in the availability of the geologic formations in the western mountainous region, they assumed to be a constant values based on western-most available elevation data. In order to allow GW flow to occur in the mountainous region, this assumption was necessary.

The model setup requires designating boundary conditions (i.e. time series river level and GW recharge data for a simulation period) as well as initial hydraulic heads to describe the exchange between GW model and external system, such as streams or water bodies. The boundary conditions are needed to achieve a numerical solution, and are used to calculate water flows

coming into or out of the model area due to external factors, such as lakes, streams, recharge, evapotranspiration and wells (Langevin et al., 2017). The initial hydraulic head are simulated through MODFLOW by allowing for equilibrium with river and recharge boundary conditions (Bailey et al., 2016). Once equilibrium is achieved, these initial hydraulic heads can be used to represent the initial conditions, and then will be utilized to develop the coupled SWAT-MODFLOW model, which can be further used to analyze snow water - GW interactions.

2.3 Surface water and GW modeling

2.3.1 SWAT model and calibration – validation procedure

SWAT model solves a soil water balance equation and it can simulate various hydrologic processes including surface runoff, snow accumulation, snowmelt, GW recharge, evapotranspiration, soil moisture, plant growth and transpiration, and soil temperature for each spatial unit, among other processes (Neitsch et al., 2011). Snow simulation in the SWAT model requires various input parameters to initiate the modelling procedure as follows:

$$SNO_{day} = SNO_{day-1} + R_{day} - E_{sub} - SNO_{melt} \quad (1)$$

Where, SNO is the total water content of the snow pack on a given day (mm H₂O), SNO_{day-1} is the water content of the snow pack of the previous day, E_{sub} is the amount of sublimation on a given day (mm H₂O), SNO_{melt} is the amount of snowmelt on a given day (mm H₂O), and R_{day} (mm), is snow precipitation, and is only added when the average atmospheric temperature is below a threshold temperature (T_{thr}) (Neitsch et al., 2011). The snow cover component of SWAT allows non-uniform cover due to shading, drifting, topography and land cover. The user defines a threshold snow depth above which snow coverage will always extend over 100% of the area. As

the snow depth in an HRU decreases below this value, the snow coverage is allowed to decline non-linearly based on an area depletion curve.

Snowmelt is controlled by snow temperature, melting factor, as well as areal coverage of snow, which is then further controlled by the atmospheric temperature and a snow temperature lag factor that represents the degree to which mean air temperature influences snowpack temperature:

$$SNO_{melt} = b_{melt} \cdot sno_{cov} \cdot \left[\frac{T_{snow} + T_{mx}}{2} - SMTMP \right] \quad (2)$$

Where, SNO_{melt} is the amount of snowmelt on a given day (mm H₂O), b_{melt} is the melt factor of the day (mm H₂O day⁻¹ °C), SNO_{cov} is the fraction of HRU area that is covered by snow, T_{snow} is the snowpack temperature on a given day (°C), T_{mx} is the maximum daily air temperature (°C), and $SMTMP$ is the threshold temperature at which the snowmelt will occurs (°C). In this equation, T_{snow} is a function of the lag factor and atmospheric temperature, as well as the previous days snow temperature, and b_{melt} is melt factor that is calculated from below formula, where $SMFMX$ and $SMFMN$ are melt factors for June 21st and December 21st respectively, and d_n is day number of the year (Neitsch et al., 2011).

$$b_{melt} = \frac{SMFMX + SMFMN}{2} + \frac{SMFMX - SMFMN}{2} \cdot \sin\left(\frac{2\pi}{365} \cdot (d_n - 81)\right) \quad (3)$$

Due to the spatial variability within each HRU, especially in mountainous region where elevation change is sharp, five elevation bands within each HRU were applied in the SWAT model. Elevation bands are used to divide the sub-basins into different zones based on elevation, leading to model discretization of hydrological processes based on sub-basin topography (Pradhanang et al., 2011). SWAT model defines temperature and precipitation within each band by using following equations:

$$P_B = P_{st} + (Z_B - Z_{st}) \times PLAPS \times 10^{-3} \quad (4)$$

$$T_B = T_{st} + (Z_B - Z_{st}) \times TLAPS \times 10^{-3} \quad (5)$$

where P_B is the precipitation band within the particular elevation band (mm), P_{st} is total precipitation recorded at station (mm), Z_B is the midpoint of the elevation band (m), Z_{st} is the station elevation (m), T_B is the temperature within the elevation band ($^{\circ}C$), T_{st} is the temperature recorded at station ($^{\circ}C$), PLAPS is the precipitation lapse rate (mm/km) and TLAPS is temperature lapse rate ($^{\circ}C/km$), where lapse rate represents the precipitation loss and temperature decrease due to increasing elevation (Rahman et al., 2013). In this study, TLAPS and PLAPS were optimized through calibration and uncertainty assessment procedure (see following sections).

For calibration of the SWAT model, SUFI2 algorithm of the SWATCUP software was used (Abbaspour et al., 2015). Various parameters that are sensitive to snowmelt and streamflow simulation were selected from literature review (Neitsch et al., 2011; Faramarzi et al., 2017). An initial range for each parameter was assigned, and they were modified by examining 1000 parameter set samples drawn using Latin Hypercube Sampling technique, which is embodied in SUFI2 program. The SWAT hydrologic model was forced using each of the parameter sets and at least three performance statistics for each simulation were calculated, which included bR^2 value, *r-factor*, and *p-factor*. The bR^2 is calculated based on R^2 and b slope of the measured and simulated variables (e.g., monthly streamflow). The *r-factor* and *p-factor* are used to assess model uncertainty and performance in reproducing historical observations. The *r-factor* varies from 0 to ∞ and represents the model uncertainty range, for which a value of 1.0-1.5 is considered satisfactory in regional modeling. The *p-factor* is the fraction of observed data bracketed within model prediction uncertainty range, varies from 0 to 1 (Abbaspour et al., 2015). The calibration of the SWAT model is completed through several iterations to refine parameter ranges until the

optimal range for the parameter combination is achieved for certain period. Once calibration goal is achieved, the calibrated parameters are utilized to another time period for validation purposes. This study utilizes monthly streamflow observations at 13 hydrometric gauges in NSRB for streamflow calibration for the 1991-2013 period (Figure 1).

The calibrated and validated model was forced to simulate snow depth for verification of the model in SWE simulations. The weighted average snow depth in each EHG region was calculated based on the area of each sub-basin (Mountains, Foothills, and Plains), and then was compared with observed snow depth within that region. The model simulated Snow Water Equivalent (SWE) were converted to snow depth using a snow density function that was suggested for Canadian Prairies (Pomeroy et al., 1998). Finally, the snow depth was calculated as:

$$SNO_d = \frac{SNO}{S_d} \quad (6)$$

Where, SNO_d is the snow depth for day t (mm), and S_d is the snow density (g cm^{-3}).

However, the goal of this research is not streamflow projection but the effects of snow drought on GW drought and the propagation mechanism through landscape processes.

2.3.2 MODFLOW model and calibration – validation procedure

MODFLOW is a physically based GW model that utilizes a Finite Difference method to solve Darcy's equation for GW flow and calculate hydraulic head fluctuations in multiple saturated subsurface layers (Langevin et al., 2017). It is able to simulate multiple GW hydrologic processes, including GW recharge and discharge, vadose zone percolation, pumping, GW level variation, and water exchange between river and aquifer, i.e., GW-SW interactions (Bailey et al., 2016). The NSRB MODFLOW model was developed using Visual MODFLOW Flex 6.0 (Waterloo Hydrogeologic, 2018) and Newton's formulation (Niswonger, 2011) that can resolve wetting and

drying issues for each MODFLOW cell (Bailey et al., 2016). The total area covered for GW simulation was 181,500m² in order to cover the entire NSRB and to capture GW movement from the mountains to the prairies. The spatial resolution of the model was 10km×10 km and the layout of the model was 55 rows×33 columns (Zaremehrijardy et al., 2022).

MODFLOW calibration involves the adjustment of many input parameters, including horizontal hydraulic conductivity, ratio of horizontal to vertical hydraulic conductivity, and storativity parameters including specific storage and specific yield across the NSRB (Domenico & Mifflin, 1965; Heath, 1983; Morris & Johnson, 1967). Within each geologic layer, horizontal hydraulic conductivity and its ratio to vertical hydraulic conductivity value were initially adapted from Zaremehrijardy et al. (2022), where initial hydraulic conductivity was obtained from previous borehole studies (Smerdon et al., 2017), and the initial ratio of horizontal to vertical hydraulic conductivity were obtained from several studies (Chen et al., 2017; Tanachaichoksirikun et al., 2020). Similar to Zaremehrijardy et al. (2022) we used a pseudo-SUFI2 algorithm to sample 1000 sets of horizontal hydraulic conductivity as well as their ratio to vertical hydraulic conductivity. For the validation of MODFLOW model, we used simulated hydraulic heads and compared them to observed hydraulic heads from 20 observation wells for the 1983-2007 period. For evaluation of model results we used R², Mean Absolute Error (MAE), and Normalized Root Mean Squared Error (NRMSE), and ideally, these values should be 1, 0, and 0 respectively (Chunn et al., 2019). The observation wells are mostly located in downstream regions (Foothills and Plains) and there is lack of data availability in mountainous region. However, due to the nature of mountainous region bedrock geology, which exhibits a low permeability, parameter values for bedrock geology in mountainous region was assumed based on a reasonable range (Zaremehrijardy et al., 2022).

The list of selected parameters for calibration of SWAT and MODFLOW models, and their initial and final optimized ranges are provided in Table S4-1 and Table S4-2. The calibrated SWAT surface model and MODFLOW GW model were further used to construct a coupled SWAT-MODFLOW model. The coupled model was used to simulate snow depth and GW level to perform drought analysis under historical and future scenarios.

2.4 Snow drought and GW drought calculation

Most drought studies use analytical approaches and parametric indices such as the Standardized Precipitation Index (SPI) (Thomas B. McKee, 1993) or the Standardized GW Index method (Bloomfield & Marchant, 2013). While these analytical approaches are advantageous in explicitly identifying drought characteristics, the definition of drought intensity is often arbitrary and dependent on the author's judgement (Thomas B. McKee, 1993). Here, to study drought characteristics for both GW drought and snow drought, an approach similar to SPI method was implemented, and two indices including of Snow Water Equivalent Index (SWEI) and Standardized GW Index (SGWI) were constructed. Overall, the SPI approach quantifies a given variable (i.e., SWE and GW levels, in this study) as standardized departure from a selected probability distribution function that models the raw data (i.e., simulated SWE or GW level in this study). The raw data are typically fitted to a best performing probability function distribution, and then transformed to a normal distribution to generate the SPI indices (i.e., SWEI and GWI, in this study). The constructed indices (i.e., SWEI and SGWI values) can be then interpreted as the number of standard deviations by which the observed anomaly deviates from the long-term mean (Thomas B. McKee, 1993). In this approach, negative index values indicate drought events and positive values indicate wet events.

The assessment of drought severity utilizes the US Drought Monitor D scale classification method to classify and characterize drought (Svoboda et al., 2002). This method characterizes drought from D0 to D4 (abnormally dry, moderately dry, severely dry, extremely dry, and exceptionally dry). Table S5 summarizes each drought event and their features (Svoboda et al., 2002).

To calculate standardized drought indices, a proper distribution method was selected using the L-moment ratio method, where five distribution methods, including Generalized Logistics (GLO), Generalized Normal (GNO), Generalized Extreme Value (GEV), Generalized Pareto (GPA) and Pearson Type III (PE3) were examined using simulated monthly SWE and GW level data (Masud et al., 2015; Hosking, 2022).

To fit simulated SWE and GW level data into a specific probability distribution, its parameters were computed using the R package “lmom” function “pelxxx” where “xxx” stands for any probability distribution being determined, e.g., Pearson Type III distribution or Log Normal distribution, for each month (Hosking J.R.M, 1996), and used to obtain the cumulative probability function using “cdfxxx” function (Hosking & Wallis, 1997). Finally, the calculated cumulative probability function was fitted into an inverse normal distribution to generate SWEI and SGWI. Both SWEI and SGWI are dimensionless values that were calculated based on different accumulation periods for both SWE and GW level data (i.e., 1 month, 2 month, ..., 12 month accumulated data). The accumulation period is any period of interest that quantifies the standardized surplus or deficit of precipitation (Pieper et al., 2020), and under this context, instead of using precipitation, we used SWE and GW head. The indices constructed based on different accumulated data can indicate whether for a certain period of time, the amount of snow or GW is in deficit or surplus condition. Using the data generated for different accumulation periods, we

also opted to quantify how long snow can accumulate on the surface before it affects the GW (see section 2.5). Both SWEI and SGWI can capture drought features, including drought intensity, duration, and frequency.

2.5 Assessment of propagation and response time

To determine the lag time for GW to respond the changes in SWE, the cross-correlation between simulated GW level time series and SWE time series was analyzed. Cross-correlation is a widely used method for the estimation of correlation between two variables at various lag times (Pathak & Dodamani, 2021). The cross-correlation between two time series can be examined graphically as a function of a lag “h”, where “h” is user defined arbitrary range of values indicating the lag time between two time series (Shumway and Stoffer, 2017). For example, consider the following relationship,

$$y_t = x_{t-h} + \omega_t \quad (7)$$

Where x_t is selected variables for examining their correlations with y_t , and ω_t is the white noise indicating random error between two time series. The model above indicates that x_t leads y_t for h units of time. Resulted cross-correlation function graph at $t=h$ displays a highest bar where the correlation between two time series x_t and y_t is at maximum. In this study, each region (Mountains, Foothills, and Plains) possessed one time series for GW head and one time series for SWE, and hence total of three cross-correlation function graphs were obtained, where x_t was set to be SWE time series and y_t was GW head time series. Because this study target at a regional scale SWE and GW connection, we performed the cross correlation analysis at each EGH regions.

In the example above, there is no auto-correlation within x_t and y_t data, meaning that the time series of both x_t and y_t are not correlated with the lagged version of themselves, e.g. the

correlation between x_t and $x_{t-1,2,3,\dots}$ or y_t and $y_{t-1,2,3,\dots}$. However, with strongly auto-correlated time series, it is difficult to assess the relationship between the two processes and the response time of one to the other variable. Thus, it is imperative to distinguish the correlation between x_t and y_t from the correlation of the time series itself. In addition, before performing a cross-correlation analysis, it is necessary to ensure that the time series are stationary. Stationarity of data indicates that data is a stochastic process that the unconditional joint probability distribution, their mean, and their variance do not change over time (Gagniuc, 2017). Input data joint stationarity is necessary because stationarity essentially allows us to estimate mean and cross-correlation (Shumway and Stoffer, 2017). Due to the nature of GW head or SWE time series, which usually possesses seasonality or trend, cross-correlation function cannot be applied directly unless all trends and / or seasonality are removed. As a result, pre-whitening is often performed before the cross-correlation analysis to maintain time series stationarity. Since pre-whitening is a linear operation, any linear relationships between original time series are preserved after pre-whitening and it is assumed that at least one of the variables (variables x_t and y_t) are independent (Cryer and Chan, 2011). More details about pre-whitening is provided in Cryer and Chan (2011) and presented in supplementary material N1.

2.6 Assessment of driving physical processes

In order to understand how various physical processes control the formation of snow drought, GW drought, and the signal propagation from SWE to GW across each of the EHG regions, we assess the dominant physical processes by implementing Least Absolute Shrinkage and Selection Operator algorithm (LASSO) (Tibshirani, 1996). The LASSO algorithm allows performing variable selection based on criteria that is examined through an iterative procedure and provided

by the user. The LASSO is able to select the most relevant variables by making the coefficients of non-relevant variables exactly zero (Tibshirani, 1996).

The selected input time series for our LASSO analyses in this study included simulated GW level time series as the response variable Y_i , and the simulated exogenous variables X_i , which are the time series of other hydrological variables that control the formation of GW level time series. The exogenous variables were selected based on their potential influence on GW levels based on model simulated results. Table S6 shows total of 12 hydrological variables being selected as input time series for LASSO analysis (Neitsch et al., 2011). Note that our GW-SW model generates daily time series for each of hydrologic variables at a sub-basin scale. The LASSO analyses, however, was performed at EHG regional scale, i.e., Mountains, Foothills, and Plains. Therefore, the model generated time series for each hydrologic variable were aggregated from the sub-basin level to EHG regional scale, based on a weighted average area approach in each of the three EHG regions. Note that before performing LASSO operation, data stationarity was also performed using similar procedure as conducted in cross-correlation function analysis, where we identified and removed any trend and /or seasonality within the time series. We also performed pre-whitening analysis to allow the LASSO to start. In LASSO technique, a hyper-parameter λ (a value greater than zero) is used as a criterion to control the selection or withdrawal of the input variables that are / or not influential on GW variations. The increase of the number of input variables for selection in LASSO stops when $\log \lambda$ is equal to 0. The larger the λ , indicates the more coefficients are exactly zero, meaning that more irrelevant variables are removed and vice versa. To examine the relevant variables X_i , we employed a range of λ values. At each λ , we recorded the number of non-zero coefficients for each variable X_i . Before the selection of a new exogenous variable (i.e., new hydrological variable that is influential on GW level), we also performed LASSO analysis on

lagged time series of the selected variables to study the memory effect exerted to the GW level time series. For instance, we considered not only the original time series of soil water content, we also lagged soil water content time series with 1 month, 2 months, ..., 12 months to study whether a lagged soil water content time series would impact the variation of GW head time series. To achieve this, each time series are lagged 12 times (1-month lag, 2-month lag ... 12-month lag), hence a total of 13 time series per variable were included in the LASSO matrix (1 original time series + 12 lagged time series), which gave overall of 13×12 exogenous variables = 156 time series for each EHG region. By doing so, we opted to study not only which exogenous variables are dominant to control the variation of GW head time series, but also how long before present can one variable be influential on the GW level time series. Similar to the original time series, all lagged time series for each variable that exhibited non-zero λ values were recorded, otherwise they were removed. Therefore, we count the number of non-zero elements in the parameter matrix representing relevant time series. The parameter matrix allows us to determine the relevant variable graphically by creating a heat plot, and the result of which will be further explained in later section. More specifically, each column of the heat plot corresponds to a λ value, which increases from left to the right. Each row of the heat plot corresponds to a specific variable X_i . Each cell is color-coded to reflect the size of parameter matrix. In this study, we used red or red-like color to indicate large parameter matrix and green or green-like color to indicate small parameter matrix. Therefore, the variable that corresponds to the row with more red-like cell is more relevant compared to the variable that corresponds to the row with fewer red-like cells. More details about the LASSO method is provided in supplementary materials N2

3. Results and discussion

3.1 Model calibration, validation, and verification

3.1.1 SWAT model calibration and validation results

The overall model performance for calibration (1991-2013) and validation (1983-1990) periods was satisfactory for most of the hydrometric stations (Figure 3, and Table S7). With a regional *r-factor* of 0.88 for calibration and 0.99 for validation periods, the model reproduced over 60% of the observed data (*p-factor* of 0.66) for both periods. The regional averaged R^2 and bR^2 based on the final optimum range of parameters were 0.64 and 0.58 for calibration and 0.60 and 0.54 for validation periods, respectively. It is suggested that *p-factor* between 0.6 to 0.8 and *r-factor* around 1 can lead to a reasonable performance for a regional-scale hydrologic model (Abbaspour, 2015; Faramarzi et al., 2015, 2017). However, there were a few gauges in the Mountains and Plains that demonstrated a lower performance with relatively higher *r-factor*, and lower *p-factor*, R^2 , and bR^2 as compared to other stations. The large uncertainty and low model performance in Mountains is generally attributed to input climate data scarcity, i.e., scattered distribution of climate stations and insufficient data length in high topographic regions (Chaponniere et al., 2007; Islam et al., 2017; Mizukami et al., 2014). The climate data (e.g., precipitation, temperature, solar radiation, wind speed, and air humidity) drive most of snow processes such as snowfall, snow accumulation, and snowmelt in Mountains, and they are primary drivers of hydrological processes in Mountains. In addition, the lower *p-factor*, R^2 , and bR^2 in some tributaries of the Mountains is related to glacier melt runoff, which is additional source of streamflow during warm seasons, while the glacier melt runoff were not systematically simulated in this study.

The comparison of simulated versus observed snow depth indicated an R^2 of > 0.8 and bR^2 of > 0.77 across EHG regions, demonstrating satisfactory model performance in snow depth

simulation, as a result in simulating SWE which are used to perform snow drought analyses for the study regions (Figure 3, right column). Note that due to limitation in snow depth data we only performed a model verification, where we used calibrated model parameters based on streamflow to simulate snow depth.

3.1.2 MODFLOW model calibration and validation results

MODFLOW model performance was assessed by comparing the simulated hydraulic heads and observation head data, which were retrieved from 20 observation wells. The comparison of the best-simulated monthly head with observed data resulted in an R^2 of 0.97, MAE of 23.12 m, and NRMSE of 0.040 for entire study area, indicating a satisfactory model performance (Aliyari et al., 2019; Chunn et al., 2019; Clark et al., 2011). Note that all observation wells are located in the Foothills and Plains and lacking measurements for Mountains. Given the connectivity of underground water flow between upstream and downstream EHG regions (Nepal et al., 2014), we assumed acceptable model performance in Foothills and or Plains can satisfy model performance in the Mountains. A relatively high mean square error value might be related to several reasons: First, the observation wells data represented local GW heads, whereas the model simulated GW heads represent average head for each grid cell of 10km×10 km of resolution. In grid cells, where in reality elevation differences is significant, this coarse resolution cannot capture the sharp change of GW head because the grid assumes uniform elevation within the particular grid cell while observation well might locate at a higher (lower) elevation location than the average cell elevation. The second reason could be due to boundary condition such as river stage accuracy, as well as lakes or pumping wells, which were not adequately represented in the model. . For the purpose of this study, the results statistics can be considered as satisfactory even though the model is under the circumstance where more reliable data should be implemented.

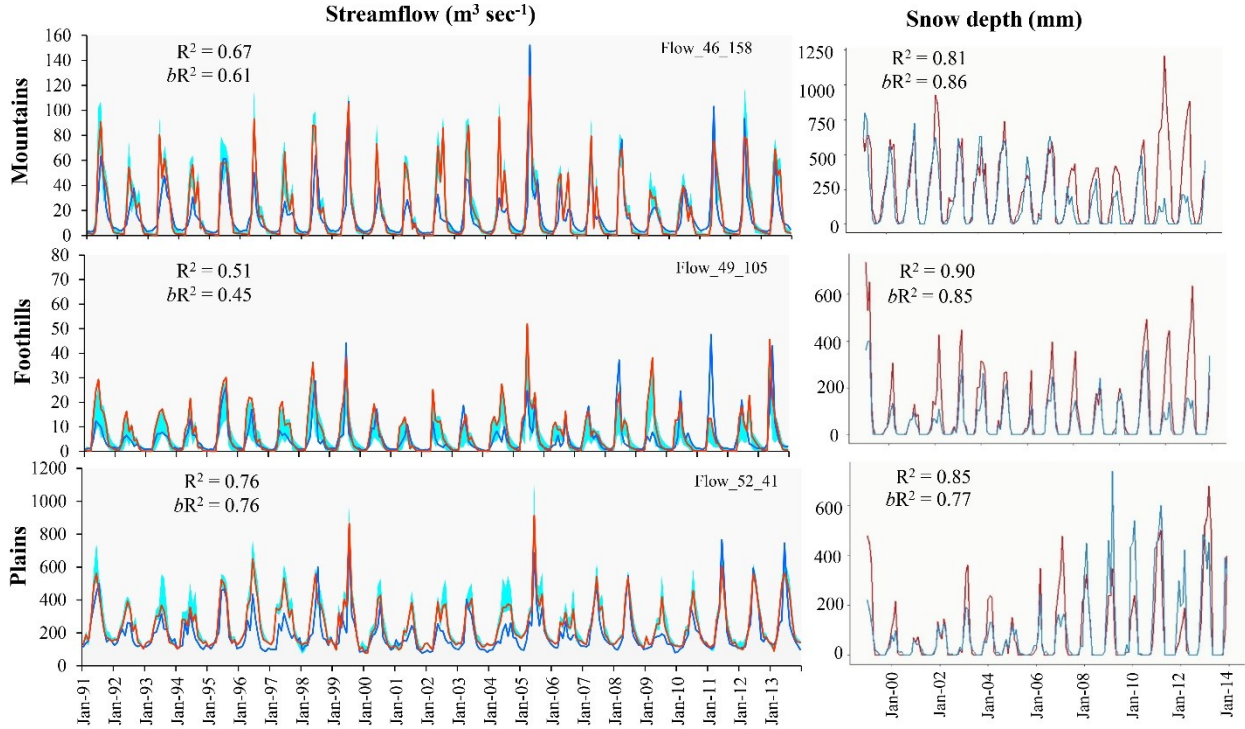


Figure 2. Model calibration performance for selected hydrometric stations across different EHG regions (left column). The shaded range indicates the 95PPU based on calibrated parameter range. Comparison of model simulated snow depth (red) with the observed (blue) used for model verification (right column).

3.2 Drought characteristics (frequency, duration and intensity)

3.2.1 Snow drought

Given that the NSRB is historically prone to hydrologic droughts (Yadete et al., 2008), we used model simulated SWE data to evaluate the historical and future snow drought characteristics through analysis of cumulative probability distribution (CDF) of drought intensity, duration, and frequency of drought events in each EHG region (Fig. 3). To achieve this, we firstly selected the suitable probability distribution function. The L-moment parameters of the simulated data points (demonstrated with plus signs in Fig. S1) matched the best with PE3 L-moment curve. Therefore, the Pearson Type III distribution was selected as the most suitable distribution to both SWE and GW levels. Then, we are able to utilize the index construction method to determine aforementioned

drought characteristics. The analysis of historical CDF indicated that the cumulative probability of the occurrence of all snow drought events with intensity of ≤ 1 is 75% in Mountains (Fig. 3, upper row). The historical CDF also demonstrated that there was an evidence of exceptional snow drought event (D4) where snow density exceeded 3. The CDF plot of the projected snow drought events for future period, indicated that the probability of drought events of different intensity follows an overall similar pattern as the historical events, however depending of the GCM type and SSP scenario a range of drought intensity was projected for a given probability value (shaded range in Fig 3, upper row). For example, it was found that the cumulative chance of occurrence of snow drought events with intensity of $SWEI \leq 1$ and $SWEI \leq 1.2$ in the future is 75% in Mountains. Overall, the CDF results for Mountains showed a lower intensity drought events in the future as compared to the historical period, e.g., the future projected SWEI did not exceed 2.8 whereas it was ≤ 3.2 for the historical period. The historical snow drought intensity for Foothills and Plains were both less severe than the mountainous regions because the maximum historical SWEI was less than 3. Such pattern is consistent with previous study, which pointed out that precipitation can gradually increase from barren land to grassland, then cropland and finally forest (Fan et al., 2015).

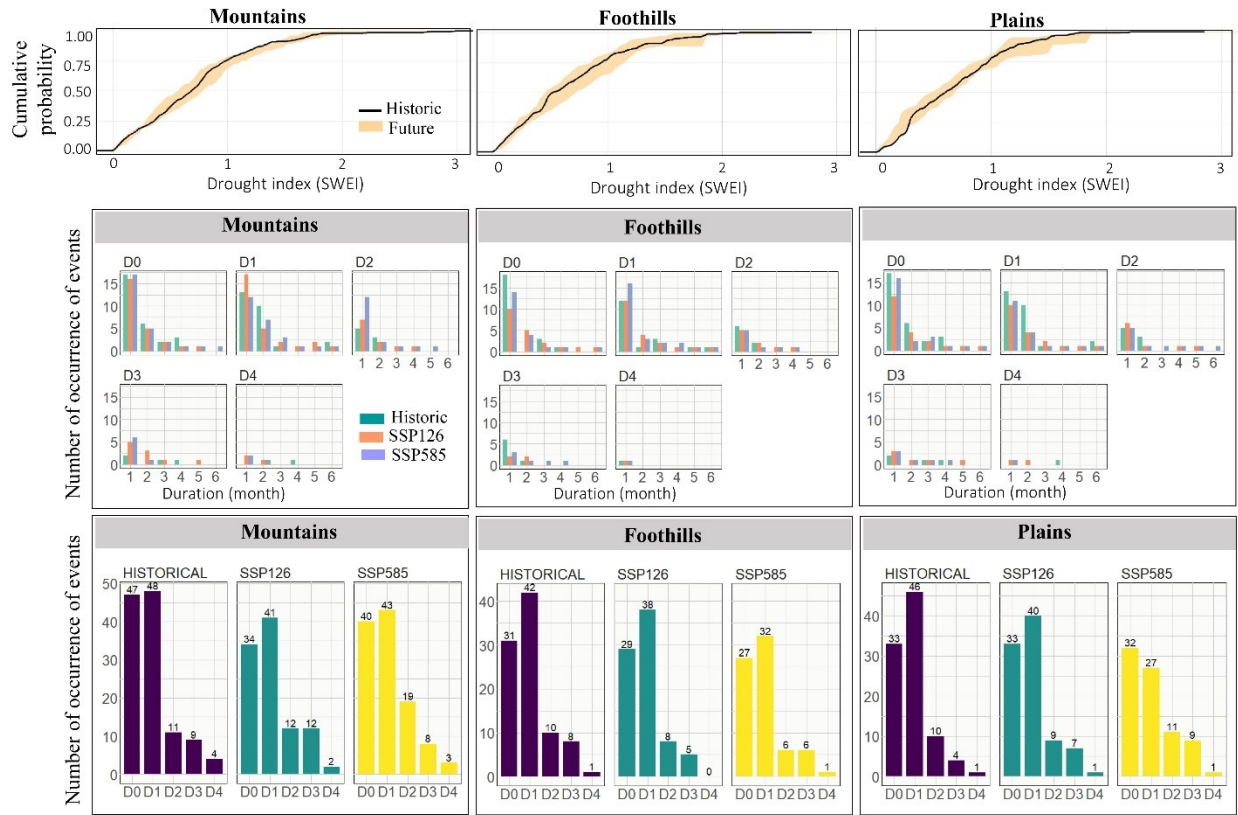


Figure 3. Historical and future snow drought characteristics: cumulative snow drought intensity (upper row), snow drought duration for each class of drought (middle row), and snow drought frequency (bottom row). Upper row: illustrates the cumulative probability of snow drought intensity for historical and future periods. The x-axis illustrates the snow drought intensity (SWEI), whereas y-axis indicate the cumulative probability for a particular snow drought intensity. The black curve in the center shows the historical snow drought intensity and shaded area around elaborates possible future intensity.

However, the multi-model and multi-scenario projected SWEI for the future in both regions suggested potentially more severe events, which is shown by wider range falling beyond historical maximum intensity (exceeding 3) for a given probability level in Figure 3 (upper row). Possible cause of such difference is that Mountains is less influenced by human activities, and hence the climatic condition, geologic formation and ecologic settings would remain relatively unchanged, whereas foothill and plain region would experience more change due to more frequent human activities such as agricultural, industrial or municipal alteration. Even we did not explicitly simulate anthropogenic activities in this study, but the potential impact of human activities are

reflected in the climate data, because all GCM simulated future climate data incorporated anthropogenic impact, such as radiative forcing due to anthropogenic greenhouse gas emissions (Döscher et al., 2022; Wu et al., 2021; Voltaire et al., 2019; Yukimoto et al., 2019).

Analysis of snow drought duration for the historical period (1983-2013) and SSP scenarios for the future (2040-2073), indicated that nearly 60% of droughts lasted for one month, and 23% lasted for two months. Overall, projected data in Mountains suggested more frequent and longer duration for abnormal (D0) and moderate (D1) snow droughts, followed by severe (D2) as compared to extreme (D3) and exceptional (D4) in all scenarios. However, more frequent severe droughts lasting for longer time (e.g., D2 and D3 of up to 5 months), were projected in future scenarios (SSP126 and SSP585) as compared to historical period in the Mountains (Figure 3, middle row). Also, the duration for D4 snow drought events in SSP126 and SSP585 scenarios decreased as compared to historical records, suggesting more frequent exceptional droughts (D4) with shorter duration. On the other hand, SSP126 scenario indicates more D3 drought events compared to SSP585, with a few events lasting longer than two months in Mountains. In Foothills, we observed fewer drought events in the future as compared to Mountains (Fig. 3, middle row). The D4 drought for all scenarios was identical, and historical D3 events outnumbered both future scenarios, but SSP585 scenario suggested that more D3 events with longer duration might occur, similar to D2 events for both SSP126 and SSP585 scenarios. On the other side of the spectrum, the number of D0 and D1 events for all scenarios are similar, suggesting a less variate projection. The severity of snow drought events in Plains were mainly D0 and D1, with nearly 77% of droughts falling within these categories, where both future scenarios suggested less frequent drought events with shorter duration (1 to 3 months) and more frequent drought events with longer duration (4-6 months) comparing to historical records (Fig. 3, middle row). For D2 and D3 events,

both future scenarios showed more events for all durations compared to historical records, and SSP585 scenario showed more events lasted longer than 3 months. As for D3 and D4 events, historical records indicated more drought events with longer duration than future scenarios. In short, projected future scenarios suggest that the plain regions will likely experience more snow drought events with less severity, implying a milder drought in the future, and extreme and exceptional drought would likely occur in the mountainous regions.

The frequency of all snow drought events, regardless of their duration, indicated that most of the droughts were abnormal and moderate for historical and future scenarios in all EHG regions (Fig. 3, bottom row). In Mountains, the SSP585 scenario showed more frequent snow droughts than SSP126, whereas the opposite was observed in Foothills and Plains. Focusing on D2 to D4 events, the overall number of drought events for SSP585 prevails SSP126. Moreover, the results suggested less abnormal and moderate droughts for both future scenarios, which implies that mild droughts tend to be milder, whereas severe droughts will likely be more severe.

Overall, the results of snow drought characteristics suggested that mountainous region is more likely to experience intensified, long-lasting, and frequent snow droughts in the future as compared to the historical period. One possible reason is related to the projected snow cover depletion. DeBeer and Pomeroy (2017) pointed out that spatial heterogeneity of snow accumulation can be a primary control of the pattern of snow cover depletion, or at least equally important as the effects of other factors such as net radiation in a mountainous region (DeBeer & Pomeroy, 2017). Although, Pomeroy and Brun (2000) argued that the depth of snow cover usually increases with elevation due to more frequent snowfall and less melt events, but the underlying condition is that vegetation and small-scale surface topographic irregularities such as bumps or hollows, which is not what is observed in upstream of NSRB. On the other hand, snow sublimation

can transfer a large amount of SWE back to the atmosphere as water vapor. In SWAT model, snow sublimation is impacted by degree of shading, which directly relates to the land cover type in each region (Neitsch et al., 2011). In mountainous region, nearly 50% of the land are barren land or sparsely distributed vegetated land, which leads to a more exposure of snow to atmosphere, hence higher chance of sublimation.

Moreover, as described in section 2.3.1, snowmelt calculated in SWAT model depends on maximum and minimum melt factors. In the final calibrated model, melt factor in Mountains sub-basins are higher than Foothills and Plains. The optimized maximum and minimum snowmelt factors in Mountains are 5.84 and 5.77 respectively, whereas maximum and minimum snowmelt factors in Foothills and Plains are 4.5. Hence, mountain region will likely experience more snowmelt compared to Foothills and Plains, leading to lower snow accumulation in Mountains.

In addition, needle leaf forests can impact energy exchange between atmosphere and snow, because it not only suppresses turbulent energy fluxes (Harding & Pomeroy, 1996; Link & Marks, 1999), leading to a significant shortwave radiation reduction (Ellis et al., 2010), but may also alter snow surface albedo due to the falling of forest litters (Hardy et al., 2000; Melloh et al., 2002). Such effect is less obvious in the forests located at a more leveled terrains such as foothill and plains, because the decrease in shortwave radiation reduction is compensated by the longwave radiation emitted from canopy, and hence only a small amount of radiation loss to the snow will occur (Ellis et al., 2011). This can consequently reduce the severity of the snow cover depletion in foothill and plain regions than that of mountainous region. While our model did not explicitly simulate these detailed physical processes, but it implicitly addressed them through calibration of physical parameters. In future projections, these processes are indirectly reflected in GCM simulated climate data, which are inputs to our model for future projections.

3.2.2 GW drought

To understand GW drought characteristics we performed cumulative probability distribution (CDF) of drought intensity, duration, and frequency analysis using GW head time series that were simulated by our coupled GW-SW model in each EHG region and for past and future scenarios (Fig. 4).

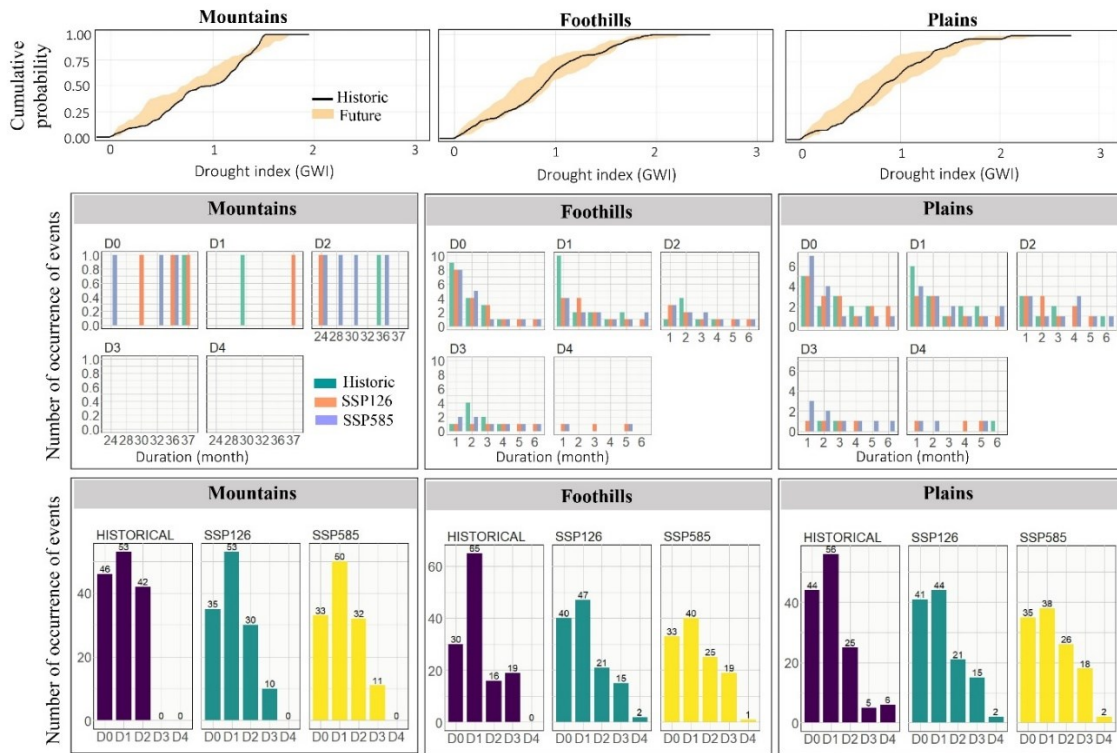


Figure 4. Historical and future standardized GW index (SGWI) characteristics for (a) cumulative GW drought intensity. The black line shows the historical GW drought intensity and shaded area around elaborates possible future intensity. (b) GW drought duration for each class of drought, and (c) GW drought frequency for each EHG region.

The analysis of historical CDF suggests that the cumulative probability of occurrence of all GW drought events with intensity of ≤ 1 is 50% in Mountains (Fig.4, upper row). The results also revealed that cumulative probability of all drought events that has intensity of ≤ 2 in Mountains is 100%, hence only abnormal (D0) to extreme (D3) drought were observed in Mountains. The CDF plot for the projected GW drought events for future period, suggests that the probability of the

majority of droughts of different intensity in the future will likely be smaller than historical events. However, depending on the type of GCM and SSP scenario, a drought intensity range was projected for a given probability value (shaded range in Fig. 4, upper row). For example, we notice that the chance of occurrence of GW drought with an intensity of $SGWI \leq 1.1$ and $SGWI \leq 1.3$ in the future is 75% in Mountains. Overall, the CDF results for Mountains showed that most of the future SGWI intensity are lower than historical events, but small portion of projected SGWI intensity are greater than historical events. For instance, at nearly 80% cumulative probability, almost all GCMs and all scenarios indicated an intensity of $SGWI \leq 1.4$, and the future projected SGWI did not exceed 1.7, whereas it was ≤ 1.9 for the historical period. In contrast to snow drought, the historical GW drought intensity for Foothills and Plains were both more severe than the mountainous region because the maximum historical SGWI exceeded 2. However, the multi-model and multi-scenario predicted SGWI for both regions suggested potentially less severe GW drought as compared to historical period, which is shown by wider shade falling in the left side of historical curve for a given probability level in Figure 4 (upper row). However, the shaded areas for Foothills and Plains are wider than Mountains, indicating a larger uncertainty and a wider range of drought possibilities in the future. Moreover, soil texture can also contribute to variation in GW drought intensity. Soylu et al. (2011) discussed how soil texture can influence the evapotranspiration from water table, and argued that silty loam can crucially impact surface evapotranspiration (Soylu et al., 2011), and based on NSRB soil information, Foothills and Plains possess more silty texture soils than Mountains.

The analysis of GW drought duration for the historical period (1983-2013), and that of SSP scenarios for the future period (2040-2073), indicated that around 36% to 44% of all drought types and for Foothills and Plains and all periods lasted for one month, and around 18% to 28% lasted

for two months (Fig. 4, middle row). However, mountainous region showed extremely long durations (24 months to 37 months) for both historical and future drought events. Overall, all drought events in Mountains are abnormal (D0), moderate (D1), and severe (D2) during historical period, and projected data in Mountains suggested longer duration for abnormal (D0) and moderate (D1) GW droughts in SSP126 scenarios, and longer duration for severe (D2) drought for SSP 585 scenarios. An implication is that even though mountainous region is the source of water for many streams, but the aquifer still displays below-normal GW level for a long time. This further supports our previous discussion that in mountainous region aquifer is less capable of storing snow water due to the existence of exposed bedrock landscape. Even though other landforms exist in the alpine environment, there is also a large quantity of snowmelt loss from the aquifer to other places, such as streamflow or downstream aquifers. In Foothills, The D1 event showed longest duration during historical period, which was 5 months, and historical D1 event outnumbered both future scenarios. The future projections showed a slightly longer drought duration in both SSP126 and SSP585 scenarios as compared to historical events. The duration of D2, D3 and D4 events in SSP126 and SSP585 scenarios are similar, with nearly identical number of droughts and duration. In short, future projections are similar in both scenarios for Foothills, and both scenarios suggested slightly longer-duration drought events in the future. The severity of GW drought events in Plains for SSP126 scenario were mainly D0 and D1, where historical D0 and D1 droughts outnumbered both future scenarios, and the distribution of duration in all scenarios for D0, D1, and D2 were relatively uniform, meaning that the number of drought events with same duration in different scenarios are all similar. For D0 events, SSP126 projection possesses longer duration (3 to 6 months) as compared to historical. For D2 and D3 events, SSP585 scenario showed more drought events compared to historical and SSP126 scenario, with long duration (can all reach 6 months). For D4

events, SSP126 projection exhibited slightly longer duration than SSP585 scenario, but both scenarios had shorter duration compared to historical events. In short, projected future scenarios indicated that plain regions will likely experience less abnormal (D0), moderate (D1) and severe (D2) droughts with longer duration; and more extreme (D3) and exceptional (D4) droughts with shorter duration.

Similar to snow drought, the frequency of all GW drought events, regardless of their duration, suggests that most of the droughts were abnormal and moderate for both historical and future scenarios in all EHG regions (Fig. 4, bottom row). In all EHG regions, SSP585 showed more frequent severe (D2) and extreme (D3) drought than SSP126. However, focusing on D4 events, the overall number of drought events for SSP126 slightly outnumbered SSP585. Overall, in the plain region, projected GW drought tends to be the more severe than historical period, and foothill region is relatively less variable with time comparing to other two regions.

Overall, the results of GW drought characteristics suggested that all regions are expected to experience less intense, but long-lasting and less frequent GW drought in the future as compared to historical period. Especially for Mountains, it is highly likely to experience less intense GW drought, but with relatively longer duration, where the frequency of D0, D1 and D2 droughts are projected to decrease while it is projected to increase in D3 droughts.

3.3 Propagation time for GW response to SWE

The comparison of cross-correlation factors (CCF) between SWE and GW level time series for the historical (1983-2013) period indicated that the propagation time of drought from snow to groundwater varies across EHG regions (Fig 5). The results showed that the response time from snow to GW in each region are 4-month in Mountains (CCF=0.187), 5-month in Foothills

(CCF=0.134), and 6-month in Plains (CCF=0.254), respectively (Fig. 5a-c, maximum bar in the left side of each plot). The difference in response time (i.e., time required for GW levels to respond to the changes in SWE) across entire region implies that under different EHG settings, the hydrologic processes that control propagation mechanism also differs. This indicates different physical processes under each EHG settings can be the potential driver for such mechanism, including the difference in precipitation, temperature, evapotranspiration, antecedent soil moisture, curve number that represents soil permeability among others. Note that all cross-correlation factors are low even though the cross correlation factor values are above the criteria threshold (the black horizontal line in the figures, see Supplementary Materials N1). This might indicate that the connection between snow and GW is rather weak. One reason is the time series data that are weighted area averaged across each of the EHG regions and they may not represent the spatiotemporal variability of SWE and GW head within each region. Therefore, the assumption that SWE and GW head are constant in each region is not realistic.

A stronger correlation between snow and groundwater that is reported in some studies, is mainly due to the scale of their study, for a relatively small-scale catchment reasonable amount of recorded data were available (Bloomfield & Marchant, 2013; Fendeková & Fendek, 2012; Pathak & Dodamani, 2021; Yeh, 2021). A smaller-scale study with sufficient recorded data can more accurately represent hydrologic, geologic, and ecologic conditions, whereas large-scale

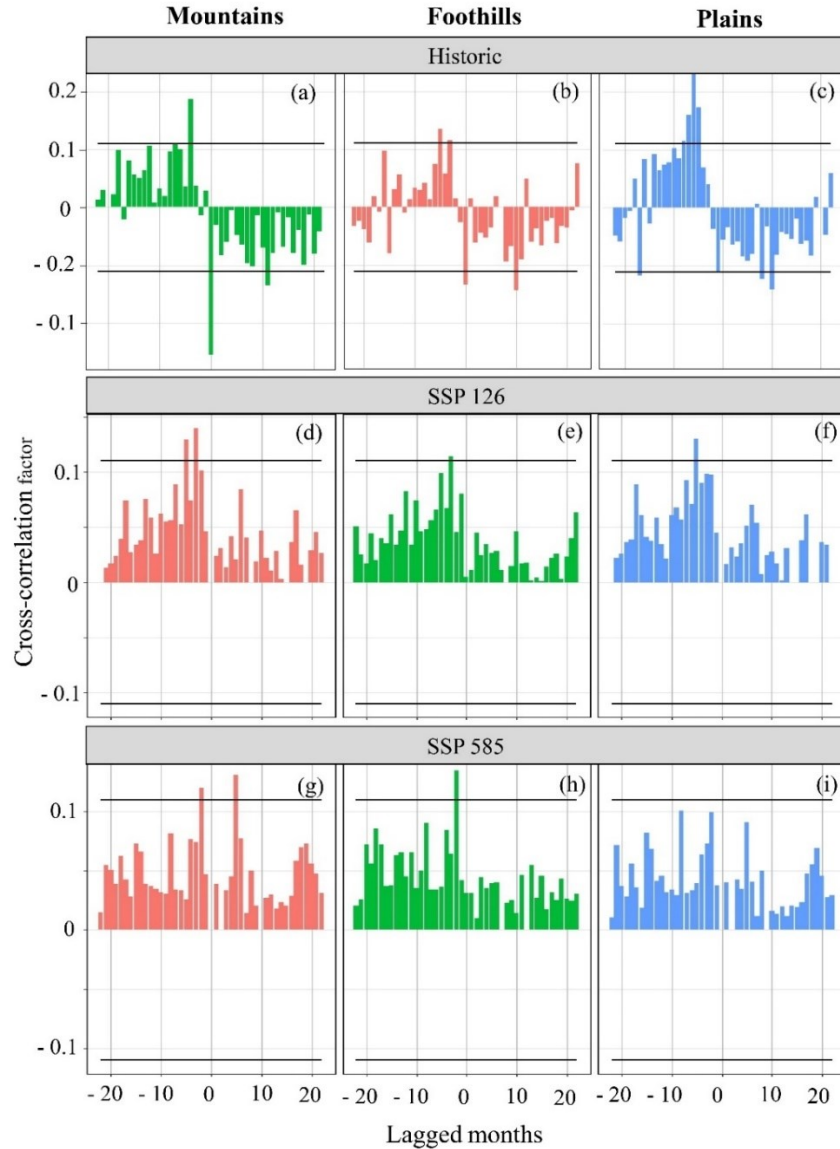


Figure 5. Historical cross-correlation analysis result for (a) Mountains, (b) Foothills and (c) Plains. (d) to (f) shows cross-correlation analysis result for SSP126 scenario for corresponding regions, and (g) to (i) shows the results for SSP585 scenario. The x-axis indicates lag time between SWE and GW levels. The negative lag months indicates that in SWE and GW time series, the variation of SWE occur before GW variations (i.e., GW responds to changes in SWE), whereas right-hand-side means GW time series leads SWE time series (not realistic and usually below the horizontal threshold, suggesting meaningless correlation, or negative CCF values, suggesting inverse correlation).

modelling can potentially possess uncertainty in representing detailed heterogeneity. Another potential reason is that SWE is based on precipitation, which doesn't occur during summer across large portion of study area, and hence GW head would mainly respond to rainfall precipitation or

GW recharge from stream or lakes. During melt season, depending on the vegetation types, soil texture, and climate factors (temperature, wind, air humidity), the accumulated snow can melt and transform into other hydrologic components such as evapotranspiration, snowmelt runoff, infiltration to soil moisture, lateral flow, and GW recharge. Hence, the amount of SWE that enters the aquifer can be smaller in less permeable soils than others, resulting in a relatively less impact on the variation of GW head. Moreover, in our models the simulated snow and GW head time series ignore certain source of uncertainties, such as human exploitation of GW, and snow redistribution such as avalanche or wind-related redistribution (Freudiger et al., 2017). The poor CCF could also be due to aquifer water flow and connectivity underneath EHG regions, from Mountain to Plain, which can become weaker as terrain gets flatter and the water permeability gets poorer (Cai et al., 2020). Nonetheless, performing cross-correlation on SWE and GW time series can still provide an insight of possible physical connection between snow and GW.

Interestingly, our results indicated that the response time of GW to changes in SWE is the shortest in Mountains as compared to the other EHG regions. This is counterintuitive because often bedrock is characterized with low hydraulic conductivity, where snowmelt can flow over the exposed bedrock instead of infiltration (Hayashi, 2020). However, apart from exposed bedrock in the Mountains, there are also various types of alpine landforms in the NSRB, such as talus, meadows, moraine or rock glacier, which dominantly possess coarse material, and allow snowmelt infiltration and storage to occur (Hayashi, 2020). In Foothills, the dominant land cover is needleleaf forests, pasture and grassland, with nearly no agricultural land present. In Plains, most of the land cover is composed of agricultural lands, pasture, and a large urban area. Such land cover (or land use) can increase the amount of water being consumed by vegetation, enhancing plant water uptake from soil and evapotranspiration. This can lead to a decreasing amount of water

recharging to the aquifer, hence a longer response time of GW to changes in SWE. Moreover, soil hydraulic conductivity is crucial to the response time, since it determines the rate of water being conducted from surface to the ground. Comparing to Foothills and Plains, soil type in the Mountains is relatively uniform possessing a soil hydraulic conductivity of about 300 mm/hr, whereas in Plains, the hydraulic conductivity is around 100 mm/hr. This results in a slower response of GW to changes in SWE (Fig 5a, 4-month response time, left side of the plot).

The ensemble mean projections of propagation time for SSP126 indicated that response time of GW to alterations in SWE is shorter in the future (3-month for Mountains, 3-month for Foothills, and 5-month for Plains) as compared to historic period in all regions (Fig. 5d-f). The mountainous region showed shorter response time compare to other regions. The projection response time was relatively shorter under SSP 585 with 2-month for Mountains, 3-month for Foothills, and no obvious relations in Plains. This suggests that under future global warming scenarios, hydrologic processes such as evapotranspiration will likely be intensified, leading to higher amount of water vapor in the atmosphere, leading to more precipitation events (IPCC, 2013), and most likely in the form of rain than snow (Mote et al., 2005). The change in hydrologic regime is likely more accelerate in the mountainous region than other EHG regions (Feng & Wu, 2016; Khalili et al., 2023). It is noteworthy that the lower than threshold CCF projected under SSP585 in Plains doesn't necessarily mean that the amount of snow is less than other scenarios where obvious cross-correlation were observed between SWE and GW levels, and in fact, most of the SSP585 models showed relatively the same amount of snow in each region (see Fig. S3). However, changes in the precipitation pattern caused by climate change can lead to more disconnected snow-GW relationship. Because warming temperature can result in earlier and more accelerated snowmelt, reducing propagation time for infiltration or recharge to GW (Vano et al., 2010). Hence, the

snowmelt cannot replenish groundwater reserves, leading to a less connected relationship between snow and GW.

3.4 Dominant driving physical processes

The analysis of heat plots using the simulated data for the historical period indicated that among all three EHG regions, the soil water content and percolation play fundamental role in variation of GW head (Fig. 6, shown by the far distance to the right that the red-like cell can go, as the color didn't change to the lightest green color). Percolation is defined as the volume of snowmelt and excessive surface water that directly enters soil layer, and eventually drains into shallow and /or deep aquifer, resulting in a direct quantity change of GW head. In SWAT model, percolation is directly calculated based on soil water content, soil temperature, and the effects of damping depth (Neitsch et al., 2011). Percolation is also directly dependent on the travel time of the percolation water, which further depends on the soil saturated hydraulic conductivity (Neitsch et al., 2011). The hydraulic conductivity depends on the soil texture which can seasonally vary by soil temperature and freezing-thaw processes (Gao & Shao, 2015). In SWAT model, soil temperature is simulated based on near surface maximum and minimum air temperature, which is then calculated based on soil depth to reflect the effects of damping depth. The damping depth is the depth at which the soil temperature variation due to climatic temperature no longer occurs. Damping depth can directly impact percolation flux rate (Corona et al., 2018). As a result, SWAT model considers the above parameters that directly or indirectly affect percolation processes, and eventually influence MODFLOW simulated GW head variation.

Overall, the temperature variation within soil layer can impact water movement (Neitsch et al., 2011). On the one hand, during warm and wet season, soil water content can accelerate the flux of water from surface to GW system, because of stored-full runoff mechanism (Han et al.,

2019). On the other hand, soil water content might also be inversely related to snowmelt infiltration during cold season, because in frozen soils, a larger amount of soil water content might block the infiltration process because of refreezing of existing soil water content,

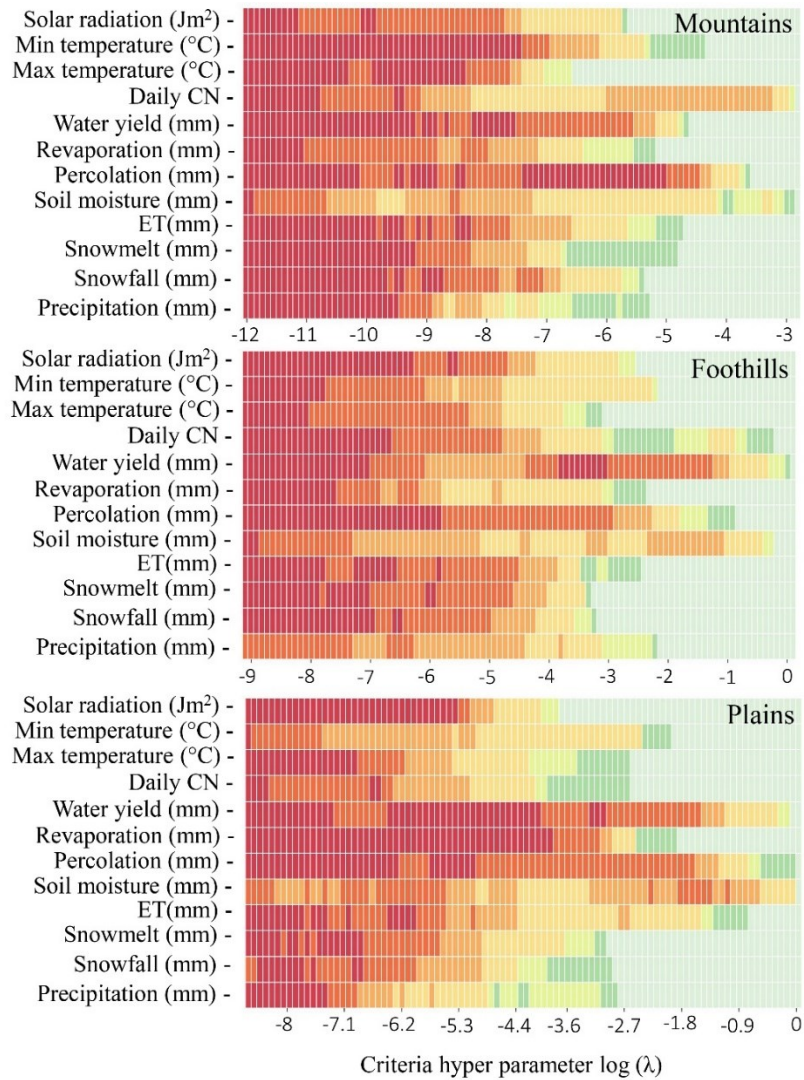


Figure 6. Heat plot indicating dominant physical processes for each EHG region. More cells with red-like color indicate that the particular parameter is more influential on GW head variation.

which can make the soil impermeable if an ice lens is formed near the surface (Gray & Landine, 1988; Mohammed et al., 2018; Stähli et al., 2004). On top of that, soil with frozen water can impact lateral runoff, which then indirectly influence the amount of water entering GW system, and frozen

soil can heavily reduce infiltration capacity when pre-freeze soil water content is high (Ireson et al., 2015). Especially in Canadian Prairies, frozen soils are commonly seen, and permeability of frozen soils can heavily impact the quantity of water available for GW recharge (Mohammed et al., 2019).

Looking at mountainous and foothill regions, CN exhibits a fundamental role, whereas plain region suggests prevailing controlling force of evapotranspiration. Curve number is a parameter employed in the Soil Conservation Services (SCS) runoff method, which indicates the runoff potential and is calculated based on soil permeability, land cover, and antecedent soil conditions in the calculation of runoff (Neitsch et al., 2011). It measures the ability a particular HRU can transform excess precipitation into surface runoff or infiltration. The curve number can indirectly affect GW head, because it controls the amount of water not entering the soil and therefore the GW system. Unlike Mountains, where CN significantly affected GW head (Fig. 6), the GW head variation in Plains and Foothills demonstrated sensitivity to water yield. Total water yield in SWAT model is calculated as the summation of surface runoff, GW discharge, and lateral (or subsurface) flow entering main channel within each HRU, subtracting total amount of water loss by transmission through streambed and pond abstractions (Arnold, J., Kiniry, R., Williams, E., Haney, S., Neitsch, 2012). One possible reason for total water yield not displaying a dominant role in Mountains is that the major portion of water contributed to streamflow instead of GW system in Mountains, which is also explained in section 3.3, and can be further supported from Fig. S4 (see Fig. S4, bottom row right corner).

The plain region demonstrated less GW sensitivity to CN as compared to Mountains and Foothills, mainly because of an enhanced actual evapotranspiration. Note that this doesn't necessarily mean that evapotranspiration in Plains is more than that of Mountains and Foothills,

but the impact from evapotranspiration on the formation of GW is significant in plain region. In fact, the monthly average of evapotranspiration in Foothills is the highest among all regions (see Fig. S4). The first potential factor is the higher atmospheric water demand in plain region comparing to that of Mountains and Foothills, because high atmospheric water demand is usually associated with higher temperature (Condon et al., 2020). Since we applied temperature lapse rate based on elevation, the plain region is expected to have higher temperature than Mountains and Plains, which can also be seen in Fig. S4 where Plain generally has highest maximum and minimum temperature (Fig. S4, third row). Also, in Mountains and Foothills the GW tends to be more related with snowpack and snowmelt (Condon et al., 2020). That being said, GW variation in Mountains and Foothills are likely to be more corresponded to surface water processes, which can be justified by looking at Fig. S4 where Mountains tend to have highest snowmelt during melt season (Fig. S4, second row). Another potential factor is soil water availability for evapotranspiration among different EHG. From Fig. S4, we can observe that the plain region generates the least available soil water comparing to Mountains and Foothills, yet the evapotranspiration is more than that of Mountains, which could imply that large amount of soil moisture is lost due to evapotranspiration, leading to less water input to GW system (Neitsch et al., 2011).

4. Implication of the study results

This study advances our understanding of the propagation mechanism between snow and GW droughts, as well as the physical driving processes that controls the interaction of snow water and GW. As also pointed out by other researchers, most of the recent studies did not address the connection between any forms of hydrological or meteorological droughts with GW droughts (Petersen-Perlman et al., 2022). Given that snow is a primary driver of hydrologic processes in

most of mid-to-high latitude watersheds, the result of our study can provide valuable information for better understanding of snow water - groundwater relationship, which can inform water management and environmental protection. While droughts are inevitable and parts of natural hydrologic cycle, but their frequency, intensity, and duration are projected to change due to the changes in climate under future global warming scenarios (Mianabadi et al., 2020). Hence, the understanding of how drought and groundwater relate is crucial (Brauns et al., 2020; Langridge & Van Schmidt, 2020). Our projections under two most extreme global warming scenarios (i.e., SSP126, known as the most environmental-friendly scenario; and SSP 585, as the worst global warming scenario, show strong regional differences of future drought characteristics, where Mountains GW drought tends to be less severe than historical record in the future, while Plains tends to be worse. This is consistent with a recent study arguing that drought can slow groundwater level recovery in agricultural areas compared to forested areas (Park et al., 2021). Such trend in Plains might result in prolonged groundwater deficit, which can potentially impact agricultural and ecosystem groundwater use in the region (Park et al., 2021). However, in Mountains, the intensified snow drought and slightly relieved GW drought implies that there might be a slight shift of water storage from snow to the groundwater system. This is likely due to the accelerated snowmelt as a result of global warming, which can potentially generate more excess water infiltration to the root zone which can make its way to recharge GW compared to rainfall precipitation in the future (Earman et al., 2006; W. Y. Wu et al., 2020). Under this context, our result can be used as reference to discover what land management techniques can be implemented to mitigate different future droughts in each region. For example, in Plains, GW droughts might be relieved by improving land management techniques such as increasing coverage of fallow land, crop type selection (Gebremichael et al., 2021), or changing irrigation patterns (Yimam et al., 2021)

and increasing irrigation water use monitoring (Zhang & Long, 2021). Another management technique is consideration of a more strategic groundwater use to protect against GW drought. Faramarzi et al (2017) argued that the NSRB has shown an increasing trend of groundwater use, leading to over extraction of renewable groundwater (Faramarzi et al., 2017). Based on this, GW droughts might be relieved by considering the balance between supply, demand and connectivity between aquifers (Best and Lowry, 2014).

Also, droughts can significantly affect GW quality (Petersen-Perlman et al., 2022), such as increase in nitrate concentrations (Jutglar et al., 2021) or increase in certain redox-sensitive ions and metals (Aladejana et al., 2020). Note that even though our study doesn't focus on water quality, but our modelling framework, and the simulated processes that drive interconnection between snow and GW droughts, can incorporate nutrient data and simulate nutrient transport, such as nitrate quantity in the shallow aquifer (Neitsch et al., 2011). Prediction and future projection of GW quality under various drought types can be beneficial in determining the best agricultural or industrial practices in drought-prone regions (Aravinthasamy et al., 2021). It is also worth noting that our study does not consider the impacts of large-scale natural climate variabilities including El-Nino Southern Oscillation (ENSO) or Pacific Decal Oscillation (PDO) (Corona et al., 2018; Han et al., 2019). Hence, future study is needed to consider the ensemble contemporary impacts of global warming and large-scale climatic variation to better capture the snow and GW drought characteristics.

Furthermore, our results showed how the propagation time varies in each region, as well as the variation in dominant physical processes, including the different weight for curve number, soil water, evapotranspiration, water yield and percolation. Then based on the regional differences, future studies can incorporate different regional-scale water resource management strategies such

as conjunctive management for surface water and groundwater (Amundsen & Jensen, 2019; Apurv & Cai, 2020; Long et al., 2020), or managed aquifer recharge (MAR) (Dillon et al., 2020), to explore impacts of surface water - GW management strategies in improving drought characteristics.

5. Study caveats and future directions

Unlike surface hydrologic modelling, where model performance mainly depends on availability of geospatial and time series input data, as well as streamflow observation; the GW modelling is affected by proper setting of geological formations in the model, resolution of spatial units delineated in the model, boundary condition such as river bed elevations, local pumping, lakes and river water levels (Waterloo Hydrogeologic, 2018). The performance of GW models are also affected by the GW head observations, which are less available as compared to surface water data at a regional scale. In this regional-scale study, the grid resolution of $10\text{km} \times 10\text{km}$ created some areas of limitations in GW head simulation. The simulated GW head in the grids that contained the boundary of watershed, exerted mismatch with observation well data. Because the groundwater in these grids that contained partial watershed, did not receive recharge from the full grid area, whereas in reality the GW recharge is not limited to the watershed border in any given grid cell. Also, large grid size ($10\text{km} \times 10\text{km}$) can contain elevation change within the grid area. The simulated GW head is based on the overall average elevation of each grid cell, whereas in reality the observation well might locate in high (or low) elevation region within that grid cell. Hence, the GW head can be heavily underestimated or overestimated. Moreover, when an observation well is located near stream, the GW head gradually changes from river bottom to the GW level in observation well, but in the simulation, the model can force the GW head to satisfy boundary condition in each cell immediately with no possibility for gradual change due to the coarse spatial resolution. As a result, the simulated head can mismatch with observation. While all

these limitations are common in most large-scale GW-SW modelling studies (Barthel & Banzhaf, 2016; Candela et al., 2014; Refsgaard et al., 2010; Zhou & Li, 2011), but comparison of the current model with a more high-resolution one, would provide direction on the magnitude of the changes in model results and conclusions.

Alternatively, partial refinement of grid can improve model performance, especially for grids that contains drastic elevation change. MODFLOW is able to perform partial refinement on grid size, which can improve GW head simulation at local scale. However, the simulation time of the coupled SWAT-MODFLOW with larger number of grid cells at a regional-scale is a limiting factor. Alternatively, a comparison with other state-of-the-art tools that allow partial refinement can inform about model performance. For future projections, we assumed that quantity of glacier melt runoff contributing to headwater tributaries would remain similar to historical period. This assumption adds uncertainty to streamflow simulation for future scenarios, and therefore, on processes that affect GW recharge in upstream catchments, and consequently the GW head fluctuations. Coupling a process-based glacier modeling with GW-SW modeling can improve model reliability.

6. Summary and conclusion

Droughts are features of natural hydrology, while their intensity, duration, and frequency is projected to change under global warming scenarios. Snow and groundwater droughts are connected through various physical processes within a hydrologic cycle. Snow processes are primary driver of hydrologic balance in most of mid-to-high-latitude watersheds. Understanding of both snow and GW drought characteristics and projection of their future propagation and interconnection is vital for sustainable management of water resources. To address how snow and

GW droughts characteristics may change under future global warming scenarios and how their interconnection and propagation mechanism might change in the future, we constructed a coupled SW-GW model of a relatively large watershed in western Canada using a calibrated SWAT hydrologic model and a calibrated MODFLOW GW model. For future projection of snow and GW droughts, we forced our SW-GW model with downscaled climate data projected through an ensemble of five GCMs of the CMIP6 series for SSP126 and SSP585 scenarios for the 2040-2073 period. Using model outputs we performed statistical analysis to assess the snow and GW drought characteristics, the propagation time and propagation mechanism between snow water and GW, and their variation across different eco-hydro(geo)logical settings such as Mountains, Foothills, and Plains for historical (1983-2013) and future periods. We draw the main conclusions as follows:

1. The characteristics of snow and GW droughts were reversed across different EHG regions under future SSP scenarios as compared to the historical period. Mountainous region experienced the worst historical snow drought as compared to Foothills and Plains, and the future projections indicated more intensified and prolonged droughts with higher frequency in the future, leading to lower snow accumulation in Mountains. Among all regions, Plains experienced worst groundwater drought historically, and it was projected to experience higher intensity droughts in the future. Mountains, on the other hand, were projected to experience less frequent and low intensity GW droughts compared to other two regions. This implies that snow droughts might shift to GW droughts in Plains and the opposite is true for Mountains.
2. The historical drought propagation time from snow to GW increased from Mountains to Plains with 4-, 5-, 6-month predicted for Mountains, Foothills, and Plains, respectively. Also, the rather low cross-correlation between snow and GW indicated a relatively weak

connection between snow and GW during historical period. In both future scenarios, the propagation time for all regions decreased, suggesting accelerated water cycle and hydrologic processes.

3. The dominant physical processes that control GW head and its connection to snow processes vary across different EHG regions. While all regions are very sensitive to the changes in soil water content and percolation processes, the physical processes that move soil water into GW system is different among regions. In Mountains and Foothills the curve number (or runoff potential) is inversely but strongly related to GW variation. The GW levels in Foothills and Plains are more responsive to the variation in total water yield, while the plain region alone is extremely sensitive to evapotranspiration due to the nature of its landform, landcover, and soil properties. Given the nonstationary response of these processes to variation in climate (Broberg et al., 2019; X. Li et al., 2020; Porter & Semenov, 2005), the response of GW to surface water processes and in particular, changes in snow can be very different across different EHG regions.

This study presented a novel approach to address regionalized snow drought and GW drought characteristics for both historical and future scenarios, which provides a comprehensive understanding of possible future, albeit realizing the existence of assumptions and limitations. This study can also advance our understanding of the propagation mechanism between snow water and GW, as well as the physical driving processes that control the interaction of snow water and GW. This study provides a basis for further studies concerning the GW management strategies in relation to changes in snow processes due to global warming in cold watersheds of the mid-to-high latitude regions. It also provides a unified approach for the analysis of snow drought and GW drought relationship.

Acknowledgment

This research was funded by the Alberta Innovates - Water Innovation Program (AI-WIP, Grant# G2020000145), Campus Alberta Innovation Program Chair (Grant# RES0034497), and Natural Sciences and Engineering Research Council of Canada Discovery Grant (Grant# RES0043463). We also thank EPCOR for their contribution to the AI-WIP funding.

Declaration of Competing Interest

The authors declare that they have no known competing financial interests or personal relationships that could have appeared to influence the work reported in this paper.

Credit authorship contribution statement

Yinlong Huang: Data curation, Formal analysis, Methodology, Software, Validation, Visualization, Writing - original draft, Writing - review & editing. Yang di: Statistical analysis and review & editing. Ryan T Bailey: Software. Monireh Faramarzi: Funding acquisition, Supervision, Conceptualization, Formal analysis, Writing - review & editing, Project administration.

References

- Abbas, S. A., Xuan, Y., & Bailey, R. T. (2022). Assessing Climate Change Impact on Water Resources in Water Demand Scenarios Using SWAT-MODFLOW-WEAP. *Hydrology*, 9(10). <https://doi.org/10.3390/hydrology9100164>
- Abbaspour, K. C. (2015). SWAT-CUP: SWAT Calibration and Uncertainty Programs- A User Manual. Department of Systems Analysis, Integrated Assessment and Modelling (SIAM),EAWAG. Swiss Federal Institute of Aquatic Science and Technology, Dübendorf, Switzerland. Doi: DOI: 10.1007/s00402-009-1032-4
- Abbaspour, K. C., Vaghefi, S. A., & Srinivasan, R. (2017). A guideline for successful calibration and uncertainty analysis for soil and water assessment: A review of papers from the 2016 international SWAT conference. *Water (Switzerland)*, 10(1). <https://doi.org/10.3390/w10010006>
- Abbaspour, K. C., Yang, J., Maximov, I., Siber, R., Bogner, K., Mieleitner, J., Zobrist, J., & Srinivasan, R. (2007). Modelling hydrology and water quality in the pre-alpine/alpine Thur watershed using SWAT. *Journal of Hydrology*, 333(2–4), 413–430. <https://doi.org/10.1016/j.jhydrol.2006.09.014>
- Acreman, M., & Bullock, a. (2003). The role of wetlands in the hydrological cycle. *Hydrology and Earth System Sciences*, 7(3), 358–389.
- Agriculture and Agri-Food Canada (AAFC), (2011). Soils of Alberta [WWW Document]. URL <https://sis.agr.gc.ca/cansis/soils/ab/soils.html> (accessed 6.15.21)
- Aladejana, J. A., Kalin, R. M., Sentenac, P., & Hassan, I. (2020). Assessing the impact of climate change on groundwater quality of the shallow coastal aquifer of eastern dahomey basin, Southwestern Nigeria. *Water (Switzerland)*, 12(1). <https://doi.org/10.3390/w12010224>
- Alberta Geological Survey, 2019. 3D provincial geological framework model of Alberta, version 2.
- Aliyari, F., Bailey, R. T., Tasdighi, A., Dozier, A., Arabi, M., & Zeiler, K. (2019). Coupled SWAT-MODFLOW model for large-scale mixed agro-urban river basins. *Environmental Modelling and Software*, 115(February), 200–210. <https://doi.org/10.1016/j.envsoft.2019.02.014>
- Amundsen, E. S., & Jensen, F. (2019). Groundwater management: Waiting for a drought*. *Natural Resource Modeling*, 32(4). <https://doi.org/10.1111/nrm.12209>
- Apurv, T., & Cai, X. (2020). Drought Propagation in Contiguous U.S. Watersheds: A Process-Based Understanding of the Role of Climate and Watershed Properties. *Water Resources Research*, 56(9), 1–23. <https://doi.org/10.1029/2020WR027755>

- Aravinthasamy, P., Karunanidhi, D., Subramani, T., & Roy, P. D. (2021). Demarcation of groundwater quality domains using GIS for best agricultural practices in the drought-prone Shanmuganadhi River basin of South India. *Environmental Science and Pollution Research*, 28(15), 18423–18435. <https://doi.org/10.1007/s11356-020-08518-5>
- Arnold, J., Kiniry, R., Williams, E., Haney, S., Neitsch, S. (2012). *Soil & Water Assessment Tool, Texas Water Resources Institute-TR-439*.
- Bailey, R.T., Wible, T.C., Arabi, M., Records, R.M., Ditty, J., 2016. Assessing regional-scale spatio-temporal patterns of groundwater–surface water interactions using a coupled SWAT-MODFLOW model. *Hydrological Processes* 30, 4420–4433. <https://doi.org/10.1002/hyp.10933>
- Barnett, T. P., Adam, J. C., & Lettenmaier, D. P. (2005). Potential impacts of a warming climate on water availability in snow-dominated regions. *Nature*, 438(7066), 303–309. <https://doi.org/10.1038/nature04141>
- Barthel, R., & Banzhaf, S. (2016). Groundwater and Surface Water Interaction at the Regional-scale – A Review with Focus on Regional Integrated Models. *Water Resources Management*, 30(1), 1–32. <https://doi.org/10.1007/s11269-015-1163-z>
- Best, L.C., Lowry, C.S., (2014). Quantifying the potential effects of high-volume water extractions on water resources during natural gas development. Marcellus Shale, NY. *Journal of Hydrology.: Regional Studies* 1, 1-16.
- Bloomfield, J. P., & Marchant, B. P. (2013). Analysis of groundwater drought building on the standardised precipitation index approach. *Hydrology and Earth System Sciences*, 17(12), 4769–4787. <https://doi.org/10.5194/hess-17-4769-2013>
- Bloomfield, J. P., Marchant, B. P., Bricker, S. H., & Morgan, R. B. (2015). Regional analysis of groundwater droughts using hydrograph classification. *Hydrology and Earth System Sciences*, 19(10), 4327–4344. <https://doi.org/10.5194/hess-19-4327-2015>
- Brauns, B., Cuba, D., Bloomfield, J. P., Hannah, D. M., Jackson, C., Marchant, B. P., Heudorfer, B., Van Loon, A. F., Bessière, H., Thunholm, B., & Schubert, G. (2020). The Groundwater Drought Initiative (GDI): Analysing and understanding groundwater drought across Europe. *Proceedings of the International Association of Hydrological Sciences*, 383, 297–305. <https://doi.org/10.5194/piahs-383-297-2020>
- Broberg, M. C., Högy, P., Feng, Z., & Pleijel, H. (2019). Effects of elevated CO₂ on wheat yield: Non-linear response and relation to site productivity. *Agronomy*, 9(5), 1–18. <https://doi.org/10.3390/agronomy9050243>

- Brown, R.D., B. Bransnett, 2010. Canadian Meteorological Centre (CMC) Daily Snow Depth Analysis Data, Version 1. [WWW Document]. Boulder, Color. USA. NASA Natl. Snow Ice Data Cent. Distrib. Act. Arch. Cent. <https://doi.org/10.5067/W9FOYWH0EQZ3>
- Cai, Z., Wang, W., Zhao, M., Ma, Z., Lu, C., & Li, Y. (2020). Interaction between surface water and groundwater in yinchuan plain. *Water (Switzerland)*, *12*(9), 1–23. <https://doi.org/10.3390/w12092635>
- Candela, L., Elorza, F. J., Tamoh, K., Jiménez-Martínez, J., & Aureli, A. (2014). Groundwater modelling with limited data sets: The Chari-Logone area (Lake Chad Basin, Chad). *Hydrological Processes*, *28*(11), 3714–3727. <https://doi.org/10.1002/hyp.9901>
- Castle, S. L., Thomas, B. F., John T. Reager, M. R., & Sean C. Swenson, J. S. F. (2014). future water security of the Colorado River Basin. *Geophysical Research Letters*, *41*, 5904–5911. <https://doi.org/10.1002/2014GL061055.Received>
- Chaponniere, A., Boulet, G., Chehbouni, A., & Aresmouk, M. (2007). Understanding hydrological processes with scarce data in a mountain environment. *Hydrological Processes*, 1908–1921. <https://doi.org/10.1002/hyp>
- Chen, M., Izady, A., Abdalla, O.A., 2017. An efficient surrogate-based simulation-optimization method for calibrating a regional MODFLOW model. *Journal of Hydrology* 544, 591–603. <https://doi.org/10.1016/j.jhydrol.2016.12.011>
- Chou, F. N. F., & Wu, C. W. (2010). Reducing the impacts of flood-induced reservoir turbidity on a regional water supply system. *Advances in Water Resources*, *33*(2), 146–157. <https://doi.org/10.1016/j.advwatres.2009.10.011>
- Chunn, D., Faramarzi, M., Smerdon, B., Alessi, D.S., 2019. Application of an integrated SWAT-MODFLOW model to evaluate potential impacts of climate change and water withdrawals on groundwater-surface water interactions in west-central Alberta. *Water (Switzerland)* 11. <https://doi.org/10.3390/w11010110>
- Clark, B. R., Hart, R. M., & Gurdak, J. J. (2011). Groundwater availability of the Mississippi Embayment: Professional Paper 1785. In *U.S. Geological Survey*.
- Condon, L. E., Atchley, A. L., & Maxwell, R. M. (2020). Evapotranspiration depletes groundwater under warming over the contiguous United States. *Nature Communications*, *11*(1). <https://doi.org/10.1038/s41467-020-14688-0>
- Corona, C. R., Gurdak, J. J., Dickinson, J. E., Ferré, T. P. A., & Maurer, E. P. (2018). Climate variability and vadose zone controls on damping of transient recharge. *Journal of Hydrology*, *561*, 1094–1104. <https://doi.org/10.1016/j.jhydrol.2017.08.028>

- DeBeer, C. (2012). *Simulating Areal Snow cover Depletion and Snowmelt Runoff in Alpine Terrain* (Issue May) *PhD Thesis* [University of Saskatchewan]. <https://library-archives.canada.ca/eng/services/services-libraries/theses/Pages/item.aspx?idNumber=1032965929>
- DeBeer, C. M., & Pomeroy, J. W. (2017). Influence of snowpack and melt energy heterogeneity on snow cover depletion and snowmelt runoff simulation in a cold mountain environment. *Journal of Hydrology*, 553, 199–213. <https://doi.org/10.1016/j.jhydrol.2017.07.051>
- Dierauer, J. R., Allen, D. M., & Whitfield, P. H. (2019). Snow Drought Risk and Susceptibility in the Western United States and Southwestern Canada. *Water Resources Research*, 55(4), 3076–3091. <https://doi.org/10.1029/2018WR023229>
- Dillon, P., Escalante, E. F., Megdal, S. B., & Massmann, G. (2020). Managed aquifer recharge for water resilience. *Water (Switzerland)*, 12(7), 1–11. <https://doi.org/10.3390/W12071846>
- Domenico, P. A., & Mifflin, M. D. (1965). Water from low-permeability sediments and land subsidence. *Water Resources Research*, 1(4), 563–576. <https://doi.org/10.1029/wr001i004p00563>
- Döscher, R., Acosta, M., Alessandri, A., Anthoni, P., Arsouze, T., Bergman, T., Bernardello, R., Boussetta, S., Caron, L. P., Carver, G., Castrillo, M., Catalano, F., Cvijanovic, I., Davini, P., Dekker, E., Doblas-Reyes, F. J., Docquier, D., Echevarria, P., Fladrich, U., ... Zhang, Q. (2022). The EC-Earth3 Earth system model for the Coupled Model Intercomparison Project 6. *Geoscientific Model Development*, 15(7), 2973–3020. <https://doi.org/10.5194/gmd-15-2973-2022>
- Earman, S., Campbell, A. R., Phillips, F. M., & Newman, B. D. (2006). Isotopic exchange between snow and atmospheric water vapor: Estimation of the snowmelt component of groundwater recharge in the southwestern United States. *Journal of Geophysical Research Atmospheres*, 111(9), 1–18. <https://doi.org/10.1029/2005JD006470>
- Ellis, C. R., Pomeroy, J. W., Brown, T., & MacDonald, J. (2010). Simulation of snow accumulation and melt in needleleaf forest environments. *Hydrology and Earth System Sciences*, 14(6), 925–940. <https://doi.org/10.5194/hess-14-925-2010>
- Ellis, C. R., Pomeroy, J. W., Essery, R. L. H., & Link, T. E. (2011). Effects of needleleaf forest cover on radiation and snowmelt dynamics in the Canadian Rocky Mountains. *Canadian Journal of Forest Research*, 41(3), 608–620. <https://doi.org/10.1139/X10-227>
- Eyring, V., Bony, S., Meehl, G. A., Senior, C. A., Stevens, B., Stouffer, R. J., & Taylor, K. E. (2016). Overview of the Coupled Model Intercomparison Project Phase 6 (CMIP6) experimental design and organization. *Geoscientific Model Development*, 9(5), 1937–1958. <https://doi.org/10.5194/gmd-9-1937-2016>

- Fan, X., Ma, Z., Yang, Q., Han, Y., & Mahmood, R. (2015). Land use/land cover changes and regional climate over the Loess Plateau during 2001–2009. Part II: interrelationship from observations. *Climatic Change*, 129(3–4), 441–455. <https://doi.org/10.1007/s10584-014-1068-5>
- Faramarzi, M., Abbaspour, K.C., Adamowicz, W.L.V., Lu, W., Fennell, J., Zehnder, A.J.B., Goss, G.G., (2017). Uncertainty based assessment of dynamic freshwater scarcity in semi-arid watersheds of Alberta, Canada. *Journal of Hydrology: Regional Studies* 9, 48–68. <https://doi.org/10.1016/j.ejrh.2016.11.003>
- Faramarzi, M., Srinivasan, R., Irvani, M., Bladon, K.D., Abbaspour, K.C., Zehnder, A.J.B., Goss, G.G., (2015). Setting up a hydrological model of Alberta: Data discrimination analyses prior to calibration. *Environmental Modelling and Software* 74, 48–65. <https://doi.org/10.1016/j.envsoft.2015.09.006>
- Flerchinger, G. N., Deng, Y., & Cooley, K. R. (1993). Groundwater response to snowmelt in a mountainous watershed: testing of a conceptual model. *Journal of Hydrology*, 152(1–4), 201–214. [https://doi.org/10.1016/0022-1694\(93\)90146-Z](https://doi.org/10.1016/0022-1694(93)90146-Z)
- Food and Agricultural Organization of the United Nations, 2003. Digital soil map of the world and derived soil properties. Rome, Italy: FAO.
- Francioli, D., Cid, G., Kanukollu, S., Ulrich, A., Hajirezaei, M. R., & Kolb, S. (2021). Flooding Causes Dramatic Compositional Shifts and Depletion of Putative Beneficial Bacteria on the Spring Wheat Microbiota. *Frontiers in Microbiology*, 12(November), 1–15. <https://doi.org/10.3389/fmicb.2021.773116>
- Freudiger, D., Kohn, I., Seibert, J., Stahl, K., & Weiler, M. (2017). Snow redistribution for the hydrological modeling of alpine catchments. *Wiley Interdisciplinary Reviews: Water*, 4(5), 1–16. <https://doi.org/10.1002/WAT2.1232>
- Gagniuc, Paul A. (2017). *Markov Chains: From Theory to Implementation and Experimentation*. USA, NJ: John Wiley & Sons. pp. 1–256. [ISBN 978-1-119-38755-8](https://doi.org/10.1002/9781119387558).
- Gao, H., & Shao, M. (2015). Effects of temperature changes on soil hydraulic properties. *Soil and Tillage Research*, 153, 145–154. <https://doi.org/10.1016/j.still.2015.05.003>
- Gebremichael, M., Krishnamurthy, P. K., Ghebremichael, L. T., & Alam, S. (2021). What drives crop land use change during multi-year droughts in California’s central valley? Prices or concern for water? *Remote Sensing*, 13(4), 1–19. <https://doi.org/10.3390/rs13040650>
- Government of Alberta, Alberta Climate and Atlas Maps [WWW document]. URL <http://agriculture.alberta.ca/acis/climate-maps.jsp> (accessed 6.15.21)
- Government of Alberta, Alberta River Basins map [WWW Document] URL <https://rivers.alberta.ca/> (accessed 8.10.21)

- Government of Alberta, Alberta Water Well Information Database [WWW Document] URL <http://environment.alberta.ca/apps/GOWN/#> (accessed 12.14.21)
- Government of Canada, (2019). Historical Climate Data [WWW Document]. URL http://climate.weather.gc.ca/historical_data/search_historic_data_e.html (accessed 6.15.21)
- Government of Canada, 2017. Canadian Land Cover, Circa 2000 (Vector) - GeoBase Series, 1996-2005 [WWW Document]. URL <https://open.canada.ca/data/en/dataset/97126362-5a85-4fe0-9dc2-915464cfdbb7> (accessed 4.15.20).
- Gray, D. M., & Landine, P. G. (1988). An energy-budget snowmelt model for the Canadian Prairies. *Canadian Journal of Earth Sciences*, 25(8), 1292–1303. <https://doi.org/10.1139/e88-124>
- H.Shumway and D.S. Stoffer. *Time Series Analysis and Its Applications: With R Examples*. Springer, 2017. pp-32
- Han, Z., Huang, S., Huang, Q., Leng, G., Wang, H., Bai, Q., Zhao, J., Ma, L., Wang, L., & Du, M. (2019). Propagation dynamics from meteorological to groundwater drought and their possible influence factors. *Journal of Hydrology*, 578(September). <https://doi.org/10.1016/j.jhydrol.2019.124102>
- Harding, R. ., & Pomeroy, J. . (1996). The Energy Balance of the Winter Boreal Landscape. *Journal of Climate*, 9(11), 2778–2787. https://journals.ametsoc.org/view/journals/clim/9/11/1520-0442_1996_009_2778_tebotw_2_0_co_2.xml
- Hardy, J. P., Melloh, R., Robinson, P., & Jordan, R. (2000). Incorporating effects of forest litter in a snow process model. *Hydrological Processes*, 14(18), 3227–3237. [https://doi.org/10.1002/1099-1085\(20001230\)14:18<3227::AID-HYP198>3.0.CO;2-4](https://doi.org/10.1002/1099-1085(20001230)14:18<3227::AID-HYP198>3.0.CO;2-4)
- Hayashi, M. (2020). Alpine Hydrogeology: The Critical Role of Groundwater in Sourcing the Headwaters of the World. *Groundwater*, 58(4), 498–510. <https://doi.org/10.1111/gwat.12965>
- Hayashi, M., & Rosenberry, D. O. (2002). Effects of Groundwater Exchange on the Hydrology and Ecology of Surface Water. *Ground Water*, 40, 309–316. <https://doi.org/10.1111/j.1745-6584.2002.tb02659.x>
- Heath, R. C. (1983). *Basic Ground-Water Hydrology* (Water Supply Paper 2220). U.S. Geological Survey.
- Hokanson, K. J., Mendoza, C. A., & Devito, K. J. (2019). Interactions between Regional Climate, Surficial Geology, and Topography: Characterizing Shallow Groundwater Systems in Sub-

- humid, Low-Relief Landscapes. *Water Resources Research*, 55(1), 284–297. <https://doi.org/10.1029/2018WR023934>
- Hosking, J. R. M. (1996). Fortran routines for use with the method of L-moments, Version 3. Research Report RC20525, IBM Research Division, Yorktown Heights, N.Y.
- Hosking, J. R. M. (2022). *Package ‘lmom .’* [WWW Document]. URL <https://cran.r-project.org/web/packages/lmom/lmom.pdf>
- Hosking, J. R. M. and Wallis, J. R. (1997). Regional frequency analysis: an approach based on L-moments, Cambridge University Press, Appendix A.10.
- Huang, J., Cao, L., Yu, F., Liu, X., & Wang, L. (2021). Groundwater Drought and Cycles in Xuchang City, China. *Frontiers in Earth Science*, 9(September), 1–13. <https://doi.org/10.3389/feart.2021.736305>
- Huning, L. S., & AghaKouchak, A. (2020). Global snow drought hot spots and characteristics. *Proceedings of the National Academy of Sciences of the United States of America*, 117(33), 19753–19759. <https://doi.org/10.1073/PNAS.1915921117>
- IPCC. (2022). Climate Change 2022 - Mitigation of Climate Change - Working Group III. Cambridge University Press, 1454. <https://www.ipcc.ch/site/assets/uploads/2018/05/uncertainty-guidance-note.pdf>.%0Awww.cambridge.org
- Ireson, A. M., Barr, A. G., Johnstone, J. F., Mamet, S. D., van der Kamp, G., Whitfield, C. J., Michel, N. L., North, R. L., Westbrook, C. J., Debeer, C., Chun, K. P., Nazemi, A., & Sagin, J. (2015). The changing water cycle: the Boreal Plains ecozone of Western Canada. *Wiley Interdisciplinary Reviews: Water*, 2(5), 505–521. <https://doi.org/10.1002/WAT2.1098>
- Islam, S. ul, Déry, S. J., & Werner, A. T. (2017). Future Climate Change Impacts on Snow and Water Resources of the Fraser River Basin, British Columbia. *Journal of Hydrometeorology*, 18(2), 473–496. <https://doi.org/10.1175/jhm-d-16-0012.1>
- J.D.Cryer and K.S. Chan. *Time Series Analysis with Applications in R*. Springer, 2011 pp-265
- Jacobs, J. M., Mergelsberg, S. L., Lopera, A. F., & Myers, D. A. (2002). Evapotranspiration from a wet prairie wetland under drought conditions: Paynes prairie preserve, Florida, USA. *Wetlands*, 22(2), 374–385. [https://doi.org/10.1672/0277-5212\(2002\)022\[0374:EFAWPW\]2.0.CO;2](https://doi.org/10.1672/0277-5212(2002)022[0374:EFAWPW]2.0.CO;2)
- Jarvis, A., Guevara, E., Reuter, H.I., Nelson, A.D., 2008. Hole-filled SRTM for the globe : version 4 : data grid.

- Jódar, J., Cabrera, J. A., Martos-Rosillo, S., Ruiz-Constán, A., González-Ramón, A., Lambán, L. J., Herrera, C., & Custodio, E. (2017). Groundwater discharge in high-mountain watersheds: A valuable resource for downstream semi-arid zones. The case of the Bérchules River in Sierra Nevada (Southern Spain). *Science of the Total Environment*, 593–594, 760–772. <https://doi.org/10.1016/j.scitotenv.2017.03.190>
- Jutglar, K., Hellwig, J., Stoelzle, M., & Lange, J. (2021). Post-drought increase in regional-scale groundwater nitrate in southwest Germany. *Hydrological Processes*, 35(8), 1–11. <https://doi.org/10.1002/hyp.14307>
- Kapnick, S., & Hall, A. (2012). Causes of recent changes in western North American snowpack. *Climate Dynamics*, 38(9–10), 1885–1899. <https://doi.org/10.1007/s00382-011-1089-y>
- Khalili, P., Razavi, S., Davies, E.G.R., Alessi, D.S., Faramarzi, M., 2023. Assessment of blue water-green water interchange under extreme warm and dry events across different ecohydrological regions of western Canada, *Journal of Hydrology*, In review.
- Kriauciuniene, J., Meilutyte-barauskiene, D., Rimkus, E., Kazys, J., & Vincevicius, A. (2008). Climate change impact on hydrological processes in Lithuanian Nemunas river basin. *Baltica*, 21(1), 13–23.
- Langevin, C. D., Hughes, J. D., Banta, E. R., Niswonger, R. G., Panday, S., & Provost, A. M. (2017). Documentation for the MODFLOW 6 Groundwater Flow Model: U.S. Geological Survey Techniques and Methods. In *Book 6, Modeling Techniques*. <https://pubs.usgs.gov/tm/06/a55/tm6a55.pdf>
- Langridge, R., & Van Schmidt, N. D. (2020). Groundwater and Drought Resilience in the SGMA Era. *Society and Natural Resources*, 33(12), 1530–1541. <https://doi.org/10.1080/08941920.2020.1801923>
- Lee, J. M., Park, J. H., Chung, E., & Woo, N. C. (2018). Assessment of groundwater drought in the Mangyeong River Basin, Korea. *Sustainability (Switzerland)*, 10(3). <https://doi.org/10.3390/su10030831>
- Li, B., & Rodell, M. (2015). Evaluation of a model-based groundwater drought indicator in the conterminous U.S. *Journal of Hydrology*, 526, 78–88. <https://doi.org/10.1016/j.jhydrol.2014.09.027>
- Li, X., Dong, J., Gruda, N. S., Chu, W., & Duan, Z. (2020). Interactive effects of the CO2 enrichment and nitrogen supply on the biomass accumulation, gas exchange properties, and mineral elements concentrations in cucumber plants at different growth stages. *Agronomy*, 10(1). <https://doi.org/10.3390/agronomy10010139>

- Link, T. E., & Marks, D. (1999). Point simulation of seasonal snow cover dynamics beneath boreal forest canopies. *Journal of Geophysical Research Atmospheres*, *104*(D22), 27841–27857. <https://doi.org/10.1029/1998JD200121>
- Long, D., Yang, W., Scanlon, B. R., Zhao, J., Liu, D., Burek, P., Pan, Y., You, L., & Wada, Y. (2020). South-to-North Water Diversion stabilizing Beijing's groundwater levels. *Nature Communications*, *11*(1). <https://doi.org/10.1038/s41467-020-17428-6>
- Lundberg, A., Ala-Aho, P., Eklo, O., Klöve, B., Kværner, J., & Stumpp, C. (2016). Snow and frost: Implications for spatiotemporal infiltration patterns - a review. *Hydrological Processes*, *30*(8), 1230–1250. <https://doi.org/10.1002/hyp.10703>
- MacDonald, R. J., Byrne, J. M., Boon, S., & Kienzle, S. W. (2012). Modelling the Potential Impacts of Climate Change on Snowpack in the North Saskatchewan River Watershed, Alberta. *Water Resources Management*, *26*(11), 3053–3076. <https://doi.org/10.1007/s11269-012-0016-2>
- Masud, B., Cui, Q., Ammar, M. E., Bonsal, B. R., Islam, Z., & Faramarzi, M. (2021). Means and extremes: Evaluation of a CMIP6 multi-model ensemble in reproducing historical climate characteristics across Alberta, Canada. *Water* DOI: <https://doi.org/10.3390/w13050737>
- Masud, M. B., Khaliq, M. N., & Wheeler, H. S. (2015). Analysis of meteorological droughts for the Saskatchewan River Basin using univariate and bivariate approaches. *Journal of Hydrology*, *522*, 452–466. <https://doi.org/10.1016/j.jhydrol.2014.12.058>
- Melloh, R. A., Hardy, J. P., Bailey, R. N., & Hall, T. J. (2002). An efficient snow albedo model for the open and sub-canopy. *Hydrological Processes*, *16*(18), 3571–3584. <https://doi.org/10.1002/hyp.1229>
- Meng, Y., Liu, G., & Li, M. (2015). Tracing the sources and processes of groundwater in an alpine glacierized region in Southwest China: Evidence from environmental isotopes. *Water (Switzerland)*, *7*(6), 2673–2690. <https://doi.org/10.3390/w7062673>
- Mianabadi, A., Derakhshan, H., Davary, K., Hasheminia, S. M., & Hrachowitz, M. (2020). A Novel Idea for Groundwater Resource Management during Megadrought Events. *Water Resources Management*, *34*(5), 1743–1755. <https://doi.org/10.1007/s11269-020-02525-4>
- Mizukami, N., Clark, M. P., Slater, A. G., Brekke, L. D., Elsner, M. M., Arnold, J. R., & Gangopadhyay, S. (2014). Hydrologic implications of different large-scale meteorological model forcing datasets in mountainous regions. *Journal of Hydrometeorology*, *15*(1), 474–488. <https://doi.org/10.1175/JHM-D-13-036.1>
- Mohammed, A. A., Pavlovskii, I., Cey, E. E., & Hayashi, M. (2019). Effects of preferential flow on snowmelt partitioning and groundwater recharge in frozen soils. *Hydrology and Earth System Sciences*, *23*(12), 5017–5031. <https://doi.org/10.5194/hess-23-5017-2019>

- Morris, D. A., & Johnson, A. I. (1967). *Summary of Hydrologic and Physical Properties of Rock and Soil Materials, as Analyzed by the Hydrologic Laboratory of the U.S. Geological Survey* (Geological Survey Water-Supply Paper 1839-D). U.S. Geological Survey.
- Mote, P. W., Hamlet, A. F., Clark, M. P., & Lettenmaier, D. P. (2005). Declining mountain snowpack in western north America. *Bulletin of the American Meteorological Society*, 86(1), 39–49. <https://doi.org/10.1175/BAMS-86-1-39>
- National Oceanic and Atmospheric Administration. (2018). Snow drought. Drought.gov. <https://www.drought.gov/what-is-drought/snow-drought>. (accessed 3.12.20).
- Neitsch, S. ., Arnold, J. ., Kiniry, J. ., & Williams, J. . (2011). Soil & Water Assessment Tool Theoretical Documentation Version 2009. *Texas Water Resources Institute*, 1–647. <https://doi.org/10.1016/j.scitotenv.2015.11.063>
- Nepal, S., et al (2014). Upstream–downstream linkages of hydrological processes in the Himalayan region. *Ecological Processes*, 2014 3:19. <https://doi.org/10.1186/s13717-014-0019-4>
- Niswonger, R. G. (2011). MODFLOW-NWT , A Newton Formulation for MODFLOW-2005. In *Book 6, Modeling Techniques*.
- Niu, Q., Liu, L., Heng, J., Li, H., & Xu, Z. (2020). A Multi-Index Evaluation of Drought Characteristics in the Yarlung Zangbo River Basin of Tibetan Plateau, Southwest China. *Frontiers in Earth Science*, 8(June), 1–16. <https://doi.org/10.3389/feart.2020.00213>
- North Saskatchewan Watershed Alliance, 2005. The State of the North Sask River Watershed Report [WWW Document] URL <https://www.nswa.ab.ca/our-watershed/> (accessed 7.16.21)
- O’Neill, B. C., Tebaldi, C., Van Vuuren, D. P., Eyring, V., Friedlingstein, P., Hurtt, G., Knutti, R., Kriegler, E., Lamarque, J. F., Lowe, J., Meehl, G. A., Moss, R., Riahi, K., & Sanderson, B. M. (2016). The Scenario Model Intercomparison Project (ScenarioMIP) for CMIP6. *Geoscientific Model Development*, 9(9), 3461–3482. <https://doi.org/10.5194/gmd-9-3461-2016>
- Park, S., Kim, H., & Jang, C. (2021). Impact of groundwater abstraction on hydrological responses during extreme drought periods in the boryeong dam catchment, korea. *Water (Switzerland)*, 13(15). <https://doi.org/10.3390/w13152132>
- Pathak, A. A., & Dodamani, B. M. (2019). Trend Analysis of Groundwater Levels and Assessment of Regional Groundwater Drought: Ghataprabha River Basin, India. *Natural Resources Research*, 28(3), 631–643. <https://doi.org/10.1007/s11053-018-9417-0>

- Pathak, A. A., & Dodamani, B. M. (2021). Connection between Meteorological and Groundwater Drought with Copula-Based Bivariate Frequency Analysis. *Journal of Hydrologic Engineering*, 26(7), 05021015. [https://doi.org/10.1061/\(asce\)he.1943-5584.0002089](https://doi.org/10.1061/(asce)he.1943-5584.0002089)
- Paznekas, A., & Hayashi, M. (2016). Groundwater contribution to winter streamflow in the Canadian Rockies. *Canadian Water Resources Journal*, 41(4), 484–499. <https://doi.org/10.1080/07011784.2015.1060870>
- Petersen-Perlman, J. D., Aguilar-Barajas, I., & Megdal, S. B. (2022). Drought and groundwater management: Interconnections, challenges, and policy responses. *Current Opinion in Environmental Science and Health*, 28, 100364. <https://doi.org/10.1016/j.coesh.2022.100364>
- Pieper, P., Düsterhus, A., & Baehr, J. (2020). A universal Standardized Precipitation Index candidate distribution function for observations and simulations. *Hydrology and Earth System Sciences*, 24(9), 4541–4565. <https://doi.org/10.5194/hess-24-4541-2020>
- Pomeroy, J. W., & Brun, E. (2000). Physical properties of snow. In *Encyclopedia of Earth Sciences Series: Vol. Part 3* (pp. 859–863). https://doi.org/10.1007/978-90-481-2642-2_422
- Pomeroy, J. W., Gray, D. M., Shook, K. R., Toth, B., Essery, R. L. H., Pietroniro, A., & Hedstrom, N. (1998). An evaluation of snow accumulation and ablation processes for land surface modelling. *Hydrological Processes*, 12(15), 2339–2367. [https://doi.org/10.1002/\(SICI\)1099-1085\(199812\)12:15<2339::AID-HYP800>3.0.CO;2-L](https://doi.org/10.1002/(SICI)1099-1085(199812)12:15<2339::AID-HYP800>3.0.CO;2-L)
- Porter, J. R., & Semenov, M. A. (2005). Crop responses to climatic variation. *Philosophical Transactions of the Royal Society B: Biological Sciences*, 360(1463), 2021–2035. <https://doi.org/10.1098/rstb.2005.1752>
- Pradhanang, S. M., Anandhi, A., Mukundan, R., Zion, M. S., Pierson, D. C., Schneiderman, E. M., Matonse, A., & Frei, A. (2011). Application of SWAT model to assess snowpack development and streamflow in the Cannonsville watershed, New York, USA. *Hydrological Processes*, 25(21), 3268–3277. <https://doi.org/10.1002/hyp.8171>
- Rahman, K., Maringanti, C., Beniston, M., Widmer, F., Abbaspour, K., & Lehmann, A. (2013). Streamflow Modeling in a Highly Managed Mountainous Glacier Watershed Using SWAT: The Upper Rhone River Watershed Case in Switzerland. *Water Resources Management*, 27(2), 323–339. <https://doi.org/10.1007/s11269-012-0188-9>
- Refsgaard, J. C., Højberg, A. L., Møller, I., Hansen, M., & Søndergaard, V. (2010). Groundwater modeling in integrated water resources management - visions for 2020. *Ground Water*, 48(5), 633–648. <https://doi.org/10.1111/j.1745-6584.2009.00634.x>
- Sauchyn, D., Rehan, A. M., Basu, S., Andreichuk, Y., Gurrupu, S., Kerr, S., & Bedoya, J. M. (2020). *Natural and Externally Forced Hydroclimatic Variability in the North Saskatchewan River Basin : Support for EPCOR ' s Climate Change Strategy* (Issue September).

- Schuol, J., Abbaspour, K. C., Srinivasan, R., & Yang, H. (2008). Estimation of freshwater availability in the West African sub-continent using the SWAT hydrologic model. *Journal of Hydrology*, 352(1–2), 30–49. <https://doi.org/10.1016/j.jhydrol.2007.12.025>
- Shabani, A., Woznicki, S. A., Mehaffey, M., Butcher, J., Wool, T. A., & Whung, P. Y. (2021). A coupled hydrodynamic (HEC-RAS 2D) and water quality model (WASP) for simulating flood-induced soil, sediment, and contaminant transport. *Journal of Flood Risk Management*, 14(4), 1–17. <https://doi.org/10.1111/jfr3.12747>
- Smerdon, B.D., Hughes, A.T., Jean, G., 2017. Permeability Measurements of Upper Cretaceous and Paleogene Bedrock Cores made from 2004-2015 (tabular data, tab-delimited format, to accompany Open File Report 2016-03).
- Soylu, M. E., Istanbuluoglu, E., Lenters, J. D., & Wang, T. (2011). Quantifying the impact of groundwater depth on evapotranspiration in a semi-arid grassland region. *Hydrology and Earth System Sciences*, 15(3), 787–806. <https://doi.org/10.5194/hess-15-787-2011>
- Spruill, C. A., Workman, S. R., & Taraba, J. L. (2000). Simulation of daily and monthly stream discharge from small watersheds using the SWAT model. *Transactions of the American Society of Agricultural Engineers*, 43(6), 1431–1439. <https://doi.org/10.13031/2013.3041>
- Stähli, M., Bayard, D., Wydler, H., & Flühler, H. (2004). Snowmelt infiltration into alpine soils visualized by dye tracer technique. *Arctic, Antarctic, and Alpine Research*, 36(1), 128–135. [https://doi.org/10.1657/1523-0430\(2004\)036\[0128:SIASV\]2.0.CO;2](https://doi.org/10.1657/1523-0430(2004)036[0128:SIASV]2.0.CO;2)
- Staudinger, M., Stahl, K., & Seibert, J. (2014). *A drought index accounting for snow*. 5375–5377. <https://doi.org/10.1002/2013WR014979.Reply>
- Stocker, T. , Qin, D., Plattner, G.-K., Tignor, M., Allen, S. , Boschung, J., Nauels, A., Xia, Y., Bex, V., & Midgley, P. . (2013). Climate Change 2013: The Physical Science Basis. Contribution of Working Group I to the Fifth Assessment Report of the Intergovernmental Panel on Climate Change. In *Cambridge University Press*.
- Stouffer, R. J., Eyring, V., Meehl, G. A., Bony, S., Senior, C., Stevens, B., & Taylor, K. E. (2017). CMIP5 scientific gaps and recommendations for CMIP6. *Bulletin of the American Meteorological Society*, 98(1), 95–105. <https://doi.org/10.1175/BAMS-D-15-00013.1>
- Tanachaichoksirikun, P., Seeboonruang, U., Fogg, G.E., 2020. Improving Groundwater Model in Regional Sedimentary Basin Using Hydraulic Gradients. *KSCE Journal of Civil Engineering* 24, 1655–1669. <https://doi.org/10.1007/s12205-020-1781-8>
- Teshager, A. D., Gassman, P. W., Secchi, S., Schoof, J. T., & Misgna, G. (2016). Modeling Agricultural Watersheds with the Soil and Water Assessment Tool (SWAT): Calibration and

- Validation with a Novel Procedure for Spatially Explicit HRUs. *Environmental Management*, 57(4), 894–911. <https://doi.org/10.1007/s00267-015-0636-4>
- Texas A&M University, (2012). *SWAT: Soil & Water Assessment Tool* [WWW Document]. URL <https://swat.tamu.edu/> (accessed 3.12.21)
- Thomas B. McKee, N. J. D. and J. K. (1993). THE RELATIONSHIP OF DROUGHT FREQUENCY AND DURATION TO TIME SCALES. *Journal of Surgical Oncology*, 105(8), 818–824. <https://doi.org/10.1002/jso.23002>
- Tibshirani, R. (1996). Regression Shrinkage and Selection Via the Lasso. *Journal of the Royal Statistical Society: Series B (Methodological)*, 58(1), 267–288, 1996. ISSN 00359246. <https://doi.org/10.1111/j.2517-6161.1996.tb02080.x>
- United States Geological Survey. (2016). USGS: Groundwater and Drought. <https://water.usgs.gov/ogw/drought/#:%7E:text=A%20groundwater%20drought%20typically%20refers,for%20humans%20and%20the%20environment.> (accessed 3.12.20).
- United States Geological Survey. (2019). USGS: Snowmelt Runoff and Water Cycle. https://www.usgs.gov/special-topic/water-science-school/science/snowmelt-runoff-and-water-cycle?qt-science_center_objects=0#qt-science_center_objects. (accessed 10.18.21).
- Van der Kamp, G., & Hayashi, M. (2009). Groundwater-wetland ecosystem interaction in the semiarid glaciated plains of North America. *Hydrogeology Journal*, 17(1), 203–214. <https://doi.org/10.1007/s10040-008-0367-1>
- Van Lanen, H. A. J., & Peters, E. (2000). *Definition, Effects and Assessment of Groundwater Droughts*. 49–61. https://doi.org/10.1007/978-94-015-9472-1_4
- Van Loon, A. F., Van Lanen, H. A. J., Hisdal, H., Tallaksen, L. M., Fendeková, M., Oosterwijk, J., Horvát, O., & Machlica, A. (2010). Understanding hydrological winter drought in Europe. *IAHS-AISH Publication*, 340(January), 189–197.
- Vano, J. A., Scott, M. J., Voisin, N., Stöckle, C. O., Hamlet, A. F., Mickelson, K. E. B., Elsner, M. M. G., & Lettenmaier, D. P. (2010). Climate change impacts on water management and irrigated agriculture in the Yakima River Basin, Washington, USA. *Climatic Change*, 102(1–2), 287–317. <https://doi.org/10.1007/s10584-010-9856-z>
- Voldoire, A., Saint-Martin, D., Sénési, S., Decharme, B., Alias, A., Chevallier, M., Colin, J., Guérémy, J. F., Michou, M., Moine, M. P., Nabat, P., Roehrig, R., Salas y Méliá, D., Sférian, R., Valcke, S., Beau, I., Belamari, S., Berthet, S., Cassou, C., ... Waldman, R. (2019). Evaluation of CMIP6 DECK Experiments With CNRM-CM6-1. *Journal of Advances in Modeling Earth Systems*, 11(7), 2177–2213. <https://doi.org/10.1029/2019MS001683>

- Water for Life: Facts about Water in Alberta 2002*. (2010). Alberta Environment Information Centre.
- Waterloo Hydrogeologic. (2018). User 's Manual Visual MODFLOW Flex 5.1. In *Waterloo Hydrogeologic*.
- Weedon, G. P., Balsamo, G., Bellouin, N., Gomes, S., Best, M. J., & Viterbo, P. (2014). The WFDEI meteorological forcing data set: WATCH Forcing Data methodology applied to ERA-Interim reanalysis data. *Water Resources Research*, 50(9), 7505–7514. <https://doi.org/10.1002/2014WR015638>
- Wu, J., Chen, X., Gao, L., Yao, H., Chen, Y., & Liu, M. (2016). Response of Hydrological Drought to Meteorological Drought under the Influence of Large Reservoir. *Advances in Meteorology*, 2016. <https://doi.org/10.1155/2016/2197142>
- Wu, T., Lu, Y., Fang, Y., Xin, X., Li, L., Li, W., Jie, W., Zhang, J., Liu, Y., Zhang, L., Zhang, F., Zhang, Y., Wu, F., Li, J., Chu, M., Wang, Z., Shi, X., Liu, X., Wei, M., ... Liu, X. (2019). The Beijing Climate Center Climate System Model (BCC-CSM): The main progress from CMIP5 to CMIP6. *Geoscientific Model Development*, 12(4), 1573–1600. <https://doi.org/10.5194/gmd-12-1573-2019>
- Wu, T., Yu, R., Lu, Y., Jie, W., Fang, Y., Zhang, J., Zhang, L., Xin, X., Li, L., Wang, Z., Liu, Y., Zhang, F., Wu, F., Chu, M., Li, J., Li, W., Zhang, Y., Shi, X., Zhou, W., ... Hu, A. (2021). BCC-CSM2-HR: A high-resolution version of the Beijing Climate Center Climate System Model. *Geoscientific Model Development*, 14(5), 2977–3006. <https://doi.org/10.5194/gmd-14-2977-2021>
- Wu, W. Y., Lo, M. H., Wada, Y., Famiglietti, J. S., Reager, J. T., Yeh, P. J. F., Ducharme, A., & Yang, Z. L. (2020). Divergent effects of climate change on future groundwater availability in key mid-latitude aquifers. *Nature Communications*, 11(1), 1–9. <https://doi.org/10.1038/s41467-020-17581-y>
- Yadete, H., Kalinga, O., Beersing, A., & Biftu, G. (2008). Assessment of Climate Change Effects on Water Yield From the North Saskatchewan River Basin. In *North Saskatchewan Watershed Alliance* (Issue July).
- Yeh, H.-F. (2021). Spatiotemporal Variation of the Meteorological and Groundwater Droughts in Central Taiwan. *Frontiers in Water*, 3(February), 1–12. <https://doi.org/10.3389/frwa.2021.636792>
- Yimam, A. Y., Assefa, T. T., Sishu, F. K., Tilahun, S. A., Reyes, M. R., & Vara Prasad, P. V. (2021). Estimating surface and groundwater irrigation potential under different conservation agricultural practices and irrigation systems in the ethiopian highlands. *Water (Switzerland)*, 13(12). <https://doi.org/10.3390/w13121645>

- Yukimoto, S., Kawai, H., Koshiro, T., Oshima, N., Yoshida, K., Urakawa, S., Tsujino, H., Deushi, M., Tanaka, T., Hosaka, M., Yabu, S., Yoshimura, H., Shindo, E., Mizuta, R., Obata, A., Adachi, Y., & Ishii, M. (2019). The meteorological research institute Earth system model version 2.0, MRI-ESM2.0: Description and basic evaluation of the physical component. *Journal of the Meteorological Society of Japan*, 97(5), 931–965. <https://doi.org/10.2151/jmsj.2019-051>
- Zaremehrijardy, M., Razavi, S., & Faramarzi, M. (2021). *Assessment of the cascade of uncertainty in future snow depth projections across watersheds of mountainous, foothill, and plain areas in northern latitudes*. *Journal of Hydrology*, 598(November), 125735. <https://doi.org/10.1016/j.jhydrol.2020.125735>
- Zaremehrijardy, M., Victor, J., Park, S., Smerdon, B., Alessi, D., Faramarzi, M. (2022) *Assessment of snowmelt and groundwater-surface water dynamics in mountainous, foothills, and plains regions in northern latitudes*, *Journal of Hydrology*, in review.
- Zhang, C., & Long, D. (2021). Estimating Spatially Explicit Irrigation Water Use Based on Remotely Sensed Evapotranspiration and Modeled Root Zone Soil Moisture. *Water Resources Research*, 57(12), 1–27. <https://doi.org/10.1029/2021WR031382>
- Zhou, Y., & Li, W. (2011). A review of regional groundwater flow modeling. *Geoscience Frontiers*, 2(2), 205–214. <https://doi.org/10.1016/j.gsf.2011.03.003>

CHAPTER III – CONCLUSION

Research Summary

This research study used a calibrated and validated surface water and groundwater models to simulate snow water equivalent (SWE) and groundwater heads (GW) under historical (1983-2013) and future (2040-2073) periods. The simulated SWE and GW time series were used to construct SWE drought index (SWEI) and standardized GW drought index (SGWI) to analyze both historical and future drought characteristics, including intensity, duration, and, frequency across different eco-hydro(geo)logical settings (EHGs). Also, the propagation mechanism from snow drought to GW drought was studied in each EHG region, which determined the propagation time from surface to the GW system and the driving physical process that can potentially impact the variation of GW level time series. The study area was the North Saskatchewan River Basin (NSRB), which is selected because it is a snow dominated watershed with abundant GW resources (Maccagno.M & Kupper, 2009), as well as three distinctively different EHG regions (Mountains, Foothills, and Plains). Meanwhile, the study area possesses relatively sufficient hydrometric stations and observation wells data available for calibration and validation purposes. Given that the watershed encompasses diverse EHG settings and that snow processes is a primary process controlling hydrological cycle, it resembles watershed behaviors in mid-to-high latitude regions. Moreover, this watershed plays a fundamental role in the local ecosystem and downstream water consumption in socioeconomic sectors.

The future projections in this study were based on downscaled climate data (Masud et al., 2021) from an ensemble of five Global Climate Models (GCMs) of the Coupled Model Intercomparison Project Phase 6 (CMIP6) for two extreme Shared Socio-economic Pathways

(SSPs) including SSP126 and SSP585 (Riahi et al., 2017). The projected SWEI and SGWI were used to identify different classes of snow droughts and GW droughts based on US drought monitoring D-scale method (Svoboda et al., 2002) for each EHG. The results of the study indicated that characteristics of snow and GW droughts were reversed across different EHG regions under future SSP scenarios as compared to the historical period. Mountainous region experienced the worst historical snow drought as compared to Foothills and Plains, and the multi-model ensemble mean projections indicated more intensified and prolonged droughts with higher frequency in Mountains, leading to lower snow accumulation in Mountains. Among all regions, Plains experienced worst historical groundwater drought, and it was projected to experience higher intensity droughts in the future. Mountains, on the other hand, were projected to experience relatively less frequent and low intensity GW droughts compared to other two regions. This implies a potential shift of snow drought events to GW droughts in Plains and the opposite processes in the Mountains in the future.

The cross-correlation statistical analysis of the SWE and GW time series indicated that the historical propagation time for Mountains, Foothills, and Plains were 4 months, 5 months and 6 months respectively. This indicated that GW drought has the quickest response time in mountainous region compared to other regions, mainly due to its nature of landform. Nevertheless, the highest correlation among all regions was related to the plain region, indicating that variation in snow in the plain region is more related to the variation in groundwater, implying that snow droughts in the plain region can contribute more to the formation of groundwater droughts. Moreover, statistical analysis of the simulated SWE and GW time series and multi-model ensemble mean data indicated that future snow - GW drought propagation time for SSP 126 is shorter in the future (3-month for Mountains, 3-month for Foothills, and 5-month for Plains)

compared to historic period in all regions. The response time, based on multi-model ensemble mean analysis, was relatively shorter under SSP 585 with 2-month for Mountains, 3-month for Foothills, and no obvious relations in Plains, all of which suggesting intensified hydrologic processes such as evapotranspiration.

Using the SW-GW model outputs, we were also able to perform statistical analysis using LASSO variable selection method to determine what physical processes can exert dominant control on the GW level formation, which can provide an idea of how the propagation mechanism is being affected by other physical processes. We selected total of 12 physical parameters and determined the spatial variation for dominant physical processes under different EHG, and found out that soil water content and percolation are the most significant processes among all to impact the snow / GW propagation mechanism, and curve number was the most sensitive factor impacting mountain and foothill regions more than plain region. However, the propagation mechanism in the plain region is heavily impacted by evapotranspiration.

Study Conclusions and Implications

This study advances our understanding of the propagation mechanism between snow water and GW, as well as the physical driving processes that controls the interaction of snow water and GW. As also pointed out by other researchers, most of the recent studies did not address the connection between any forms of hydrological or meteorological droughts with GW droughts (Petersen-Perlman et al., 2022). Given that snow is a primary driver of hydrologic processes in most of mid-to-high latitude watersheds, the result of our study can provide valuable information for better understanding of snow water - groundwater relationship, which can inform water management and environmental protection. While droughts are inevitable and parts of natural

hydrologic cycle, but their frequency, intensity, and duration are projected to change due to the changes in climate under future global warming scenarios (Mianabadi et al., 2020). Hence, the understanding of how drought and groundwater relate is crucial (Brauns et al., 2020; Langridge & Van Schmidt, 2020). Our projections under two most extreme global warming scenarios (i.e., SSP126, known as the most environmental-friendly scenario; and SSP 585, as the worst global warming scenario) show strong regional differences of future drought characteristics, where Mountains GW drought tends to be less severe than historical record in the future, while Plains tends to be worse. This is consistent with a recent study arguing that drought can slow groundwater level recovery in agricultural areas compared to forested areas (Park et al., 2021). Such trend in Plains might result in prolonged groundwater deficit, which can potentially impact agricultural and ecosystem groundwater use in the region (Park et al., 2021). However, in Mountains, the intensified snow drought and slightly relieved GW drought implies that there might be a slight shift of water storage from snow to the groundwater system. This is like due to the accelerated snowmelt as a result of global warming, which can potentially generate more excess water infiltration to the root zone which can make its way to recharge GW compared to rainfall precipitation in the future (Earman et al., 2006; W. Y. Wu et al., 2020). Under this context, our result can be used as reference to discover what land management techniques can be implemented to mitigate different future droughts in each region. For example, in Plains, GW droughts might be relieved by improving of land management techniques such as increasing coverage of fallow land, crop type selection (Gebremichael et al., 2021), or changing irrigation patterns (Yimam et al., 2021) and increasing irrigation water use monitoring (Zhang & Long, 2021).

Also, droughts can significantly affect GW quality (Petersen-Perlman et al., 2022), such as increase in nitrate concentrations (Jutglar et al., 2021) or increase in certain redox-sensitive ions

and metals (Aladejana et al., 2020). Note that even though our study doesn't focus on water quality, but our modelling framework, and the simulated processes that drive interconnection between snow and GW droughts, can incorporate nutrient data and simulate nutrient transport, such as nitrate quantity in the shallow aquifer (Neitsch et al., 2011). Prediction and future projection of GW quality under various drought types can be beneficial in determining the best agricultural or industrial practices in drought-prone regions (Aravinthasamy et al., 2021). It is also worth noting that our study does not consider the impacts of large-scale natural climate variabilities including El-Nino Southern Oscillation (ENSO) or Pacific Decal Oscillation (PDO) (Corona et al., 2018; Han et al., 2019). Hence, future study is needed to consider the ensemble contemporary impacts of global warming and large-scale climatic variation to better capture the snow and GW drought characteristics.

Furthermore, our results showed how the propagation time varies in each region, as well as the variation in dominant physical processes, including the different weight for curve number, soil water, evapotranspiration, water yield and percolation. Then based on the regional differences, future studies can incorporate different regional-scale water resource management strategies such as conjunctive management for surface water and groundwater (Amundsen & Jensen, 2019; Apurv & Cai, 2020; Long et al., 2020), or managed aquifer recharge (MAR) (Dillon et al., 2020), to explore impacts of surface water - GW management strategies in improving drought characteristics.

Overall, the main conclusions of the study are listed as follows:

1. The characteristics of snow and GW droughts were reversed across different EHG regions under future SSP scenarios as compared to the historical period. Mountainous region experienced the worst historical snow drought as compared to Foothills and Plains, and the future projections indicated more intensified and prolonged droughts with higher frequency

in the future, leading to lower snow accumulation in Mountains. Among all regions, Plains experienced worst groundwater drought historically, and it was projected to experience higher intensity droughts in the future. Mountains, on the other hand, were projected to experience less frequent and low intensity GW droughts compared to other two regions. This implies that snow droughts might shift to GW droughts in Plains and the opposite is true for Mountains.

2. The historical drought propagation time from snow to GW increased from Mountains to Plains with 4-, 5-, 6-month predicted for Mountains, Foothills, and Plains, respectively. Also, the rather low cross-correlation between snow and GW indicated a relatively weak connection between snow and GW during historical period. In both future scenarios, the propagation time for all regions decreased, suggesting accelerated water cycle and hydrologic processes.
3. The dominant physical processes that control GW head and its connection to snow processes vary across different EHG regions. While all regions are very sensitive to the changes in soil water content and percolation processes, the physical processes that move soil water into GW system is different among regions. In Mountains and Foothills the curve number (or runoff potential) is inversely but strongly related to GW variation. The GW levels in Foothills and Plains are more responsive to the variation in total water yield, while the plain region alone is extremely sensitive to evapotranspiration due to the nature of its landform, landcover, and soil properties. Given the nonstationary response of these processes to variation in climate (Broberg et al., 2019; X. Li et al., 2020; Porter & Semenov, 2005), the response of GW to surface water processes and in particular, changes in snow can be very different across different EHG regions.

This study presented a novel approach to address regionalized snow drought and GW drought characteristics for both historical and future scenarios, which provides a comprehensive understanding of possible future, albeit realizing the existence of assumptions and limitations. This study can also advance our understanding of the propagation mechanism between snow water and GW, as well as the physical driving processes that control the interaction of snow water and GW. This study provides a basis for further studies concerning the GW management strategies due to changes in snow processes that result from global warming effects in cold watersheds of the mid-to-high latitude regions. It also provides a unified approach for analyzing snow drought and GW drought relationship.

Study Limitations and Future Directions

Unlike surface hydrologic modelling, where model performance mainly depends on availability of geospatial and time series input data, as well as streamflow observation; the GW modelling is affected by proper setting of geological formations in the model, resolution of spatial units delineated in the model, boundary condition such as river bed elevations, local pumping, lakes and river water levels (Waterloo Hydrogeologic, 2018). The performance of GW models are also affected by the GW head observations, which are less available as compared to surface water data at a regional scale. In this regional-scale study, the grid resolution of $10\text{km} \times 10\text{km}$ created some areas of limitations in GW head simulation. The simulated GW head in the grids that contained the boundary of watershed, exerted mismatch with observation well data. Because the groundwater in these grids that contained partial watershed, did not receive recharge from the full grid area, whereas in reality the GW recharge is not limited to the watershed border in any given grid cell. Also, large grid size ($10\text{km} \times 10\text{km}$) can contain elevation change within the grid area. The simulated GW head is based on the overall average elevation of each grid cell, whereas in

reality the observation well might locate in high (or low) elevation region within that grid cell. Hence, the GW head can be heavily underestimated or overestimated. Moreover, when an observation well is located near stream, the GW head gradually changes from river bottom to the GW level in observation well, but in the simulation, the model can force the GW head to satisfy boundary condition in each cell immediately with no possibility for gradual change due to the coarse spatial resolution. As a result, the simulated head can mismatch with observation. While all these limitations are common in most large-scale GW-SW modelling studies (Barthel & Banzhaf, 2016; Candela et al., 2014; Refsgaard et al., 2010; Zhou & Li, 2011), but comparison of the current model with a more high-resolution one, would provide direction on the magnitude of the changes in model results and conclusions.

Alternatively, partial refinement of grid can improve model performance, especially for grids that contains drastic elevation change. MODFLOW is able to perform partial refinement on grid size, which can improve GW head simulation at local scale. However, the simulation time of the coupled SWAT-MODFLOW with larger number of grid cells at a regional-scale is a limiting factor. Alternatively, a comparison with other state-of-the-art tools that allow partial refinement can inform about model performance. For future projections, we assumed that quantity of glacier melt runoff contributing to headwater tributaries would remain similar to historical period. This assumption adds uncertainty to streamflow simulation for future scenarios, and therefore, on processes that affect GW recharge in upstream catchments, and consequently the GW head fluctuations. Coupling a process-based glacier modeling with GW-SW modeling can improve model reliability.

Both snow and groundwater drought are valuable water resources, particularly for snow-dominated regions where groundwater resource is also abundant. As climate change alters the

precipitation patterns and might cause potentially more frequent extreme events, understanding the relationship between the two droughts can also be helpful in development of snow water / groundwater reservation infrastructures, which can be responsive to potential drought events, and hence further improve the ecosystem including the changes in vegetation or soil moisture and the agricultural practices. Through the modelling methods to simulate snow and groundwater relationship, we can gain better understanding of past, current and future variation of these parameters, and their potential impact to the environment. I wish this study and other similar studies can give me a glance of near future, and can assist in protecting the valuable water resources.

BIBLIOGRAPHY

- Abbas, S. A., Xuan, Y., & Bailey, R. T. (2022). Assessing Climate Change Impact on Water Resources in Water Demand Scenarios Using SWAT-MODFLOW-WEAP. *Hydrology*, 9(10). <https://doi.org/10.3390/hydrology9100164>
- Abbaspour, K. C. (2015). SWAT-CUP: SWAT Calibration and Uncertainty Programs- A User Manual. Department of Systems Analysis, Integrated Assessment and Modelling (SIAM), EAWAG. Swiss Federal Institute of Aquatic Science and Technology, Dübendorf, Switzerland. Doi: DOI: 10.1007/s00402-009-1032-4
- Abbaspour, K. C., Rouholahnejad, E., Vaghefi, S., Srinivasan, R., Yang, H., & Kløve, B. (2015). A continental-scale hydrology and water quality model for Europe: Calibration and uncertainty of a high-resolution large-scale SWAT model. *Journal of Hydrology*, 524, 733–752. <https://doi.org/10.1016/j.jhydrol.2015.03.027>
- Abbaspour, K. C., Vaghefi, S. A., & Srinivasan, R. (2017). A guideline for successful calibration and uncertainty analysis for soil and water assessment: A review of papers from the 2016 international SWAT conference. *Water (Switzerland)*, 10(1). <https://doi.org/10.3390/w10010006>
- Abbaspour, K. C., Yang, J., Maximov, I., Siber, R., Bogner, K., Mieleitner, J., Zobrist, J., & Srinivasan, R. (2007). Modelling hydrology and water quality in the pre-alpine/alpine Thur watershed using SWAT. *Journal of Hydrology*, 333(2–4), 413–430. <https://doi.org/10.1016/j.jhydrol.2006.09.014>
- Acreman, M., & Bullock, a. (2003). The role of wetlands in the hydrological cycle. *Hydrology and Earth System Sciences*, 7(3), 358–389.
- Agriculture and Agri-Food Canada (AAFC), (2011). Soils of Alberta [WWW Document]. URL <https://sis.agr.gc.ca/cansis/soils/ab/soils.html> (accessed 6.15.21)
- Ajami, H., Meixner, T., Dominguez, F., Hogan, J., & Maddock, T. (2012). Seasonalizing Mountain System Recharge in Semi-Arid Basins-Climate Change Impacts. *Ground Water*, 50(4), 585–597. <https://doi.org/10.1111/j.1745-6584.2011.00881.x>
- Aladejana, J. A., Kalin, R. M., Sentenac, P., & Hassan, I. (2020). Assessing the impact of climate change on groundwater quality of the shallow coastal aquifer of eastern dahomey basin, Southwestern Nigeria. *Water (Switzerland)*, 12(1). <https://doi.org/10.3390/w12010224>
- Alberta Environment Information Centre. (2010). *Water for Life: Facts about Water in Alberta 2002*.
- Alberta Geological Survey, 2019. 3D provincial geological framework model of Alberta, version 2.

- Aliyari, F., Bailey, R. T., Tasdighi, A., Dozier, A., Arabi, M., & Zeiler, K. (2019). Coupled SWAT-MODFLOW model for large-scale mixed agro-urban river basins. *Environmental Modelling and Software*, 115(February), 200–210. <https://doi.org/10.1016/j.envsoft.2019.02.014>
- Amundsen, E. S., & Jensen, F. (2019). Groundwater management: Waiting for a drought*. *Natural Resource Modeling*, 32(4). <https://doi.org/10.1111/nrm.12209>
- Apurv, T., & Cai, X. (2020). Drought Propagation in Contiguous U.S. Watersheds: A Process-Based Understanding of the Role of Climate and Watershed Properties. *Water Resources Research*, 56(9), 1–23. <https://doi.org/10.1029/2020WR027755>
- Aravinthasamy, P., Karunanidhi, D., Subramani, T., & Roy, P. D. (2021). Demarcation of groundwater quality domains using GIS for best agricultural practices in the drought-prone Shanmuganadhi River basin of South India. *Environmental Science and Pollution Research*, 28(15), 18423–18435. <https://doi.org/10.1007/s11356-020-08518-5>
- Arnold, J., Kiniry, R., Williams, E., Haney, S., Neitsch, S. (2012). *Soil & Water Assessment Tool, Texas Water Resources Institute-TR-439*.
- Bailey, R. T., & Park, S. (2019). *SWAT-MODFLOW Tutorial—Documentation for Preparing and Running SWAT-MODFLOW Simulations*.
- Bailey, R. T., Wible, T. C., Arabi, M., Records, R. M., & Ditty, J. (2016). Assessing regional-scale spatio-temporal patterns of groundwater–surface water interactions using a coupled SWAT-MODFLOW model. *Hydrological Processes*, 30(23), 4420–4433. <https://doi.org/10.1002/hyp.10933>
- Bailey, R.T., Wible, T.C., Arabi, M., Records, R.M., Ditty, J., 2016. Assessing regional-scale spatio-temporal patterns of groundwater–surface water interactions using a coupled SWAT-MODFLOW model. *Hydrological Processes* 30, 4420–4433. <https://doi.org/10.1002/hyp.10933>
- Barnett, T. P., Adam, J. C., & Lettenmaier, D. P. (2005). Potential impacts of a warming climate on water availability in snow-dominated regions. *Nature*, 438(7066), 303–309. <https://doi.org/10.1038/nature04141>
- Barnett, T. P., Pierce, D. W., Hidalgo, H. G., Bonfils, C., Santer, B. D., Das, T., Bala, G., Wood, A. W., Nozawa, T., Mirin, A. a, Cayan, D. R., & Dettinger, M. D. (2008). Human-Induced Changes United States. *Science*, 319(February), 1080–1083.
- Barthel, R., & Banzhaf, S. (2016). Groundwater and Surface Water Interaction at the Regional-scale – A Review with Focus on Regional Integrated Models. *Water Resources Management*, 30(1), 1–32. <https://doi.org/10.1007/s11269-015-1163-z>

- Beran, M. ., & Rodier, J. . (1985). Hydrological aspects of drought: a contribution to the International Hydrological Programme. In *Studies and Reports in Hydrology* (Vol. 39, p. 149). UNESCO-WMO.
- Best, L.C., Lowry, C.S., (2014). Quantifying the potential effects of high-volume water extractions on water resources during natural gas development. Marcellus Shale, NY. *Journal of Hydrology.: Regional Studies* 1, 1-16.
- Bloomfield, J. P., & Marchant, B. P. (2013). Analysis of groundwater drought building on the standardised precipitation index approach. *Hydrology and Earth System Sciences*, 17(12), 4769–4787. <https://doi.org/10.5194/hess-17-4769-2013>
- Bloomfield, J. P., Marchant, B. P., Bricker, S. H., & Morgan, R. B. (2015). Regional analysis of groundwater droughts using hydrograph classification. *Hydrology and Earth System Sciences*, 19(10), 4327–4344. <https://doi.org/10.5194/hess-19-4327-2015>
- Brauns, B., Cuba, D., Bloomfield, J. P., Hannah, D. M., Jackson, C., Marchant, B. P., Heudorfer, B., Van Loon, A. F., Bessière, H., Thunholm, B., & Schubert, G. (2020). The Groundwater Drought Initiative (GDI): Analysing and understanding groundwater drought across Europe. *Proceedings of the International Association of Hydrological Sciences*, 383, 297–305. <https://doi.org/10.5194/piahs-383-297-2020>
- Broberg, M. C., Högy, P., Feng, Z., & Pleijel, H. (2019). Effects of elevated CO₂ on wheat yield: Non-linear response and relation to site productivity. *Agronomy*, 9(5), 1–18. <https://doi.org/10.3390/agronomy9050243>
- Brown, R.D., B. Bransnett, 2010. Canadian Meteorological Centre (CMC) Daily Snow Depth Analysis Data, Version 1. [WWW Document]. Boulder, Color. USA. NASA Natl. Snow Ice Data Cent. Distrib. Act. Arch. Cent. <https://doi.org/10.5067/W9FOYWH0EQZ3>
- Cai, Z., Wang, W., Zhao, M., Ma, Z., Lu, C., & Li, Y. (2020). Interaction between surface water and groundwater in yinchuan plain. *Water (Switzerland)*, 12(9), 1–23. <https://doi.org/10.3390/w12092635>
- Candela, L., Elorza, F. J., Tamoh, K., Jiménez-Martínez, J., & Aureli, A. (2014). Groundwater modelling with limited data sets: The Chari-Logone area (Lake Chad Basin, Chad). *Hydrological Processes*, 28(11), 3714–3727. <https://doi.org/10.1002/hyp.9901>
- Castle, S. L., Thomas, B. F., John T. Reager, M. R., & Sean C. Swenson, J. S. F. (2014). future water security of the Colorado River Basin. *Geophysical Research Letters*, 41, 5904–5911. <https://doi.org/10.1002/2014GL061055>.Received
- Chaponniere, A., Boulet, G., Chehbouni, A., & Aresmouk, M. (2007). Understanding hydrological processes with scarce data in a mountain environment. *Hydrological Processes*, 1908–1921. <https://doi.org/10.1002/hyp>

- Chen, M., Izady, A., Abdalla, O.A., 2017. An efficient surrogate-based simulation-optimization method for calibrating a regional MODFLOW model. *Journal of Hydrology* 544, 591–603. <https://doi.org/10.1016/j.jhydrol.2016.12.011>
- Chou, F. N. F., & Wu, C. W. (2010). Reducing the impacts of flood-induced reservoir turbidity on a regional water supply system. *Advances in Water Resources*, 33(2), 146–157. <https://doi.org/10.1016/j.advwatres.2009.10.011>
- Chunn, D., Faramarzi, M., Smerdon, B., Alessi, D.S., 2019. Application of an integrated SWAT-MODFLOW model to evaluate potential impacts of climate change and water withdrawals on groundwater-surface water interactions in west-central Alberta. *Water (Switzerland)* 11. <https://doi.org/10.3390/w11010110>
- Clark, B. R., Hart, R. M., & Gurdak, J. J. (2011). Groundwater availability of the Mississippi Embayment: Professional Paper 1785. In *U.S. Geological Survey*.
- Condon, L. E., Atchley, A. L., & Maxwell, R. M. (2020). Evapotranspiration depletes groundwater under warming over the contiguous United States. *Nature Communications*, 11(1). <https://doi.org/10.1038/s41467-020-14688-0>
- Corona, C. R., Gurdak, J. J., Dickinson, J. E., Ferré, T. P. A., & Maurer, E. P. (2018). Climate variability and vadose zone controls on damping of transient recharge. *Journal of Hydrology*, 561, 1094–1104. <https://doi.org/10.1016/j.jhydrol.2017.08.028>
- Corriveau, J., Chambers, P. A., Yates, A. G., & Culp, J. M. (2011). Snowmelt and its role in the hydrologic and nutrient budgets of prairie streams. *Water Science and Technology*, 64(8), 1590–1596. <https://doi.org/10.2166/wst.2011.676>
- Debeer, C. (2012). *Simulating Areal Snow cover Depletion and Snowmelt Runoff in Alpine Terrain* (Issue May) *PhD Thesis* [University of Saskatchewan]. <https://library-archives.canada.ca/eng/services/services-libraries/theses/Pages/item.aspx?idNumber=1032965929>
- DeBeer, C. M., & Pomeroy, J. W. (2017). Influence of snowpack and melt energy heterogeneity on snow cover depletion and snowmelt runoff simulation in a cold mountain environment. *Journal of Hydrology*, 553, 199–213. <https://doi.org/10.1016/j.jhydrol.2017.07.051>
- Dierauer, J. R., Allen, D. M., & Whitfield, P. H. (2019). Snow Drought Risk and Susceptibility in the Western United States and Southwestern Canada. *Water Resources Research*, 55(4), 3076–3091. <https://doi.org/10.1029/2018WR023229>
- Dierauer, J. R., Allen, D. M., & Whitfield, P. H. (2021). Climate change impacts on snow and streamflow drought regimes in four ecoregions of British Columbia. *Canadian Water Resources Journal*, 46(4), 168–193. <https://doi.org/10.1080/07011784.2021.1960894>

- Dillon, P., Escalante, E. F., Megdal, S. B., & Massmann, G. (2020). Managed aquifer recharge for water resilience. *Water (Switzerland)*, *12*(7), 1–11. <https://doi.org/10.3390/W12071846>
- Domenico, P. A., & Mifflin, M. D. (1965). Water from low-permeability sediments and land subsidence. *Water Resources Research*, *1*(4), 563–576. <https://doi.org/10.1029/wr001i004p00563>
- Döscher, R., Acosta, M., Alessandri, A., Anthoni, P., Arsouze, T., Bergman, T., Bernardello, R., Boussetta, S., Caron, L. P., Carver, G., Castrillo, M., Catalano, F., Cvijanovic, I., Davini, P., Dekker, E., Doblas-Reyes, F. J., Docquier, D., Echevarria, P., Fladrich, U., ... Zhang, Q. (2022). The EC-Earth3 Earth system model for the Coupled Model Intercomparison Project 6. *Geoscientific Model Development*, *15*(7), 2973–3020. <https://doi.org/10.5194/gmd-15-2973-2022>
- Earman, S., Campbell, A. R., Phillips, F. M., & Newman, B. D. (2006). Isotopic exchange between snow and atmospheric water vapor: Estimation of the snowmelt component of groundwater recharge in the southwestern United States. *Journal of Geophysical Research Atmospheres*, *111*(9), 1–18. <https://doi.org/10.1029/2005JD006470>
- Ellis, C. R., Pomeroy, J. W., Brown, T., & MacDonald, J. (2010). Simulation of snow accumulation and melt in needleleaf forest environments. *Hydrology and Earth System Sciences*, *14*(6), 925–940. <https://doi.org/10.5194/hess-14-925-2010>
- Ellis, C. R., Pomeroy, J. W., Essery, R. L. H., & Link, T. E. (2011). Effects of needleleaf forest cover on radiation and snowmelt dynamics in the Canadian Rocky Mountains. *Canadian Journal of Forest Research*, *41*(3), 608–620. <https://doi.org/10.1139/X10-227>
- Eyring, V., Bony, S., Meehl, G. A., Senior, C. A., Stevens, B., Stouffer, R. J., & Taylor, K. E. (2016). Overview of the Coupled Model Intercomparison Project Phase 6 (CMIP6) experimental design and organization. *Geoscientific Model Development*, *9*(5), 1937–1958. <https://doi.org/10.5194/gmd-9-1937-2016>
- Fan, X., Ma, Z., Yang, Q., Han, Y., & Mahmood, R. (2015). Land use/land cover changes and regional climate over the Loess Plateau during 2001–2009. Part II: interrelationship from observations. *Climatic Change*, *129*(3–4), 441–455. <https://doi.org/10.1007/s10584-014-1068-5>
- Faramarzi, M., Abbaspour, K.C., Adamowicz, W.L.V., Lu, W., Fennell, J., Zehnder, A.J.B., Goss, G.G., (2017). Uncertainty based assessment of dynamic freshwater scarcity in semi-arid watersheds of Alberta, Canada. *Journal of Hydrology: Regional Studies* *9*, 48–68. <https://doi.org/10.1016/j.ejrh.2016.11.003>
- Faramarzi, M., Srinivasan, R., Iravani, M., Bladon, K. D., Abbaspour, K. C., Zehnder, A. J. B., & Goss, G. G. (2015). Setting up a hydrological model of Alberta: Data discrimination analyses

- prior to calibration. *Environmental Modelling and Software*, 74, 48–65. <https://doi.org/10.1016/j.envsoft.2015.09.006>
- Fendeková, M., & Fendek, M. (2012). Groundwater drought in the nitra river basin - Identification and classification. *Journal of Hydrology and Hydromechanics*, 60(3), 185–193. <https://doi.org/10.2478/v10098-012-0016-1>
- Flerchinger, G. N., Deng, Y., & Cooley, K. R. (1993). Groundwater response to snowmelt in a mountainous watershed: testing of a conceptual model. *Journal of Hydrology*, 152(1–4), 201–214. [https://doi.org/10.1016/0022-1694\(93\)90146-Z](https://doi.org/10.1016/0022-1694(93)90146-Z)
- Food and Agricultural Organization of the United Nations, 2003. Digital soil map of the world and derived soil properties. Rome, Italy: FAO.
- Francioli, D., Cid, G., Kanukollu, S., Ulrich, A., Hajirezaei, M. R., & Kolb, S. (2021). Flooding Causes Dramatic Compositional Shifts and Depletion of Putative Beneficial Bacteria on the Spring Wheat Microbiota. *Frontiers in Microbiology*, 12(November), 1–15. <https://doi.org/10.3389/fmicb.2021.773116>
- Freudiger, D., Kohn, I., Seibert, J., Stahl, K., & Weiler, M. (2017). Snow redistribution for the hydrological modeling of alpine catchments. *Wiley Interdisciplinary Reviews: Water*, 4(5), 1–16. <https://doi.org/10.1002/WAT2.1232>
- Gagniuc, Paul A. (2017). *Markov Chains: From Theory to Implementation and Experimentation*. USA, NJ: John Wiley & Sons. pp. 1–256. [ISBN 978-1-119-38755-8](https://doi.org/10.1002/9781119387558).
- Gao, H., & Shao, M. (2015). Effects of temperature changes on soil hydraulic properties. *Soil and Tillage Research*, 153, 145–154. <https://doi.org/10.1016/j.still.2015.05.003>
- Gebremichael, M., Krishnamurthy, P. K., Ghebremichael, L. T., & Alam, S. (2021). What drives crop land use change during multi-year droughts in California’s central valley? Prices or concern for water? *Remote Sensing*, 13(4), 1–19. <https://doi.org/10.3390/rs13040650>
- Government of Alberta, Alberta Climate and Atlas Maps [WWW document]. URL <http://agriculture.alberta.ca/acis/climate-maps.jsp> (accessed 6.15.21)
- Government of Alberta, Alberta River Basins map [WWW Document] URL <https://rivers.alberta.ca/> (accessed 8.10.21)
- Government of Alberta, Alberta Water Well Information Database [WWW Document] URL <http://environment.alberta.ca/apps/GOWN/#> (accessed 12.14.21)
- Government of Canada, (2019). Historical Climate Data [WWW Document]. URL http://climate.weather.gc.ca/historical_data/search_historic_data_e.html (accessed 6.15.21)
- Government of Canada, 2017. Canadian Land Cover, Circa 2000 (Vector) - GeoBase Series, 1996-2005 [WWW Document]. URL <https://open.canada.ca/data/en/dataset/97126362-5a85->

4fe0-9dc2-915464cfdbb7 (accessed 4.15.20).

- Gray, D. M., & Landine, P. G. (1988). An energy-budget snowmelt model for the Canadian Prairies. *Canadian Journal of Earth Sciences*, 25(8), 1292–1303. <https://doi.org/10.1139/e88-124>
- H. Shumway and D.S. Stoffer. *Time Series Analysis and Its Applications: With R Examples*. Springer, 2017. pp-32
- Han, Z., Huang, S., Huang, Q., Leng, G., Wang, H., Bai, Q., Zhao, J., Ma, L., Wang, L., & Du, M. (2019). Propagation dynamics from meteorological to groundwater drought and their possible influence factors. *Journal of Hydrology*, 578(September). <https://doi.org/10.1016/j.jhydrol.2019.124102>
- Harbaugh, A. W. (2005). *MODFLOW-2005: the U.S. Geological Survey modular groundwater model - the groundwater flow process*. <https://doi.org/10.3133/tm6A16>
- Harding, R. ., & Pomeroy, J. . (1996). The Energy Balance of the Winter Boreal Landscape. *Journal of Climate*, 9(11), 2778–2787. https://journals.ametsoc.org/view/journals/clim/9/11/1520-0442_1996_009_2778_tebotw_2_0_co_2.xml
- Hardy, J. P., Melloh, R., Robinson, P., & Jordan, R. (2000). Incorporating effects of forest litter in a snow process model. *Hydrological Processes*, 14(18), 3227–3237. [https://doi.org/10.1002/1099-1085\(20001230\)14:18<3227::AID-HYP198>3.0.CO;2-4](https://doi.org/10.1002/1099-1085(20001230)14:18<3227::AID-HYP198>3.0.CO;2-4)
- Harpold, A. A., & Kohler, M. (2017). Potential for Changing Extreme Snowmelt and Rainfall Events in the Mountains of the Western United States. *Journal of Geophysical Research: Atmospheres*, 122(24), 13,219–13,228. <https://doi.org/10.1002/2017JD027704>
- Hatchett, B. J., & McEvoy, D. J. (2018). Exploring the origins of snow drought in the northern sierra nevada, california. *Earth Interactions*, 22(2), 1–13. <https://doi.org/10.1175/EI-D-17-0027.1>
- Hatchett, B. J., Rhoades, A. M., & Mcevoy, D. J. (2021). *Monitoring the Daily Evolution and Extent of Snow Drought. July*, 1–29.
- Hayashi, M. (2020). Alpine Hydrogeology: The Critical Role of Groundwater in Sourcing the Headwaters of the World. *Groundwater*, 58(4), 498–510. <https://doi.org/10.1111/gwat.12965>
- Hayashi, M., & Rosenberry, D. O. (2002). Effects of Groundwater Exchange on the Hydrology and Ecology of Surface Water. *Ground Water*, 40, 309–316. <https://doi.org/10.1111/j.1745-6584.2002.tb02659.x>

- He, Z., Liang, H., Yang, C., Huang, F., & Zeng, X. (2018). Temporal–spatial evolution of the hydrologic drought characteristics of the karst drainage basins in South China. *International Journal of Applied Earth Observation and Geoinformation*, 64(August 2017), 22–30. <https://doi.org/10.1016/j.jag.2017.08.010>
- Heath, R. C. (1983). *Basic Ground-Water Hydrology* (Water Supply Paper 2220). U.S. Geological Survey.
- Hokanson, K. J., Mendoza, C. A., & Devito, K. J. (2019). Interactions between Regional Climate, Surficial Geology, and Topography: Characterizing Shallow Groundwater Systems in Sub-humid, Low-Relief Landscapes. *Water Resources Research*, 55(1), 284–297. <https://doi.org/10.1029/2018WR023934>
- Hosking, J. R. M. (1996). Fortran routines for use with the method of L-moments, Version 3. Research Report RC20525, IBM Research Division, Yorktown Heights, N.Y.
- Hosking, J. R. M. (2022). *Package ‘lmom.’* [WWW Document]. URL <https://cran.r-project.org/web/packages/lmom/lmom.pdf>
- Hosking, J. R. M. and Wallis, J. R. (1997). Regional frequency analysis: an approach based on L-moments, Cambridge University Press, Appendix A.10.
- Huang, J., Cao, L., Yu, F., Liu, X., & Wang, L. (2021). Groundwater Drought and Cycles in Xuchang City, China. *Frontiers in Earth Science*, 9(September), 1–13. <https://doi.org/10.3389/feart.2021.736305>
- Hughes, J. D., Petrone, K. C., & Silberstein, R. P. (2012). Drought, GW storage and stream flow decline in southwestern Australia. *Geophysical Research Letters*, 39(3), 1–6. <https://doi.org/10.1029/2011GL050797>
- Huning, L. S., & AghaKouchak, A. (2020). Global snow drought hot spots and characteristics. *Proceedings of the National Academy of Sciences of the United States of America*, 117(33), 19753–19759. <https://doi.org/10.1073/PNAS.1915921117>
- IPCC. (2022). Climate Change 2022 - Mitigation of Climate Change - Working Group III. *Cambridge University Press*, 1454. <https://www.ipcc.ch/site/assets/uploads/2018/05/uncertainty-guidance-note.pdf>.%0Awww.cambridge.org
- IPCC. (2022). Summary for Policymakers: Climate Change 2022_ Impacts, Adaptation and Vulnerability_ Working Group II contribution to the Sixth Assessment Report of the Intergovernmental Panel on Climate Change. In *Working Group II contribution to the Sixth Assessment Report of the Intergovernmental Panel on Climate Change*. <https://doi.org/10.1017/9781009325844.Front>

- Ireson, A. M., Barr, A. G., Johnstone, J. F., Mamet, S. D., van der Kamp, G., Whitfield, C. J., Michel, N. L., North, R. L., Westbrook, C. J., Debeer, C., Chun, K. P., Nazemi, A., & Sagin, J. (2015). The changing water cycle: the Boreal Plains ecozone of Western Canada. *Wiley Interdisciplinary Reviews: Water*, 2(5), 505–521. <https://doi.org/10.1002/WAT2.1098>
- Islam, S. ul, Déry, S. J., & Werner, A. T. (2017). Future Climate Change Impacts on Snow and Water Resources of the Fraser River Basin, British Columbia. *Journal of Hydrometeorology*, 18(2), 473–496. <https://doi.org/10.1175/jhm-d-16-0012.1>
- J.D.Cryer and K.S. Chan. *Time Series Analysis with Applications in R*. Springer, 2011 pp-265
- Jacobs, J. M., Mergelsberg, S. L., Lopera, A. F., & Myers, D. A. (2002). Evapotranspiration from a wet prairie wetland under drought conditions: Paynes prairie preserve, Florida, USA. *Wetlands*, 22(2), 374–385. [https://doi.org/10.1672/0277-5212\(2002\)022\[0374:EFAWPW\]2.0.CO;2](https://doi.org/10.1672/0277-5212(2002)022[0374:EFAWPW]2.0.CO;2)
- Jarvis, A., Guevara, E., Reuter, H.I., Nelson, A.D., (2008). Hole-filled SRTM for the globe: version 4: data grid
- Jódar, J., Cabrera, J. A., Martos-Rosillo, S., Ruiz-Constán, A., González-Ramón, A., Lambán, L. J., Herrera, C., & Custodio, E. (2017). Groundwater discharge in high-mountain watersheds: A valuable resource for downstream semi-arid zones. The case of the Bérchules River in Sierra Nevada (Southern Spain). *Science of the Total Environment*, 593–594, 760–772. <https://doi.org/10.1016/j.scitotenv.2017.03.190>
- Jutglar, K., Hellwig, J., Stoelzle, M., & Lange, J. (2021). Post-drought increase in regional-scale groundwater nitrate in southwest Germany. *Hydrological Processes*, 35(8), 1–11. <https://doi.org/10.1002/hyp.14307>
- Kapnick, S., & Hall, A. (2012). Causes of recent changes in western North American snowpack. *Climate Dynamics*, 38(9–10), 1885–1899. <https://doi.org/10.1007/s00382-011-1089-y>
- Khalili, P., Razavi, S., Davies, E.G.R., Alessi, D.S., Faramarzi, M., 2023. Assessment of blue water-green water interchange under extreme warm and dry events across different ecohydrological regions of western Canada, *Journal of Hydrology*, In review.
- Kriauciuniene, J., Meilutyte-barauskiene, D., Rimkus, E., Kazys, J., & Vincevicius, A. (2008). Climate change impact on hydrological processes in Lithuanian Nemunas river basin. *Baltica*, 21(1), 13–23.
- Langridge, R., & Van Schmidt, N. D. (2020). Groundwater and Drought Resilience in the SGMA Era. *Society and Natural Resources*, 33(12), 1530–1541. <https://doi.org/10.1080/08941920.2020.1801923>

- Langevin, C. D., Hughes, J. D., Banta, E. R., Niswonger, R. G., Panday, S., & Provost, A. M. (2017). Documentation for the MODFLOW 6 Groundwater Flow Model: U.S. Geological Survey Techniques and Methods. In *Book 6, Modeling Techniques*. <https://pubs.usgs.gov/tm/06/a55/tm6a55.pdf>
- Lee, J. M., Park, J. H., Chung, E., & Woo, N. C. (2018). Assessment of groundwater drought in the Mangyeong River Basin, Korea. *Sustainability (Switzerland)*, *10*(3). <https://doi.org/10.3390/su10030831>
- Li, B., & Rodell, M. (2015). Evaluation of a model-based groundwater drought indicator in the conterminous U.S. *Journal of Hydrology*, *526*, 78–88. <https://doi.org/10.1016/j.jhydrol.2014.09.027>
- Li, X., Dong, J., Gruda, N. S., Chu, W., & Duan, Z. (2020). Interactive effects of the CO₂ enrichment and nitrogen supply on the biomass accumulation, gas exchange properties, and mineral elements concentrations in cucumber plants at different growth stages. *Agronomy*, *10*(1). <https://doi.org/10.3390/agronomy10010139>
- Link, T. E., & Marks, D. (1999). Point simulation of seasonal snow cover dynamics beneath boreal forest canopies. *Journal of Geophysical Research Atmospheres*, *104*(D22), 27841–27857. <https://doi.org/10.1029/1998JD200121>
- Liu, X., Zhu, X., Pan, Y., Li, S., Liu, Y., & Ma, Y. (2016). Agricultural drought monitoring: Progress, challenges, and prospects. *Journal of Geographical Sciences*, *26*(6), 750–767. <https://doi.org/10.1007/s11442-016-1297-9>
- Long, D., Yang, W., Scanlon, B. R., Zhao, J., Liu, D., Burek, P., Pan, Y., You, L., & Wada, Y. (2020). South-to-North Water Diversion stabilizing Beijing's groundwater levels. *Nature Communications*, *11*(1). <https://doi.org/10.1038/s41467-020-17428-6>
- Lundberg, A., Ala-Aho, P., Eklo, O., Klöve, B., Kværner, J., & Stumpp, C. (2016). Snow and frost: Implications for spatiotemporal infiltration patterns - a review. *Hydrological Processes*, *30*(8), 1230–1250. <https://doi.org/10.1002/hyp.10703>
- Maccagno, M., & Kupper, J. (2009). *North Saskatchewan River Basin: Overview of Groundwater Conditions, Issues, and Challenges. Report 1* (Issue June).
- MacDonald, R. J., Byrne, J. M., Boon, S., & Kienzle, S. W. (2012). Modelling the Potential Impacts of Climate Change on Snowpack in the North Saskatchewan River Watershed, Alberta. *Water Resources Management*, *26*(11), 3053–3076. <https://doi.org/10.1007/s11269-012-0016-2>

- Masud, B., Cui, Q., Ammar, M. E., Bonsal, B. R., Islam, Z., & Faramarzi, M. (2021). Means and extremes: Evaluation of a CMIP6 multi-model ensemble in reproducing historical climate characteristics across Alberta, Canada. *Water* DOI: <https://doi.org/10.3390/w13050737>
- Masud, M. B., Khaliq, M. N., & Wheeler, H. S. (2015). Analysis of meteorological droughts for the Saskatchewan River Basin using univariate and bivariate approaches. *Journal of Hydrology*, *522*, 452–466. <https://doi.org/10.1016/j.jhydrol.2014.12.058>
- Melloh, R. A., Hardy, J. P., Bailey, R. N., & Hall, T. J. (2002). An efficient snow albedo model for the open and sub-canopy. *Hydrological Processes*, *16*(18), 3571–3584. <https://doi.org/10.1002/hyp.1229>
- Meng, Y., Liu, G., & Li, M. (2015). Tracing the sources and processes of groundwater in an alpine glacierized region in Southwest China: Evidence from environmental isotopes. *Water (Switzerland)*, *7*(6), 2673–2690. <https://doi.org/10.3390/w7062673>
- Mianabadi, A., Derakhshan, H., Davary, K., Hasheminia, S. M., & Hrachowitz, M. (2020). A Novel Idea for Groundwater Resource Management during Megadrought Events. *Water Resources Management*, *34*(5), 1743–1755. <https://doi.org/10.1007/s11269-020-02525-4>
- Mizukami, N., Clark, M. P., Slater, A. G., Brekke, L. D., Elsner, M. M., Arnold, J. R., & Gangopadhyay, S. (2014). Hydrologic implications of different large-scale meteorological model forcing datasets in mountainous regions. *Journal of Hydrometeorology*, *15*(1), 474–488. <https://doi.org/10.1175/JHM-D-13-036.1>
- Mohammed, A. A., Pavlovskii, I., Cey, E. E., & Hayashi, M. (2019). Effects of preferential flow on snowmelt partitioning and groundwater recharge in frozen soils. *Hydrology and Earth System Sciences*, *23*(12), 5017–5031. <https://doi.org/10.5194/hess-23-5017-2019>
- Morris, D. A., & Johnson, A. I. (1967). *Summary of Hydrologic and Physical Properties of Rock and Soil Materials, as Analyzed by the Hydrologic Laboratory of the U.S. Geological Survey* (Geological Survey Water-Supply Paper 1839-D). U.S. Geological Survey.
- Mote, P. W., Hamlet, A. F., Clark, M. P., & Lettenmaier, D. P. (2005). Declining mountain snowpack in western north America. *Bulletin of the American Meteorological Society*, *86*(1), 39–49. <https://doi.org/10.1175/BAMS-86-1-39>
- Mussá, F. E. F., Zhou, Y., Maskey, S., Masih, I., & Uhlenbrook, S. (2015). GW as an emergency source for drought mitigation in the Crocodile River catchment, South Africa. *Hydrology and Earth System Sciences*, *19*(2), 1093–1106. <https://doi.org/10.5194/hess-19-1093-2015>
- National Oceanic and Atmospheric Administration. (2018). Snow drought. Drought.gov. <https://www.drought.gov/what-is-drought/snow-drought>. (accessed 3.12.20).

- Neitsch, S. ., Arnold, J. ., Kiniry, J. ., & Williams, J. . (2011). Soil & Water Assessment Tool Theoretical Documentation Version 2009. *Texas Water Resources Institute*, 1–647. <https://doi.org/10.1016/j.scitotenv.2015.11.063>
- Nepal, S., et al (2014). Upstream–downstream linkages of hydrological processes in the Himalayan region. *Ecological Processes*, 2014 3:19. <https://doi.org/10.1186/s13717-014-0019-4>
- Niu, Q., Liu, L., Heng, J., Li, H., & Xu, Z. (2020). A Multi-Index Evaluation of Drought Characteristics in the Yarlung Zangbo River Basin of Tibetan Plateau, Southwest China. *Frontiers in Earth Science*, 8(June), 1–16. <https://doi.org/10.3389/feart.2020.00213>
- Niswonger, R. G. (2011). MODFLOW-NWT , A Newton Formulation for MODFLOW-2005. In *Book 6, Modeling Techniques*.
- North Saskatchewan Watershed Alliance, 2005. The State of the North Sask River Watershed Report [WWW Document] URL <https://www.nswa.ab.ca/our-watershed/> (accessed 7.16.21)
- O’Neill, B. C., Tebaldi, C., Van Vuuren, D. P., Eyring, V., Friedlingstein, P., Hurtt, G., Knutti, R., Kriegler, E., Lamarque, J. F., Lowe, J., Meehl, G. A., Moss, R., Riahi, K., & Sanderson, B. M. (2016). The Scenario Model Intercomparison Project (ScenarioMIP) for CMIP6. *Geoscientific Model Development*, 9(9), 3461–3482. <https://doi.org/10.5194/gmd-9-3461-2016>
- Park, S., Kim, H., & Jang, C. (2021). Impact of groundwater abstraction on hydrological responses during extreme drought periods in the boryeong dam catchment, korea. *Water (Switzerland)*, 13(15). <https://doi.org/10.3390/w13152132>
- Pathak, A. A., & Dodamani, B. M. (2019). Trend Analysis of Groundwater Levels and Assessment of Regional Groundwater Drought: Ghataprabha River Basin, India. *Natural Resources Research*, 28(3), 631–643. <https://doi.org/10.1007/s11053-018-9417-0>
- Pathak, A. A., & Dodamani, B. M. (2021). Connection between Meteorological and Groundwater Drought with Copula-Based Bivariate Frequency Analysis. *Journal of Hydrologic Engineering*, 26(7), 05021015. [https://doi.org/10.1061/\(asce\)he.1943-5584.0002089](https://doi.org/10.1061/(asce)he.1943-5584.0002089)
- Paznekas, A., & Hayashi, M. (2016). Groundwater contribution to winter streamflow in the Canadian Rockies. *Canadian Water Resources Journal*, 41(4), 484–499. <https://doi.org/10.1080/07011784.2015.1060870>
- Pendergrass, A. G., Meehl, G. A., Pulwarty, R., Hobbins, M., Hoell, A., AghaKouchak, A., Bonfils, C. J. W., Gallant, A. J. E., Hoerling, M., Hoffmann, D., Kaatz, L., Lehner, F., Llewellyn, D., Mote, P., Neale, R. B., Overpeck, J. T., Sheffield, A., Stahl, K., Svoboda, M., ... Woodhouse,

- C. A. (2020). Flash droughts present a new challenge for subseasonal-to-seasonal prediction. *Nature Climate Change*, 10(3), 191–199. <https://doi.org/10.1038/s41558-020-0709-0>
- Petersen-Perlman, J. D., Aguilar-Barajas, I., & Megdal, S. B. (2022). Drought and groundwater management: Interconnections, challenges, and policy responses. *Current Opinion in Environmental Science and Health*, 28, 100364. <https://doi.org/10.1016/j.coesh.2022.100364>
- Pieper, P., Düsterhus, A., & Baehr, J. (2020). A universal Standardized Precipitation Index candidate distribution function for observations and simulations. *Hydrology and Earth System Sciences*, 24(9), 4541–4565. <https://doi.org/10.5194/hess-24-4541-2020>
- Pomeroy, J. W., & Brun, E. (2000). Physical properties of snow. In *Encyclopedia of Earth Sciences Series: Vol. Part 3* (pp. 859–863). https://doi.org/10.1007/978-90-481-2642-2_422
- Pomeroy, J. W., Gray, D. M., Shook, K. R., Toth, B., Essery, R. L. H., Pietroniro, A., & Hedstrom, N. (1998). An evaluation of snow accumulation and ablation processes for land surface modelling. *Hydrological Processes*, 12(15), 2339–2367. [https://doi.org/10.1002/\(SICI\)1099-1085\(199812\)12:15<2339::AID-HYP800>3.0.CO;2-L](https://doi.org/10.1002/(SICI)1099-1085(199812)12:15<2339::AID-HYP800>3.0.CO;2-L)
- Porter, J. R., & Semenov, M. A. (2005). Crop responses to climatic variation. *Philosophical Transactions of the Royal Society B: Biological Sciences*, 360(1463), 2021–2035. <https://doi.org/10.1098/rstb.2005.1752>
- Pradhanang, S. M., Anandhi, A., Mukundan, R., Zion, M. S., Pierson, D. C., Schneiderman, E. M., Matonse, A., & Frei, A. (2011). Application of SWAT model to assess snowpack development and streamflow in the Cannonsville watershed, New York, USA. *Hydrological Processes*, 25(21), 3268–3277. <https://doi.org/10.1002/hyp.8171>
- Qin, Y., Abatzoglou, J. T., Siebert, S., Huning, L. S., AghaKouchak, A., Mankin, J. S., Hong, C., Tong, D., Davis, S. J., & Mueller, N. D. (2020). Agricultural risks from changing snowmelt. *Nature Climate Change*, 10(5), 459–465. <https://doi.org/10.1038/s41558-020-0746-8>
- Rahman, K., Maringanti, C., Beniston, M., Widmer, F., Abbaspour, K., & Lehmann, A. (2013). Streamflow Modeling in a Highly Managed Mountainous Glacier Watershed Using SWAT: The Upper Rhone River Watershed Case in Switzerland. *Water Resources Management*, 27(2), 323–339. <https://doi.org/10.1007/s11269-012-0188-9>
- Refsgaard, J. C., Højberg, A. L., Møller, I., Hansen, M., & Søndergaard, V. (2010). Groundwater modeling in integrated water resources management - visions for 2020. *Ground Water*, 48(5), 633–648. <https://doi.org/10.1111/j.1745-6584.2009.00634.x>
- Riahi, K., van Vuuren, D. P., Kriegler, E., Edmonds, J., O'Neill, B. C., Fujimori, S., Bauer, N., Calvin, K., Dellink, R., Fricko, O., Lutz, W., Popp, A., Cuaresma, J. C., KC, S., Leimbach, M., Jiang, L., Kram, T., Rao, S., Emmerling, J., ... Tavoni, M. (2017). The Shared

- Socioeconomic Pathways and their energy, land use, and greenhouse gas emissions implications: An overview. *Global Environmental Change*, 42, 153–168. <https://doi.org/10.1016/j.gloenvcha.2016.05.009>
- Sauchyn, D., Rehan A, M., Basu, S., Andreichuk, Y., Gurrapu, S., Kerr, S., & Bedoya, J. M. (2020). *Natural and Externally Forced Hydroclimatic Variability in the North Saskatchewan River Basin : Support for EPCOR ' s Climate Change Strategy* (Issue September).
- Schuol, J., Abbaspour, K. C., Srinivasan, R., & Yang, H. (2008). Estimation of freshwater availability in the West African sub-continent using the SWAT hydrologic model. *Journal of Hydrology*, 352(1–2), 30–49. <https://doi.org/10.1016/j.jhydrol.2007.12.025>
- Shabani, A., Woznicki, S. A., Mehaffey, M., Butcher, J., Wool, T. A., & Whung, P. Y. (2021). A coupled hydrodynamic (HEC-RAS 2D) and water quality model (WASP) for simulating flood-induced soil, sediment, and contaminant transport. *Journal of Flood Risk Management*, 14(4), 1–17. <https://doi.org/10.1111/jfr3.12747>
- Sheffield, J., & Wood, E. . (2011). *Drought: Past Problems and Future Scenarios*, Earthscan, London, UK, Washington DC, USA
- Shrestha, R. R., Bonsal, B. R., Bonnyman, J. M., Cannon, A. J., & Najafi, M. R. (2021). Heterogeneous snowpack response and snow drought occurrence across river basins of northwestern North America under 1.0°C to 4.0°C global warming. *Climatic Change*, 164(3–4), 1–21. <https://doi.org/10.1007/s10584-021-02968-7>
- Smerdon, B.D., Hughes, A.T., Jean, G., 2017. Permeability Measurements of Upper Cretaceous and Paleogene Bedrock Cores made from 2004-2015 (tabular data, tab-delimited format, to accompany Open File Report 2016-03).
- Soylu, M. E., Istanbuluoglu, E., Lenters, J. D., & Wang, T. (2011). Quantifying the impact of groundwater depth on evapotranspiration in a semi-arid grassland region. *Hydrology and Earth System Sciences*, 15(3), 787–806. <https://doi.org/10.5194/hess-15-787-2011>
- Spruill, C. A., Workman, S. R., & Taraba, J. L. (2000). Simulation of daily and monthly stream discharge from small watersheds using the SWAT model. *Transactions of the American Society of Agricultural Engineers*, 43(6), 1431–1439. <https://doi.org/10.13031/2013.3041>
- Stähli, M., Bayard, D., Wydler, H., & Flühler, H. (2004). Snowmelt infiltration into alpine soils visualized by dye tracer technique. *Arctic, Antarctic, and Alpine Research*, 36(1), 128–135. [https://doi.org/10.1657/1523-0430\(2004\)036\[0128:SIASV\]2.0.CO;2](https://doi.org/10.1657/1523-0430(2004)036[0128:SIASV]2.0.CO;2)
- Staudinger, M., Stahl, K., & Seibert, J. (2014). *A drought index accounting for snow*. 5375–5377. <https://doi.org/10.1002/2013WR014979.Reply>

- Stocker, T. ., Qin, D., Plattner, G.-K., Tignor, M., Allen, S. ., Boschung, J., Nauels, A., Xia, Y., Bex, V., & Midgley, P. . (2013). *Climate Change 2013: The Physical Science Basis. Contribution of Working Group I to the Fifth Assessment Report of the Intergovernmental Panel on Climate Change*. In *Cambridge University Press*.
- Stouffer, R. J., Eyring, V., Meehl, G. A., Bony, S., Senior, C., Stevens, B., & Taylor, K. E. (2017). CMIP5 scientific gaps and recommendations for CMIP6. *Bulletin of the American Meteorological Society*, *98*(1), 95–105. <https://doi.org/10.1175/BAMS-D-15-00013.1>
- Svoboda, M. D., LeCompte, D., Hayes, M., Heim, R., & Gleason, K. (2002). The Drought Monitor. In *Bull. Amer. Meteorol. Soc* (pp. 1181–1190).
- Tanachaichoksirikun, P., Seeboonruang, U., Fogg, G.E., 2020. Improving Groundwater Model in Regional Sedimentary Basin Using Hydraulic Gradients. *KSCE Journal of Civil Engineering* *24*, 1655–1669. <https://doi.org/10.1007/s12205-020-1781-8>
- Teshager, A. D., Gassman, P. W., Secchi, S., Schoof, J. T., & Misgna, G. (2016). Modeling Agricultural Watersheds with the Soil and Water Assessment Tool (SWAT): Calibration and Validation with a Novel Procedure for Spatially Explicit HRUs. *Environmental Management*, *57*(4), 894–911. <https://doi.org/10.1007/s00267-015-0636-4>
- Texas A&M University, (2012). *SWAT: Soil & Water Assessment Tool* [WWW Document]. URL <https://swat.tamu.edu/> (accessed 3.12.21)
- Thomas B. McKee, N. J. D. and J. K. (1993). THE RELATIONSHIP OF DROUGHT FREQUENCY AND DURATION TO TIME SCALES. *Journal of Surgical Oncology*, *105*(8), 818–824. <https://doi.org/10.1002/jso.23002>
- Tibshirani, R. (1996). Regression Shrinkage and Selection Via the Lasso. *Journal of the Royal Statistical Society: Series B (Methodological)*, *58*(1), 267–288, 1996. ISSN 00359246. <https://doi.org/10.1111/j.2517-6161.1996.tb02080.x>
- United States Geological Survey. (2016). USGS: Groundwater and Drought. <https://water.usgs.gov/ogw/drought/#:%7E:text=A%20groundwater%20drought%20typically%20refers,for%20humans%20and%20the%20environment.> (accessed 3.12.20).
- United States Geological Survey. (2019). USGS: Snowmelt Runoff and Water Cycle. [https://www.usgs.gov/special-topic/water-science-school/science/snowmelt-runoff-and-water-cycle?qt-science_center_objects=0#qt-science_center_objects.](https://www.usgs.gov/special-topic/water-science-school/science/snowmelt-runoff-and-water-cycle?qt-science_center_objects=0#qt-science_center_objects) (accessed 10.18.21).
- Van der Kamp, G., & Hayashi, M. (2009). Groundwater-wetland ecosystem interaction in the semiarid glaciated plains of North America. *Hydrogeology Journal*, *17*(1), 203–214. <https://doi.org/10.1007/s10040-008-0367-1>

- Van Lanen, H. A. J., & Peters, E. (2000). *Definition, Effects and Assessment of Groundwater Droughts*. 49–61. https://doi.org/10.1007/978-94-015-9472-1_4
- Van Loon, A. F. (2015). Hydrological drought explained. *Wiley Interdisciplinary Reviews: Water*, 2(4), 359–392. <https://doi.org/10.1002/WAT2.1085>
- Van Loon, A. F., & Van Lanen, H. A. J. (2012). A process-based typology of hydrological drought. *Hydrology and Earth System Sciences*, 16(7), 1915–1946. <https://doi.org/10.5194/hess-16-1915-2012>
- Van Loon, A. F., Van Lanen, H. A. J., Hisdal, H., Tallaksen, L. M., Fendeková, M., Oosterwijk, J., Horvát, O., & Machlica, A. (2010). Understanding hydrological winter drought in Europe. *IAHS-AISH Publication*, 340(January), 189–197.
- Vano, J. A., Scott, M. J., Voisin, N., Stöckle, C. O., Hamlet, A. F., Mickelson, K. E. B., Elsner, M. M. G., & Lettenmaier, D. P. (2010). Climate change impacts on water management and irrigated agriculture in the Yakima River Basin, Washington, USA. *Climatic Change*, 102(1–2), 287–317. <https://doi.org/10.1007/s10584-010-9856-z>
- Villholth, K. G., Tøttrup, C., Stendel, M., & Maherry, A. (2013). Integrated Mapping of Groundwater Drought Risk in the Southern African Development Community (SADC) region. *Hydrogeology Journal*, 21(4), 863–885. <https://doi.org/10.1007/s10040-013-0968-1>
- Voldoire, A., Saint-Martin, D., Sénési, S., Decharme, B., Alias, A., Chevallier, M., Colin, J., Guérémy, J. F., Michou, M., Moine, M. P., Nabat, P., Roehrig, R., Salas y Méliá, D., Séférian, R., Valcke, S., Beau, I., Belamari, S., Berthet, S., Cassou, C., ... Waldman, R. (2019). Evaluation of CMIP6 DECK Experiments With CNRM-CM6-1. *Journal of Advances in Modeling Earth Systems*, 11(7), 2177–2213. <https://doi.org/10.1029/2019MS001683>
- Wang, B., Guo, S., Feng, J., Huang, J., & Gong, X. (2022). Simulation on Effect of Snowmelt on Cropland Soil Moisture within Basin in High Latitude Cold Region Using SWAT. *Nongye Jixie Xuebao/Transactions of the Chinese Society for Agricultural Machinery*, 53(1), 271–278. <https://doi.org/10.6041/j.issn.1000-1298.2022.01.030>
- Waterloo Hydrogeologic. (2018). User 's Manual Visual MODFLOW Flex 5.1. In *Waterloo Hydrogeologic*.
- Weedon, G. P., Balsamo, G., Bellouin, N., Gomes, S., Best, M. J., & Viterbo, P. (2014). The WFDEI meteorological forcing data set: WATCH Forcing Data methodology applied to ERA-Interim reanalysis data. *Water Resources Research*, 50(9), 7505–7514. <https://doi.org/10.1002/2014WR015638>
- Wu, H., Chen, B., & Li, P. (2013). Comparison of sequential uncertainty fitting algorithm (SUFI-2) and parameter solution (ParaSol) method for analyzing uncertainties in distributed hydrological modeling - A case study. *Proceedings, Annual Conference - Canadian Society for Civil Engineering*, 4(January), 3453–3456.

- Wu, J., Chen, X., Gao, L., Yao, H., Chen, Y., & Liu, M. (2016). Response of Hydrological Drought to Meteorological Drought under the Influence of Large Reservoir. *Advances in Meteorology*, 2016. <https://doi.org/10.1155/2016/2197142>
- Wu, T., Lu, Y., Fang, Y., Xin, X., Li, L., Li, W., Jie, W., Zhang, J., Liu, Y., Zhang, L., Zhang, F., Zhang, Y., Wu, F., Li, J., Chu, M., Wang, Z., Shi, X., Liu, X., Wei, M., ... Liu, X. (2019). The Beijing Climate Center Climate System Model (BCC-CSM): The main progress from CMIP5 to CMIP6. *Geoscientific Model Development*, 12(4), 1573–1600. <https://doi.org/10.5194/gmd-12-1573-2019>
- Wu, T., Yu, R., Lu, Y., Jie, W., Fang, Y., Zhang, J., Zhang, L., Xin, X., Li, L., Wang, Z., Liu, Y., Zhang, F., Wu, F., Chu, M., Li, J., Li, W., Zhang, Y., Shi, X., Zhou, W., ... Hu, A. (2021). BCC-CSM2-HR: A high-resolution version of the Beijing Climate Center Climate System Model. *Geoscientific Model Development*, 14(5), 2977–3006. <https://doi.org/10.5194/gmd-14-2977-2021>
- Wu, W. Y., Lo, M. H., Wada, Y., Famiglietti, J. S., Reager, J. T., Yeh, P. J. F., Ducharme, A., & Yang, Z. L. (2020). Divergent effects of climate change on future groundwater availability in key mid-latitude aquifers. *Nature Communications*, 11(1), 1–9. <https://doi.org/10.1038/s41467-020-17581-y>
- Yadete, H., Kalinga, O., Beersing, A., & Biftu, G. (2008). Assessment of Climate Change Effects on Water Yield From the North Saskatchewan River Basin. In *North Saskatchewan Watershed Alliance* (Issue July).
- Yeh, H.-F. (2021). Spatiotemporal Variation of the Meteorological and Groundwater Droughts in Central Taiwan. *Frontiers in Water*, 3(February), 1–12. <https://doi.org/10.3389/frwa.2021.636792>
- Yimam, A. Y., Assefa, T. T., Sishu, F. K., Tilahun, S. A., Reyes, M. R., & Vara Prasad, P. V. (2021). Estimating surface and groundwater irrigation potential under different conservation agricultural practices and irrigation systems in the ethiopian highlands. *Water (Switzerland)*, 13(12). <https://doi.org/10.3390/w13121645>
- Yukimoto, S., Kawai, H., Koshiro, T., Oshima, N., Yoshida, K., Urakawa, S., Tsujino, H., Deushi, M., Tanaka, T., Hosaka, M., Yabu, S., Yoshimura, H., Shindo, E., Mizuta, R., Obata, A., Adachi, Y., & Ishii, M. (2019). The meteorological research institute Earth system model version 2.0, MRI-ESM2.0: Description and basic evaluation of the physical component. *Journal of the Meteorological Society of Japan*, 97(5), 931–965. <https://doi.org/10.2151/jmsj.2019-051>
- Zaremehrijardy, M., Razavi, S., & Faramarzi, M. (2021). *Assessment of the cascade of uncertainty in future snow depth projections across watersheds of mountainous, foothill, and plain areas*

in northern latitudes. Journal of Hydrology, 598(November), 125735.
<https://doi.org/10.1016/j.jhydrol.2020.125735>

Zaremehrijardy, M., Victor, J., Park, S., Smerdon, B., Alessi, D., Faramarzi, M. (2022) *Assessment of snowmelt and groundwater-surface water dynamics in mountainous, foothills, and plains regions in northern latitudes*, Journal of Hydrology, in review.

Zhang, C., & Long, D. (2021). Estimating Spatially Explicit Irrigation Water Use Based on Remotely Sensed Evapotranspiration and Modeled Root Zone Soil Moisture. *Water Resources Research*, 57(12), 1–27. <https://doi.org/10.1029/2021WR031382>

Zhou, Y., & Li, W. (2011). A review of regional groundwater flow modeling. *Geoscience Frontiers*, 2(2), 205–214. <https://doi.org/10.1016/j.gsf.2011.03.003>

APPENDICES

Table S1. Input data used for SWAT model development in this study.

	Dataset	Time span	Spatial Resolution	Time step	Reference
Meteorological data source	Meteorological stations	1980-2013	-	Daily	Government of Canada: http://climate.weather.gc.ca
	CFSR	1980-2013	0.3° grid	Daily	SWAT weather generator: http://globalweather.tamu.edu
Geospatial data source	Land-use/Land cover map	2000	30 m×30 m	-	Geobase Land Cover Data (Government of Canada, 2017)
	Soil map	2003	10 km×10 km	-	Food and Agriculture Organization of the United Nations (FAO, 2003)
	Digital Elevation Maps (DEM)	2008	90 m× 90 m; 10 km×10 km	-	SRTM (Jarvis et al., 2008) http://www.altalis.com/
Other model input	Glacier melt	1985-2005			Faramarzi et al. (2015, 2017)
	Reservoirs	Since compilation	River basin River basin	Monthly Monthly	AEP, Alberta Environmental and Parks: measured data at hydrometric stations.
Observed data source	Hydrometric station data	1980-2013	River basin	Monthly	Environment Canada: https://wateroffice.ec.gc.ca/
	Snow depth data	1999-2013	24km × 24km	Daily	Canadian Meteorological Centre (CMC) Daily Snow Depth Analysis Data, Version 1.

Table S2. Climate data sources for CMIP6 GCMs projected future climate data

GCMs	Host Institute	Time span	Spatial Resolution	Time step	Reference
BCC-CSM2-MR	Beijing Climate Centre, China Meteorological Administration, China	2040-2073	250 km	Daily	Wu et al. (2019)
CNRM-CM6-1	Centre National de Recherches Météorologiques (CNRM), France	2040-2073	100 km	Daily	Voldoirie et al. (2019)
EC-Earth3	27 research institutes from 10 European countries	2040-2073	100 km	Daily	http://www.ec-earth.org
EC-Earth3-veg	27 research institutes from 10 European countries	2040-2073	100 km	Daily	http://www.ec-earth.org
MRI-ESM2.0	Meteorological Research Institute (MRI), Japan	2040-2073	100 km	Daily	Yukimoto et al. (2019)

Table S3. Input data used for MODFLOW model development for the NSRB. The data were partially adapted from Smerdon et al. (2017), Chenn et al., (2017), and Tanachaichoksirikun et al. (2020). The hydraulic head data were slightly improved in the NSRB model.

Input data for model development and			Input parameters for model calibration		Observed data for model calibration
Layer Number	Layer name	Elevation range at top of the layer (m)	Horizontal hydraulic conductivity ($m\ s^{-1}$)	Ratio of horizontal and vertical hydraulic conductivity	Monthly time series data of GW heads for the 1983-2007 period, available for 20 observation wells across NSRB. Source: Alberta water information database: all stations: http://environment.alberta.ca/apps/GOWN/#
1	Mountainous region/above sediment bedrock	500 – 3413	1.48×10^{-10} – 1.94×10^{-7}	1-100	
2	Bedrock Paskapoo	470 – 1390	1.09×10^{-10} – 5.49×10^{-5}	1-100	
3	Bedrock Scollard	367 – 963	9.53×10^{-10} – 3.55×10^{-6}	1-100	
4	Bedrock Battle	53 – 921	7.73×10^{-10} – 1.34×10^{-7}	1-100	
5	Bedrock Horseshoe	43 – 914	4.34×10^{-10} – 3.57×10^{-6}	1-100	

Table S4-1. Optimized parameters in SWAT hydrologic model calibration.

Type	Name ^a	Description	Initial range	Final range
Snow	v__SUB_SFTMP().sno	Snow fall temperature (°C)	-5 to 5	0.0084 to 0.0174
	v__SUB_SMTMP().sno	Snowfall melt base temperature (°C)	-5 to 5	0.3587 to 0.7449
	v__SUB_SMFMX().sno	Maximum melt rate for snow during the year	1.4 to 6.9	3.7506 to 7.7897
	v__SUB_SMFMN().sno	Minimum melt rate for snow during the year	1.4 to 6.9	3.7978 to 7.8878
	v__SUB_TIMP().sno	Snow pack temperature lag factor	0 to 1	0.5600 to 1.0000
Groundwater	v__ALPHA_BF.gw	Base flow alpha factor (days)	0 to 1	0.0081 to 0.1303
	v__REVAPMN.gw	Threshold depth of water in the shallow aquifer for	0 to 1000	455.90 to 1129.6
	v__GW_DELAY.gw	Groundwater delay time (days)	0 to 500	0.8705 to 134.60
	v__GW_REVAP.gw	Groundwater revap. coefficient	0.01 to 1	0.0031 to 0.3972
	v__GWQMN.gw	Threshold depth of water in the shallow aquifer	0 to 5000	326.93 to 1640.6
	v__RCHRG_DP.gw	Deep aquifer percolation fraction	0 to 1	0.0103 to 0.2974
Soil	r__SOL_AWC().sol	Soil available water storage capacity (mm H ₂ O/mm)	0 to 1	-0.376 to 0.3289
	r__SOL_K().sol	Soil conductivity (mm/hr)	0 to 2000	-0.444 to 0.4511
	r__SOL_BD().sol	Soil bulk density (g/cm ³)	0.9 to 2.5	-0.522 to 0.2523
	r__SOL_ALB().sol	Moist soil albedo	0 to 1	-0.462 to 0.4382
Soil & vegetation	v__EPCO.hru	Plant uptake compensation factor	0.01 to 1.5	0.4834 to 1.3279
	v__ESCO.hru	Soil evaporation compensation factor	0.01 to 1.5	0.4895 to 1.3355
	r__OV_N.hru	Manning's n value for overland flow	0.008 to 0.5	-0.302 to 0.5389
	r__CN2.mgt	SCS runoff curve number for moisture condition II	0 to 100	-0.524 to 0.5282
Stream	v__CH_N2.rte	Manning's n value for main channel	0.001 to 0.3	0.0074 to 0.2555
	v__CH_K2.rte	Effective hydraulic conductivity in the main channel	0.025 to 6	0.1915 to 3.9174

^a v: The parameter value is replaced by given value or absolute change; r: parameter value is multiplied by (1± a given value) or relative change.

Table S4-2. Optimized parameters in MODFLOW groundwater model calibration.

Parameter	Layer	Description	Initial range	Final value
Horizontal hydraulic conductivity	Layer 1	Horizontal hydraulic conductivity (m day ⁻¹)	0.0000127872 to 0.0167616000	0.0003072
	Layer 2			0.0135648
	Layer 3			0.00104544
	Layer 4			0.00019224
	Layer 5			0.0385344
Specific yield	Layer 1	Soil specific yield (unitless)	0.19 to 0.33	0.22
	Layer 2			0.22
	Layer 3			0.22
	Layer 4			0.22
	Layer 5			0.22
Specific storage	Layer 1	Soil specific storage (m ⁻¹)	0.00005 to 0.0001	0.00017
	Layer 2			0.00017
	Layer 3			0.00017
	Layer 4			0.00017
	Layer 5			0.00017
Vertical hydraulic conductivity	Layer 1	Vertical hydraulic conductivity (m day ⁻¹)	horizontal hydraulic conductivity / (1 to 100)	0.000063072
	Layer 2			0.00135648
	Layer 3			0.000104544
	Layer 4			0.000019224
	Layer 5			0.00385344

Table S5. US drought monitoring D-scale characteristics and detailed description

Drought Category	Description	Index Range	Possible Impacts
D0	Abnormally dry	-0.5 to -0.7	Slow farms activities and crop and pasture growth, streamflow below average, fire risk above average
D1	Moderate drought	-0.8 to -1.2	Some damage to crops and pastures, streamflow, reservoir and well levels low, development of some water shortages, high risk of fire
D2	Severe drought	-1.3 to -1.5	Crop and pasture likely to lose, common water shortages, water restrictions should be imposed, very high fire risk
D3	Extreme drought	-1.6 to -1.9	Major crop and pasture losses occurs, widespread water shortages and restrictions occurs, extremely high fire risk
D4	Exceptional drought	-2.0 or less	Exceptional and widespread crop and pasture losses, shortages of water in stream, reservoirs and wells creating emergencies, exceptionally high risk of fire dangers

Table S6. Exogenous variables selected for LASSO analysis to study dominant physical processes affecting propagation of drought from snow to GW.

Exogenous variable	Abbreviation	Description
Daily curve number	DAILYCN	The time series for average curve number in HRU representing soil permeability, land use and antecedent soil water conditions. The higher the value is, the lower permeability of the HRU is. Retrieved from output.hru file.
Actual evapotranspiration	ET	Actual evapotranspiration (soil evaporation and plant transpiration) from the HRU during the time step (mmH ₂ O)
Percolation	PERC	Water that percolates past the root zone during the time step (mmH ₂ O).
Precipitation	PRECIP	Total amount of precipitation falling on the HRU during time step (mmH ₂ O)
Water revap	REVAP	Water in the shallow aquifer returning to the root zone in response to a moisture deficit during the time step (mmH ₂ O). The variable also includes water uptake directly from the shallow aquifer by deep tree and shrub roots.
Solar radiation	SOLAR	Average daily solar radiation (MJ/m ²). Average of daily solar radiation values for time period.
Soil water content	SW_END	Soil water content (mmH ₂ O). Amount of water in the soil profile at the end of the time period (day, month or year).
Snowmelt	SNOMELT	Amount of snow or ice melting during time step (water-equivalent mmH ₂ O)
Snow fall	SNOFALL	Amount of precipitation falling as snow, sleet or freezing rain during time step (water-equivalent mmH ₂ O)
Maximum temperature	TMP_MX	Average maximum air temperature (°C). Average of maximum daily air temperatures for time period
Minimum temperature	TMP_MN	Average minimum air temperature (°C). Average of minimum daily air temperatures for time period.
Water yield	WYLD	Water yield (mmH ₂ O). Total amount of water leaving the HRU and entering main channel during the time step (WYLD = surface flow + lateral flow + groundwater discharge – transmission losses – pond abstractions)

Table S7. Calibration and validation results for streamflow simulation in SWAT model

Gauge ID used in the model	Location of hydrometric station	EHG Region	Calibration				Validation			
			<i>p-factor</i>	<i>r-factor</i>	R ²	bR ²	<i>p-factor</i>	<i>r-factor</i>	R ²	bR ²
Flow_48_56	Tributary	Mountains	0.25	0.51	0.35	0.23	0.35	0.53	0.42	0.30
Flow_144_144	Downstream of Brazeau Dam		1.00	0.04	0.99	0.98	1.00	0.02	0.99	0.99
Flow_47_148	Tributary		0.43	1.68	0.29	0.26	0.40	1.73	0.32	0.26
Flow_46_158	Main stream		0.42	0.59	0.67	0.61	0.35	0.67	0.72	0.55
Flow_43_164	Tributary		0.91	0.13	0.97	0.96	0.90	0.11	0.94	0.92
Flow_44_174	Tributary		0.73	0.10	0.66	0.59	0.68	0.10	0.62	0.54
Flow_51_76	Main stream	Foothills	0.65	0.33	0.81	0.60	–	–	–	–
Flow_77_77	Downstream of Bighorn Dam		1.00	0.38	0.96	0.94	1.00	0.21	0.95	0.93
Flow_49_105	Tributary		0.77	0.86	0.50	0.45	0.79	1.06	0.71	0.69
Flow_45_157	Main stream		0.50	0.50	0.66	0.63	0.45	0.49	0.56	0.46
Flow_54_28	Tributary	Plains	0.33	2.57	0.20	0.15	0.34	3.43	0.18	0.13
Flow_53_36	Tributary		0.34	3.20	0.49	0.36	0.53	3.07	0.09	0.06
Flow_52_41	Main stream		0.43	0.56	0.76	0.76	0.43	0.47	0.72	0.68
Average			0.60	0.88	0.64	0.58	0.60	0.99	0.60	0.54

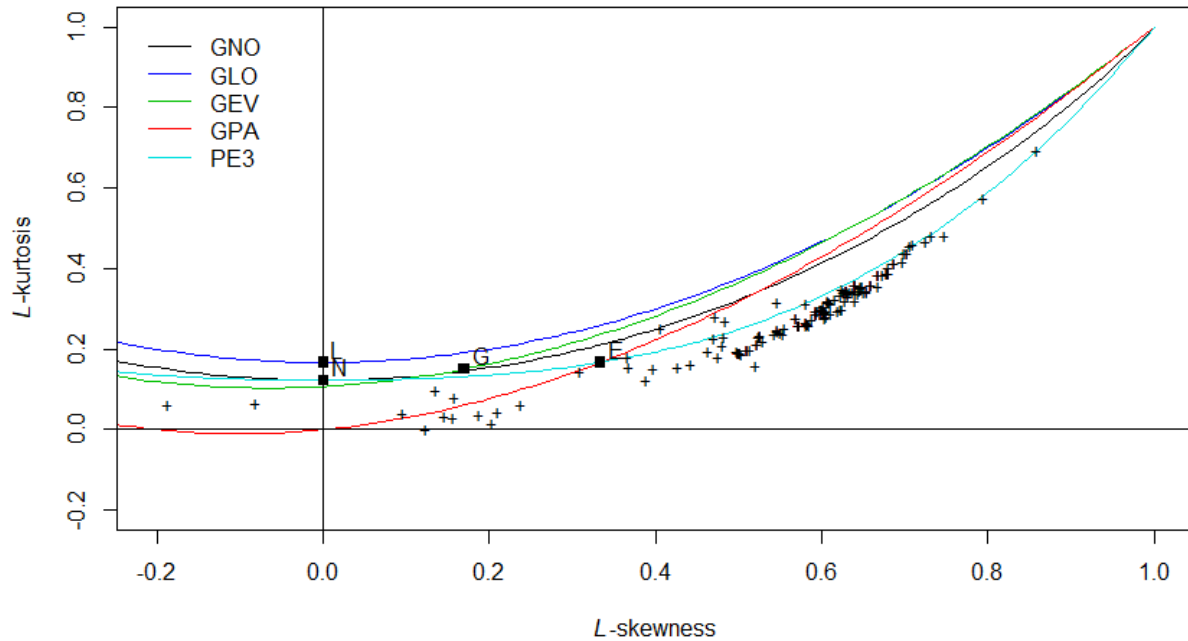


Figure S1. Comparison of the L-moment ratio diagram of simulated monthly SWE data from 174 subbasins across NSRB, and the reference L-moment curves based on five different distribution methods that were examined in this study. Demonstrated distributions in the figure are Generalized Logistics (GLO), Generalized Normal (GNO), Generalized Extreme Value (GEV), Generalized Pareto (GPA) and Pearson Type III (PE3)

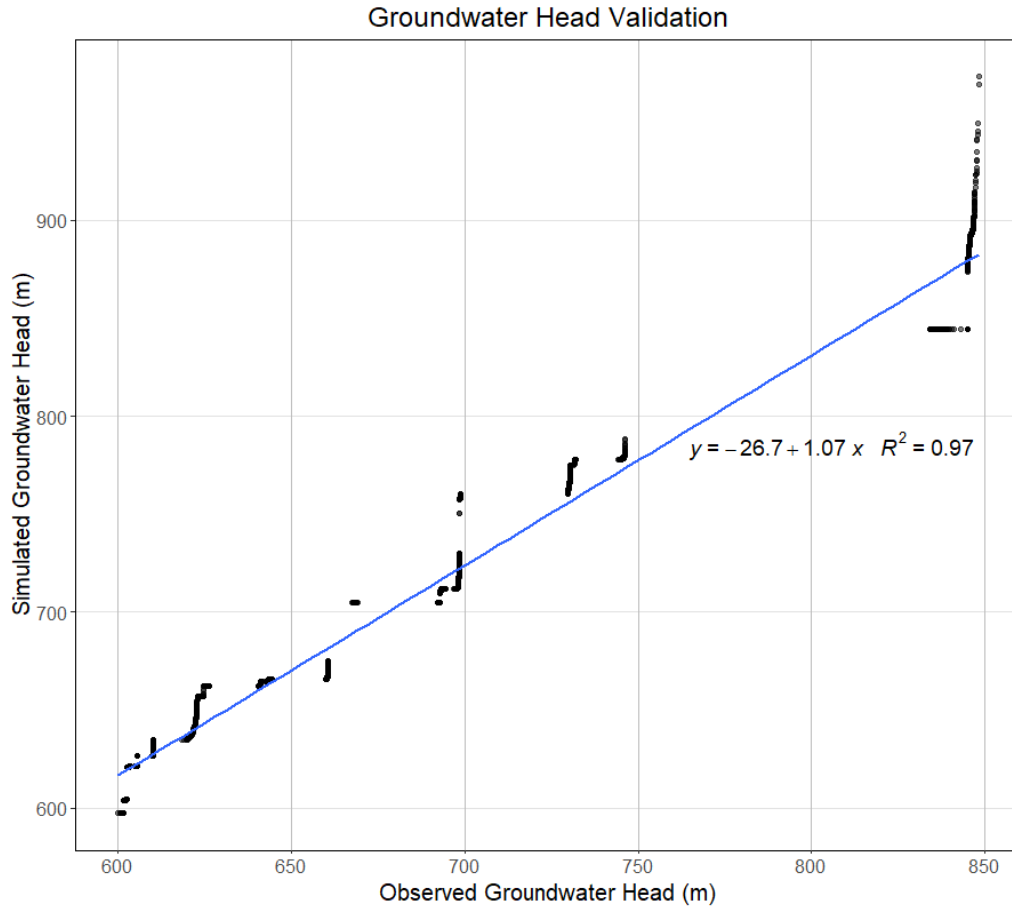


Figure S2. Observed groundwater head and simulated groundwater head comparison for entire NSRB

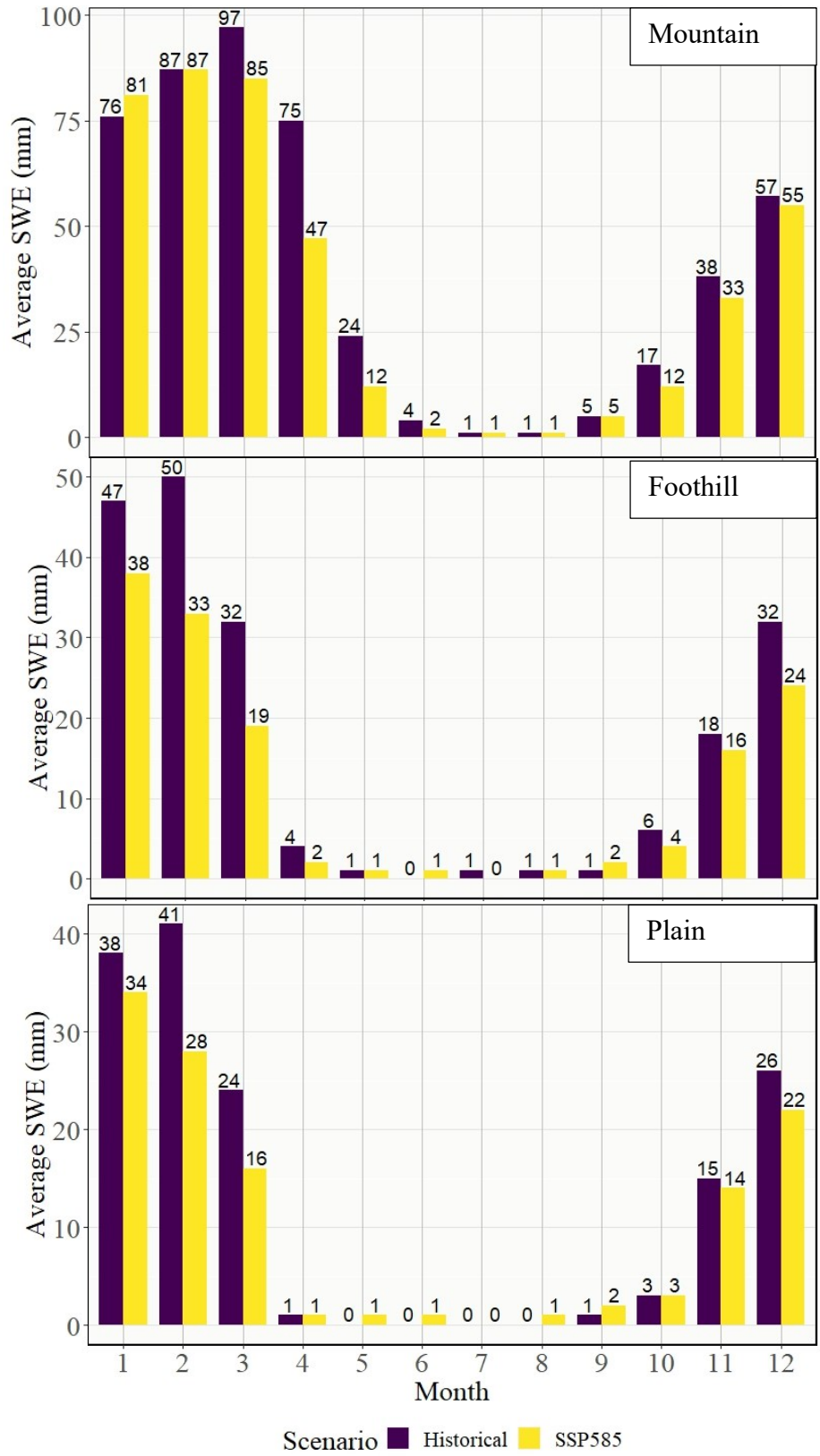


Figure S3. Monthly averaged SWE for historical and SSP585 scenario for each EHG.

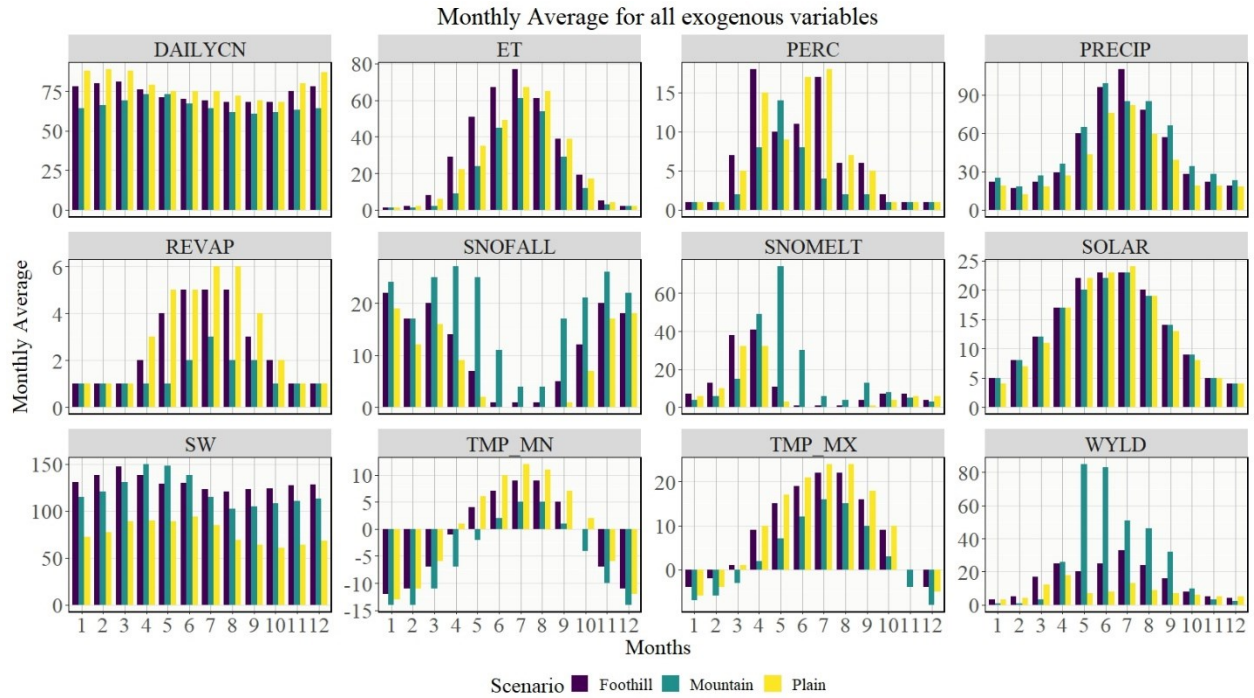


Figure S4. Monthly averaged exogenous variables for Mountains, Foothills and Plains. Each panel indicates one exogenous parameter. The first row from left to right displays daily curve number, actual evapotranspiration, percolation and precipitation. Second row from left to right displays reevaporation, snowfall, snowmelt and net solar radiation. Third row from left to right are soil water content, minimum temperature, maximum temperature and total water yield and entering the main channel.

Supplementary notes N1

The idea of pre-whitening follows from the following theorem (Shumway and Stoffer, 2017)

Firstly, the end goal of cross correlation analysis is to calculate a factor value between two time series with different lag time, hence with each lag time, a factor value is going to be calculated.

The higher the value is, the more related the two time series are and vice versa. According to the pre-whitening theorem, the large sample distribution of the sample cross-correlation function $\hat{\rho}_{xy}(h)$ (where h is the lag time) between two linear variables x_t and y_t is normal with mean zero and standard deviation of

$$\sigma_{\hat{\rho}_{xy}} = \frac{1}{\sqrt{n}}$$

, if at least one of the x_t and / or y_t variables is independent (Shumway and Stoffer, 2017).

Based on above theorem, the practical importance of maximum correlation can then be assessed by comparing their magnitudes with $d = \frac{2}{\sqrt{n}}$, where d is a base line that determines whether calculated cross-correlation factor is meaningful or not, and only the cross-correlation factor above d is considered to be meaningful.

The process of pre-whitening consists of first converting one of the two time series to a white noise process, which is a new series with mean of zero and identical variance (Cryer and Chan, 2011), via a filter and then transforming the other series using the same filter. For instance, if X_t follows an auto-correlation model with 1 unit time lag (AR(1) process) with no intercept term, then

$$\tilde{X}_t = X_t - \Phi X_{t-1} = [1 - \Phi B]X_t$$

Is the white noise via the filter $1 - \Phi B$. Then we transform Y_t to \tilde{Y} using the same filter,

$$\tilde{Y}_t = [1 - \Phi B]Y_t$$

Note that \tilde{Y}_t doesn't need to be white noise because the filter is tailor-made only to transform X_t to a white noise process, not Y_t .

We now can determine the lag relation between Y_t and X_t by computing the cross correlation factor between \tilde{Y} and \tilde{X} by comparing different cross correlation factors, and the lag time with maximum cross correlation factor is the final lag time we are looking for (Cryer and Chan, 2011).

Supplementary notes N2

Extended LASSO method for time series.

$$y_t = \sum_{i=1}^p \sum_{s=0}^h \beta_{i,s} x_{i,t-s} + \omega_t, t = h + 1, \dots, T$$

Where $x_{i,t-s}$ is the i -th variable with total number of variables of p , and a lag of s with total amount of lag h , as well as ω_t , which is a stationary error term. In this case, x_i will be the exogenous variables listed in Table S6 and y_t is the GW leveltime series. It depicts that LASSO estimator is determined through the following optimization problem,

$$\tilde{\beta}^{(\lambda)} = \underset{\beta}{\operatorname{argmin}} \|y - X\beta\|_2^2 + \lambda \|\beta\|_1$$

Where $\beta = (\beta_1^{\operatorname{Transpose}}, \dots, \beta_p^{\operatorname{Transpose}})^{\operatorname{Transpose}}$ with $\beta_i = (\beta_{i,0}, \dots, \beta_{i,h})^{\operatorname{Transpose}}$, and

$\mathbf{y} = (y_1, \dots, y_T)^{\operatorname{Transpose}}$, and

$$X = \begin{bmatrix} x_{1,h+1} & \cdots & x_{1,1} & \cdots & x_{p,h+1} & \cdots & x_{p,1} \\ \vdots & \ddots & \vdots & \ddots & \vdots & \ddots & \vdots \\ x_{1,T} & \cdots & x_{1,T-h} & \cdots & x_{p,T} & \cdots & x_{p,T-h} \end{bmatrix}$$